Received: 14 July 2022 | Revised: 6 December 2023 | Accepted: 13 December 2023

DOI: 10.1111/mec.17255

ORIGINAL ARTICLE

MOLECULAR ECOLOGY WILEY

Plastic and genomic change of a newly established lizard population following a founder event

Iva Sabolić[1] | Óscar Mira[1] | Débora Y. C. Brandt[2] | Duje Lisičić[1] | Jessica Stapley[3] | Maria Novosolov[4] | Robert Bakarić[1] | Ivan Cizelj[5] | Marko Glogoški[1] | Tomislav Hudina[6] | Maxime Taverne[7] | Morten E. Allentoft[4,8] | Rasmus Nielsen[2] | Anthony Herrel[7,9,10,11] | Anamaria Štambuk[1]

[1]Department of Biology, Faculty of Science, University of Zagreb, Zagreb, Croatia

[2]Department of Integrative Biology, University of Berkeley, Berkeley, California, USA

[3]Department of Environmental Sciences, ETH Zurich, Zurich, Switzerland

[4]Lundbeck Foundation GeoGenetics Centre, GLOBE Institute, University of Copenhagen, Copenhagen, Denmark

[5]Zoological Garden of Zagreb, Zagreb, Croatia

[6]Association Biom, Zagreb, Croatia

[7]C.N.R.S/M.N.H.N., Département d'Ecologie et de Gestion de la Biodiversité, Paris, France

[8]Trace and Environmental DNA (TrEnD) Laboratory, School of Molecular and Life Sciences, Curtin University, Perth, Western Australia, Australia

[9]Department of Biology, Evolutionary Morphology of Vertebrates, Ghent University, Ghent, Belgium

[10]Department of Biology, University of Antwerp, Wilrijk, Belgium

[11]Naturhistorisches Museum Bern, Bern, Switzerland

Correspondence
Anamaria Štambuk, Department of Biology, Faculty of Science, University of Zagreb, Zagreb, Croatia.
Email: astambuk@biol.pmf.hr

Funding information
Croatian Science Foundation, Grant/Award Number: DOK-2018-01-8879 and HRZZ-IP-06-2016-9177; National Geographic Committee for Research and Exploration

Handling Editor: Eva Stukenbrock

Abstract

Understanding how phenotypic divergence arises among natural populations remains one of the major goals in evolutionary biology. As part of competitive exclusion experiment conducted in 1971, 10 individuals of Italian wall lizard (*Podarcis siculus* (Rafinesque-Schmaltz, 1810)) were transplanted from Pod Kopište Island to the nearby island of Pod Mrčaru (Adriatic Sea). Merely 35 years after the introduction, the newly established population on Pod Mrčaru Island had shifted their diet from predominantly insectivorous towards omnivorous and changed significantly in a range of morphological, behavioural, physiological and ecological characteristics. Here, we combine genomic and quantitative genetic approaches to determine the relative roles of genetic adaptation and phenotypic plasticity in driving this rapid phenotypic shift. Our results show genome-wide genetic differentiation between ancestral and transplanted population, with weak genetic erosion on Pod Mrčaru Island. Adaptive processes following the founder event are indicated by highly differentiated genomic loci associating with ecologically relevant phenotypic traits, and/or having a putatively adaptive role across multiple lizard populations. Diverged traits related to head size and shape or bite force showed moderate heritability in a crossing experiment, but between-population differences in these traits did not persist in a common garden environment. Our results confirm the existence of sufficient additive genetic variance

Iva Sabolić and Óscar Mira joint first authorship.

for traits to evolve under selection while also demonstrating that phenotypic plasticity and/or genotype by environment interactions are the main drivers of population differentiation at this early evolutionary stage.

KEYWORDS
bottleneck, heritability, invasive success, phenotypic plasticity, population crossing experiment, rapid evolution

1 | INTRODUCTION

One of the fundamental questions in evolutionary biology is how natural selection contributes to phenotypic variability in natural populations. However, the pattern and strength of selection is dictated by temporal and spatial ecological variation, which directly affects our ability to observe adaptive processes in nature. The polygenic nature of complex phenotypic traits further hampers the detection of adaptation footprints, especially across populations inhabiting environments characterized by mild selection pressures (Pritchard & Di Rienzo, 2010). When environmental conditions abruptly change or a population occupies a novel habitat, selection may increase the genome-wide abundance of favoured alleles and create adaptive genomic divergence (Endler, 1986; Nosil et al., 2009). Such shifts can result in rapid evolution of phenotypically and genetically distinct populations over the course of only several generations (Carroll et al., 2007; Marques et al., 2018; Stuart et al., 2014). Adaptive evolution occurs through genetic changes but is often preceded by an adaptive plasticity, which increases phenotypic adaptive values (Ghalambor et al., 2007). Though plasticity appears to be most advantageous in fluctuating environments, plastic responses may also play a relevant role in species colonization and persistence in novel habitats (Aubret & Shine, 2009; Lande, 2015; Wang & Althoff, 2019). Eco-evolutionary studies focusing on phenotypic divergence in natural populations have been hard-pressed to determine the relative contributions of phenotypic plasticity and genomic divergence to adaptation across spatial and temporal scales (Hendry, 2013). Phenotypic plasticity and adaptive evolution frequently co-occur, with plasticity either constraining or facilitating genomic adaptation (Lande, 2009; Oostra et al., 2018). Both theory and empirical data suggest that initial plastic modifications attuned to adaptive demands can promote subsequent genetic adaptation to new habitats (Levis et al., 2018; Noble et al., 2019; Radersma et al., 2020). Although the role of plasticity in adaptive trajectories cannot be denied, adaptive evolution only occurs through transmission of genetic responses to selective pressures across generations. Therefore, it is the extent of the variability of the trait that can be transmitted to the next generation (i.e. its heritability) that governs the rate and magnitude of trait evolution (De Villemereuil et al., 2015; Falconer & Mackay, 1996). Narrow-sense heritability (h^2) is the proportion of total phenotypic variation that is due to additive genetic variance (V_A) among individuals. It is of special concern for adaptive evolution, as it determines the responsiveness of a trait to selection and offers a useful measure of adaptive potential of a phenotypic trait in a population (Allendorf et al., 2013; Hoffmann et al., 2017). Accordingly, estimating heritability provides a good opportunity to evaluate the relative role of genetic and plastic mechanisms underlying that trait in a specific population.

Detecting evolution by natural selection in the wild thus requires demonstrating that the phenotypic trait is variable, and adaptive (i.e. improve fitness for individuals), that the observed variability has a genetic basis (i.e. is heritable), and that it promotes genomic divergence in trait-associated loci (irrespective of any neutral sources of variation) (Endler, 1986; Pardo-Diaz et al., 2015). This can be notably difficult to achieve, as it calls for an extensive application of various experimental approaches, quantitative genetics modelling and modern population genomics techniques (Gienapp et al., 2017; Pardo-Diaz et al., 2015; Schlötterer et al., 2015). However, those are also the first steps in inferring the evolutionary potential of contemporary populations and predicting their response to subsequent ecological change.

The importance of genetic variance for population fitness has been postulated a long time ago (Nei et al., 1975). Reductions of genomic variation in natural populations are often the consequence of bottlenecks, which occur due to sharp reductions in effective population size following severe ecological disturbance. Founder effect refers to specific bottleneck event attributable to a small number of individuals establishing a novel population (Mayr & Provine, 1980). Irrespectively of their ecological cause, bottlenecks commonly increase the genetic drift and inbreeding. The size of a founding population is hence known to be one of the most important factors driving its future evolutionary trajectory in a novel environment (Allendorf, 1986) because it directly influences available phenotypic and genetic variance. Yet, many aspects of the bottleneck's determining power for colonization success and/or subsequent adaptation to novel environments still remain unresolved, especially in regard to the amount of additive genetic variance retained, or the interacting effects of phenotypic plasticity or gene flow (Dlugosch & Parker, 2008; Estoup et al., 2016; Radersma et al., 2020; Roman & Darling, 2007).

Biological invasions oftentimes represent a good model system to study the basis of adaptive responses in natural ecosystems. They are frequently well documented, enabling precise measurement of the speed of phenotypic trait evolution, and can trigger remarkable phenotypic shifts in introduced and native populations alike (Cattau et al., 2018; Moran & Alexander, 2014; Stuart et al., 2014).

Evolutionary consequences of biological invasions are recurrently studied on islands (Feiner et al., 2021; Kolbe et al., 2004; Sendell-Price et al., 2021; Warren et al., 2015), as their geographical isolation and often contrasting ecological conditions enable more accurate characterization of crucial ecological and demographic parameters. Ever since Darwin, island systems have remained one of the most fascinating scientific arenas for studying how populations and species diverge. One recent intriguing example of rapid phenotypic evolution comes from the deliberate introduction of the Italian wall lizard (*Podarcis siculus* (Rafinesque-Schmaltz, 1810)) on a small islet of Pod Mrčaru in the Adriatic Sea off the cost of Croatia. In a transplant experiment conducted in 1971, five pairs of *P. siculus* from the islet of Pod Kopište were introduced on the nearby islet Pod Mrčaru (Figure 1; Figures S1 and S2), which was at the time inhabited by Dalmatian wall lizard, *Podarcis melisellensis* (Gorman et al., 1972). Follow-up studies have revealed that in only 35 years *P. siculus* completely outcompeted the native *P. melisellensis* on the islet (Herrel et al., 2008; Vervust et al., 2007). This was not entirely unexpected, as *P. siculus* is considered an invasive species across its introduced range, known to often displace native lizard populations by reducing or taking over their habitat (D'Amico et al., 2018; Putman et al., 2020). Nevertheless, the surveys exposed something more interesting – in this short period of time the newly established *P. siculus* population exhibited spectacular phenotypic changes in ecology, morphology and physiology (Herrel et al., 2008; Taverne et al., 2019; Vervust et al., 2010; Wehrle et al., 2020). Many of the observed morphological and functional changes, such as difference in bite force, head size and shape, are reminiscent of the adaptations found in herbivorous species (Herrel, 2007; Herrel et al., 2004) and can be connected to the observed ecological shift from a predominantly insectivorous to an omnivorous diet. The adaptive role of variation in cranial shape and jaw muscles of *Podarcis* lizards is evident by consistency of ecological conditioning of their form and function across evolutionary scales, from populations to species (Taverne et al., 2021). Phenotypic head traits related to higher bite force in Italian wall lizards allow them access to a wider range of trophic resources (Taverne et al., 2020). Even though the amount of plant consumed is the major predictive ecological covariate of the head shape, sexual competition and prey hardness also affect head morphology (Taverne et al., 2020, 2021, 2023). The relative role of phenotypic plasticity and genomic adaptation in the observed differentiation, however, remained unknown, as did the signatures of small founder size and the subsequent phenotypic shift on genomic patterns in the introduced population.

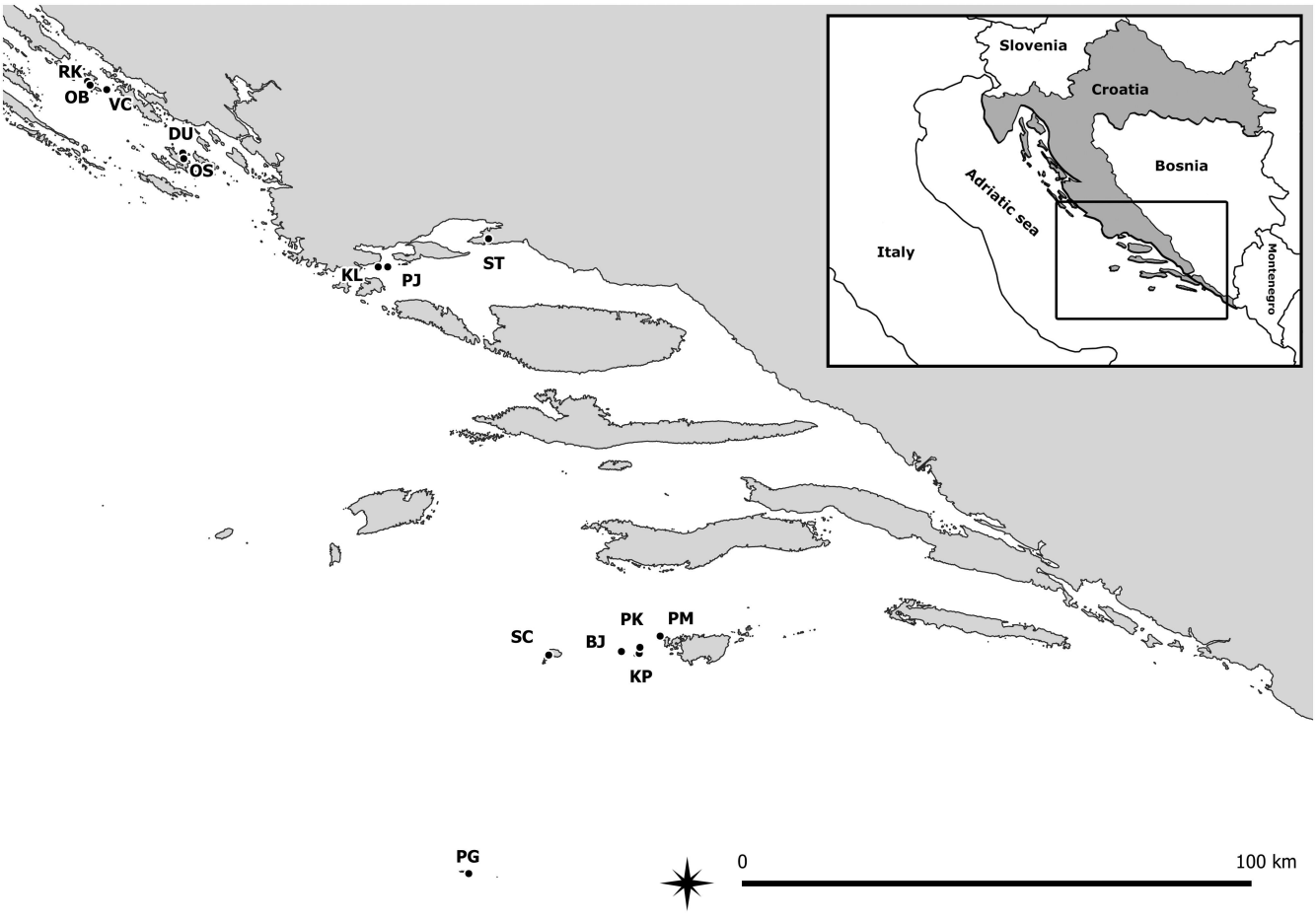

FIGURE 1 Map of the 14 sampling locations of wild *P. siculus* populations: BJ, Bijelac; DU, Veliki Dupinić; KL, Kluda; KP, Kopište; OB, Obrovanj; OS, Oštrica; PG, Mala Palagruža; PJ, Pijavica; PK, Pod Kopište; PM, Pod Mrčaru; RK, Rakita; SC, Sušac; ST, Split; VC, Visovac.

In this study, we combined genomic and quantitative genetic approaches to determine the relative role of adaptive evolution and plasticity in driving rapid phenotypic evolution of Pod Mrčaru *P. siculus*. Specifically, we: (1) quantified genome-wide divergence between the ancestral and the transplanted population; (2) determined adaptive role of a substantial number of highly diverged loci, with the prediction that those loci will be associated with divergent phenotypic traits, or environmental variation in multi-population framework; (3) tested if phenotypic differentiation between populations persists when individuals are raised in a common environment; and (4) quantified heritable variation underlining rapidly diverging traits to determine if they possess enough additive genetic variance to evolve in response to selection.

2 | MATERIALS AND METHODS

2.1 | Experimental design

To estimate the signature of founder event on genetic diversity of newly established Pod Mrčaru (PM) population and to quantify its divergence from the ancestral Pod Kopište (PK) population, we analysed genotype by sequencing data of PM and PK populations and compared the patterns with those observed across 14 *P. siculus* wild populations (Figure 1). Then, we inferred adaptive nature of the highly differentiated PK-PM loci by assessing their association with PK-PM diverged phenotypic traits and their involvement in adaptation processes across 14 wild population. Third, we performed within- and between-PK and PM population crossing experiment to test for the persistence of phenotypic divergence in common garden and assess the additive genetic variance underlying traits of interest. The research and sampling conducted within this study were executed following European and Croatian legislative guidance and were approved by the Ethical Committee of the Biological Department, University of Zagreb, and Croatian Ministry of Environmental Protection and Energy (UP/I-612-07/16-48/116, UP/I-612-07/17-48/06, UP/I-612-07/18-48/21).

2.2 | Genome assembly

The genome of *P. siculus* was assembled de novo from a female *P. siculus* individual from Pod Mrčaru islet. We generated sequencing libraries using the 10× Genomics Chromium Library Preparation and sequenced them on an Illumina HiSeq 4000 sequencer. We then assembled the genome using *supernova mkfastq* run and evaluated the completeness of our genome assembly with BUSCO using the tetrapod database. Finally, we ran BLAST with all assembly scaffolds as queries against the NCBI database to remove any scaffolds with possible contaminants. We used R package *taxonomizr* to assign taxonomy for each alignment hit and removed scaffolds that did not find a BLAST hit to Squamata from the final assembly. For more details see Supplementary Materials and methods.

2.3 | Data collection and genotyping

In summer of 2016 and 2019 we sampled 14 *P. siculus* populations from the Croatian coast of Adriatic Sea, including the two focal islands Pod Mrčaru and Pod Kopište (Figure 1). Individuals from the Pod Mrčaru and Pod Kopište islands were additionally sampled in 2017 and 2018 (and later used in a crossing experiment). For individuals sampled in 2016 and 2019 we collected a set of 14 different phenotypic measurements in situ (Table S1). We further obtained a set of 8 different environmental variables for each sampled site from WorldClim online database and previously published literature sources (Table S2). We performed vegetational surveys on Pod Kopište and Pod Mrčaru, which indicated distinct differences in floral composition, and ecological variation between the two insular habitats (Tables S3 and S9). We have further quantified prey availability on Pod Kopište, Pod Mrčaru and Kopište islands using a standard number of pitfall traps (12) left on each island for 48 h and standardized, timed sweep samples (40 min of sampling covering the different vegetation types; Tables S10 and S11). Shannon diversity and evenness indices indicated that whereas the largest island Kopiste has the greatest diversity and evenness, the smallest island, Pod Mrčaru has overall the lowest diversity in terms of mass and numerical abundance of particular taxa (Table S12). For more details see Supplementary Materials and methods and Supplementary Results.

We genotyped 585 individuals from 14 wild *P. siculus* populations, as well as lizards from the common garden experiment using a genotyping by sequencing approach. We prepared custom-made double-digest sequencing libraries (Table S4) and sequenced them on Illumina HiSeq X Ten platform. We trimmed raw reads of residual adaptor and/or barcode contamination and standardized them in length using custom-made Perl scripts. Reads with uncalled bases and/or cut sites containing more than one mismatch were removed, and those with average Phred quality score below 20 were discarded using the *process_radtags* program in Stacks. We mapped processed reads on the assembled *P. siculus* genome using default settings in the Bowtie2 software. Variant sites were called following the *ref_map* pipeline from Stacks. We discarded the reads with a minimum mapping quality lower than 20. Only the first SNP on each locus was called. We filtered out single nucleotide polymorphisms (SNPs) with a minimum allele frequency lower than 0.05 and heterozygosity higher than 0.6. We restricted the analyses only to SNPs present in all populations, in >60% of individuals in a single population, and in >70% of individuals across all populations. We filtered out variant sites with mean coverage depth lower than 4× and larger than 20×, removed loci with more than 25% of missing data and then imputed population's most frequent known genotype for any remaining missing values. The final

dataset consisted of 39,905 SNPs genotyped across 585 *P. siculus* individuals (Table S5), of which 12,381 were polymorphic in PK and PM populations. For more details see Supplementary Materials and methods.

2.4 | Genomic diversity and differentiation

For analyses of genomic diversity and divergence, we removed from the full genomic dataset loci in linkage disequilibrium (LD, $r^2 < .5$) and out of Hardy–Weinberg equilibrium ($p < .05$), resulting in dataset of 21,074 SNPs (of which 9740 SNPs were polymorphic in Pod Kopište and Pod Mrčaru populations sampled across 3 years). For estimation of genomic diversity indices and effective population size, the dataset was further randomly subsampled to a maximum of 19 samples per population (to account for the effect of sample size). Allelic richness (A_R) and observed and expected heterozygosity (H_o and H_e respectively) were assessed using the R package *diveRsity*, nucleotide diversity (π) was estimated using VCFtools software, and inbreeding coefficient (F_{IS}) using Arlequin software. Effective population size (N_E) for each sampled site was calculated using the LD method with random mating in NeEstimator.

Pair-wise F_{ST} indices were calculated using R package *StAMPP*. Genomic divergence among 14 wild populations and between PK and PM populations sampled across 3 years was further examined using a principal component analysis (PCA) of allele frequencies with the R packages *StAMPP* and *adegenet*. We used Bayesian software fastSTRUCTURE to infer ancestral genomic components in 14 wild populations, as well as in all wild Pod Mrčaru and Pod Kopište individuals and their offspring. Recent migration rates among wild populations were estimated using BayesAss approach in BA3-SNPs software. For more details see Supplementary Materials and methods.

2.5 | Adaptive nature of Pod Mrčaru and Pod Kopište genomic divergence

The main presumption of genome scan methods used to identify loci departing from neutral pattern is that the analysed populations are characterized by mutation-drift equilibrium. However, populations that have undergone a recent bottleneck – such as *P. siculus* population on Pod Mrčaru – usually suffer from nonequilibrium demography. Thus, in order to bypass this concern, we first employed genome scans to pinpoint loci that showed distinct allele patterns in Pod Mrčaru and Pod Kopište populations without directly assessing if these patterns are driven by genetic drift or environmental selection. We used three different methods to identify highly diverged, potential 'outlier' loci: non-hierarchical analysis of joint distribution of F_{ST} and heterozygosity from the software Arlequin; Bayesian F_{ST} outlier test based on Dirichlet-multinomial model for allele frequencies from BayeScan software; and a multivariate analysis of outlier loci with respect to population structure implemented in the R package *PCAdapt*. Using the datasets from three sampling years as biological pseudoreplicates (PKPM2016; PKPM2017; and PKPM2018), we chose the loci that were identified by at least two genome scan methods used in at least two out of three yearly comparisons (Figures S14 and S15). Those loci were named 'PKPM outliers' throughout the manuscript, but by the term outlier we refer here to loci which deviate from general distribution, without assuming their neutrality. We then investigated possible adaptive nature of those loci by examining their representation in loci putatively under selection and/or loci associated with environmental variance across 12 wild *P. siculus* populations (excluding PM and PK), as well as their association with diverged phenotypic traits in PM and PK populations. For more details see Supplementary Materials and methods.

We pinpointed outlier loci putatively under selection in 12 wild *P. siculus* populations using the XtX statistic from the software BayPass (Figure S5). We calibrated the thresholds for the XtX statistic outlier detection using pseudo-observed datasets with 10,000 SNPs and verified similarity among covariance matrices obtained on empirical and simulated datasets using Forstner and Moonen distances (FMD < 1). We further confirmed that covariance matrices obtained from BayPass models manifested high correlation with the matrix of 12 *P. siculus* population pairwise F_{ST} values (Mantel $r = -.93$, $p = .0001$), indicating adequate approximation of population structure. We then explored genotype-environment associations using the auxiliary model implemented in the software BayPass. SNPs considered strongly associated with environmental variation were those with BF values >20 dB (deciban units) (Figure S6). This variation among populations was modelled using scores from the first five principal components in the PCA of eight ecological variables related to climate (mean annual temperature, maximum temperature of the warmest month, minimum temperature of the coldest month, mean annual precipitation, mean annual solar radiation, and mean annual wind speed), ecological isolation (distance to large island), and area of the island (Table S2, Figure S3). The role of the same ecological covariates in the multi-population differentiation was further interrogated by partitioning phenotypic and genomic variance between spatial and ecological components for 14 populations (Figure S4) using a multivariate redundancy analysis (RDA) approach implemented in the R package *vegan*. Geographical variation was modelled using the first two dbMEM vectors obtained from distance-based Moran's eigenvector analysis. Genotype data was expressed as a matrix of population allele frequencies, and for phenotypic response matrix we used scores from the first five principal components from PCA of phenotypic variables.

We used a latent factor mixed models (LFMM) analysis implemented in the R package *lfmm* to explore genotype–phenotype associations (GPA) in our two focal populations phenotyped in 2016. We fitted LFMM models with two latent factors ($K = 2$) and recalibrated the obtained *z*-scores with modified genomic inflation factors to obtain a uniform p-value distribution which is expected under the null-hypothesis (Table S6). Loci showing significant association with analysed phenotypic variables were determined by

a Benjamini-Hochberg procedure on adjusted *p*-values with false discovery rate (FDR)=0.05 (Figures S7–S10). For more details see Supplementary Materials and methods.

2.6 | Crossing experiment in the common garden

In order to assess evolutionary potential in rapidly diverged phenotypic traits connected to head size and shape in our two focal populations, we conducted a 4-year-long crossing experiment in a common garden. We sampled adult *P. siculus* individuals on Pod Mrčaru and Pod Kopište islands in March of 2017 and 2018 and brought them to Zagreb Zoo where we set controlled crossings both within and between ancestral and transplanted population. Parental and juvenile generations were kept and raised in identical conditions and fed on the same cricket-based diet. We obtained extensive data on 7 phenotypic traits of the head and body (Figure 2) by photographing the experimental individuals (68 F0, 85 F1 and 5 backcross) and processing the photographs with image analysis software ImageJ to obtain phenotypic measures of interest using standard geometric morphometry based on landmark data and custom-made scripts in R. The repeatability of the phenotyping across both image analysis and photographing was adequate for all analysed traits (Table S7) and measures obtained using image analysis and traditional calliper-based phenotyping approach were found to be significantly correlated (Table S8). Additionally, we measured bite force in a subset of individuals from the crossing experiment (54 F0 and 75 F1 individuals), using a Kistler force transducer set in a custom-built holder and connected to a Kistler charge amplifier (Herrel et al., 1999). We assessed phenotypic differentiation in the F0 generation and F1 and backcross offspring raised in the common garden using simple t-test and analysis of variance approach in R. To evaluate whether the pattern of phenotypic differentiation in Pod Kopište and Pod Mrčaru persisted in the wild, we graphically compared raw population mean trait values obtained for Pod Mrčaru and Pod Kopište individuals in 2006 and published by Herrel et al. (2008) to those obtained for F0 individuals in our experiment. We further used quantitative genetic analysis of phenotypic traits connected to head size and shape, conducted using Bayesian animal models in *MCMCglmm* R package with group-specific additive genetic variance to assess the additive genetic variance and estimate heritability in our traits of interest. We derived the T^{-1} and D^{-1} components from the Cholesky decomposition of inverse A^{-1} relatedness matrix directly from the pedigree and then scaled them by the respective group-proportions to obtain group-specific A^{-1} relatedness matrices for each genetic group. We also included a matrix with genetic group proportions for each individual (Q) as a fixed effect in the model to account for potential differences in mean breeding values between individuals from different genetic groups (Wolak & Reid, 2017). Heritability (h^2) was calculated from posterior estimates as the ratio of additive genetic variance component to total phenotypic variance. For more details see Supplementary Materials and methods.

3 | RESULTS

3.1 | Genome assembly

We generated a highly contiguous *P. siculus* genome assembly with contig and scaffold N50 of 75.56 Kb and 37.45 Mb, respectively, and 96.43% of base pairs (1.33 Gb) in scaffolds longer than 10 kb (Table S13). Genome quality after filtering showed high completeness with 94.9% complete BUSCOs in the tetrapod database (for more details see Supplementary Materials and methods).

3.2 | The newly established Pod Mrčaru population shows genome-wide differentiation from the ancestral Pod Kopište population and weak genetic erosion

We observed genome-wide divergence of the newly established Pod Mrčaru (PM) population from its ancestral counterpart at Pod

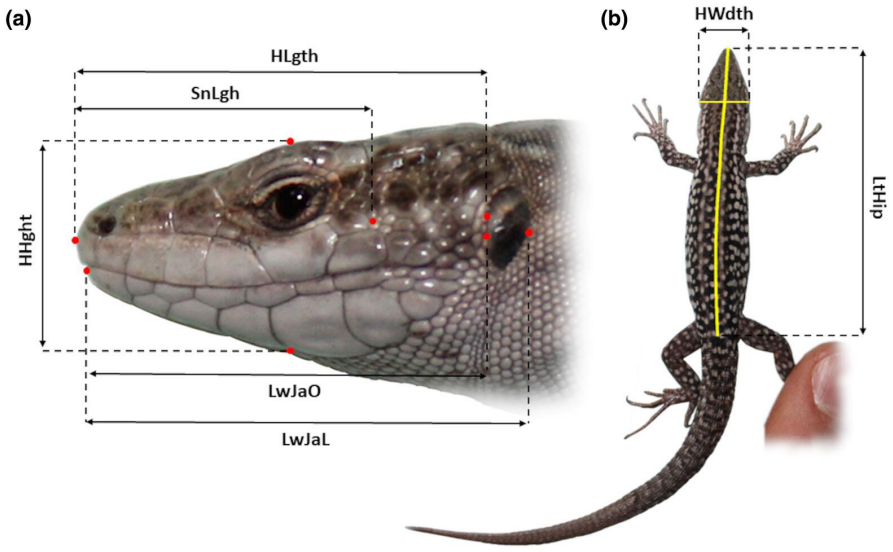

FIGURE 2 Phenotypic measures collected for lizards from the common garden experiment from images of: (a) lateral side of the head (HHgth, head height; HLgth, head length; LwJaL, lower jaw length; LwJaO, lower jaw outlever; SnLgh, snout length) and (b) dorsal side of the body (HWdth, head width; LtHip, length to hip).

Kopište (PK) 45 years after the introduction into the new environment. Principal component analysis (PCA) of allelic frequencies displayed complete separation of PK and PM populations (sampled in three consecutive years) along the first principal component, which explained modest 3.35% of genomic variance (Figure 3a). Genomic differentiation was confirmed by pairwise F_{ST} reaching a value of 0.045 (Table S14). While this is the lowest value recorded for any pairwise comparison of sampled wild populations, it is still comparable to differentiation rate observed between some other long-term isolated insular populations in the area (0.071 and 0.077; pairwise comparison between populations Kopište (KP) and Sušac (SC), and between Kopište (KP) and PK, respectively, Table S14). Furthermore, analysis of individual ancestry based on variational Bayesian inference demonstrated a clear distinction of PK and PM ancestral genomic components in individuals sampled on the islands and intra- and inter-population F1 crosses from the common garden experiment (Figure 3b).

In the multipopulation framework, the common genetic ancestry and low genomic divergence between PK and PM populations became more evident (Figures S11 and S12). We did not detect any signal of recent inter-insular migration in terms of PM individuals showing genomic introgression from PK or any other population. The lack of recent population migration among islands was confirmed by the *BayesAss* analysis, where none of the estimated pairwise population migration values were significantly different from zero (Table S15).

Lower genetic diversity was recorded for populations inhabiting southern islands, including Pod Mrčaru and Pod Kopište (Table S16, Figure 1). In comparison to the ancestral population on Pod Kopište islet, weak genetic erosion in PM population was evident across all three sampling years, with average decrease of 2% in allelic richness, 1% in nucleotide diversity and 8% in observed heterozygosity. Nonetheless, recently founded PM population exhibited higher genetic diversity across all measured indices than the population on islet Bijelac (BJ) in the same archipelago. Neither of the genetic diversity indices correlated with the island area ($p > .05$), and populations on some small islands harboured substantial amount of genetic variation (e.g. Rakita (RK) and Dupinčić (DU), Table S16). Among all populations, PK and PM had the lowest observed (and insignificant) inbreeding coefficients (F_{IS}). PM population exhibited higher number of rare alleles than PK across all three studied years (Figure S13). Effective population size (N_E) of both PK and PM populations varied across the sampling years, but fluctuation was more pronounced in PK population. Estimated N_E values of both populations were in similar range in 2016 and 2017 (220 ± 18.3 to 365.3 ± 40.7 for PK, and 230.3 ± 16.3. to 318.9 ± 4.2 for PM), while in 2018 N_E of PK population increased to 618.6 ± 132.2 (Table S16). Yet, effective population size estimates on the Pod Mrčaru islet were comparable to those recorded on some much larger islands (Kopište (KP) and Sušac (SC), Table S16). Although N_E did not correlate with the area across all populations, it did across 11 islands smaller than 0.08 km^2 (Spearman rank correlation rho = 0.64, $p < .05$). To infer how the obtained effective population size relates to the number of actual contributing parents across our data for PM and PK populations, we further calculated N_E for the F1 crosses and obtained N_E values similar to the known number of parents (F0) (Table S16).

3.3 | Highly diverged loci show a putatively adaptive role

We identified 116 loci for which distinct allelic differentiation was observed between PK and PM populations using three genome scan methods (Figure S16). As the demographic history of the PM population does not imply mutation-drift equilibrium, we could not properly test for deviations from neutrality and parse the effects of genetic drift and putative selection on patterns of per locus genomic divergence. Thus, we refer to those loci as 'PKPM outliers' in the following text. The average F_{ST} value between PM and PK populations for those 116 'outlier' loci was 0.244 across three sampling years, which is notably higher than the genome-wide average of 0.045. None of the loci reached fixation, and there were no private alleles detected in the PM population. We then investigated the possible adaptive role of these 'PKPM outliers' within 12 wild *P. siculus* populations (excluding PM and PK), and their representation among loci associated with diverged phenotypic traits in PM and PK populations.

Across 12 wild *P. siculus* populations (excluding PK and PM populations) 678 out of 39,883 loci were classified as putatively under selection using the BayPass core model, and 592 of them showed signal of directional selection. In the genotype-environment association (GEA) analysis using the genotype dataset for the same 12 populations, 4431 unique loci were found to be associated with principal components of environmental variation (Bayes factor > 20) (Table S17). Overlap between 116 PKPM 'outliers' and those 4431 GEA loci showed that 21.6% (25 out of 116) 'PKPM outliers' were also associated with environmental variation in the independent dataset of 12 other populations (Figure 4). Five 'PKPM outliers' loci were pinpointed as both associated with the environment and as putatively under selection across 12 other *P. siculus* populations (multipopulation outliers, Figure 4).

Genotype–phenotype association (GPA) analysis based on latent factor mixed model resulted in 1075 unique loci associated with male and/or female phenotypic traits in PM and PK populations, including those related to head size and shape (Table S18). Thirty of the 116 'PKPM outliers' (25.86%) were among the loci associated with the phenotype in PK and PM populations (Figure 4). Overall, 51 of 116 'PKPM outliers' (43.97%) were picked up by at least one, and 8 (6.9%) by at least two analytical approaches used to infer their adaptive role. We further found that 17.49% of the loci associated with phenotypic traits in PK and PM populations were also pinpointed as multipopulation outliers or environmentally associated loci in the independent dataset of 12 other *P. siculus* populations (Figure 4). All detected overlaps among 'PKPM outliers', loci found as putatively under selection (multipopulation outliers) or those associated with environmental variation among 12 *P. siculus* populations (GEA), and

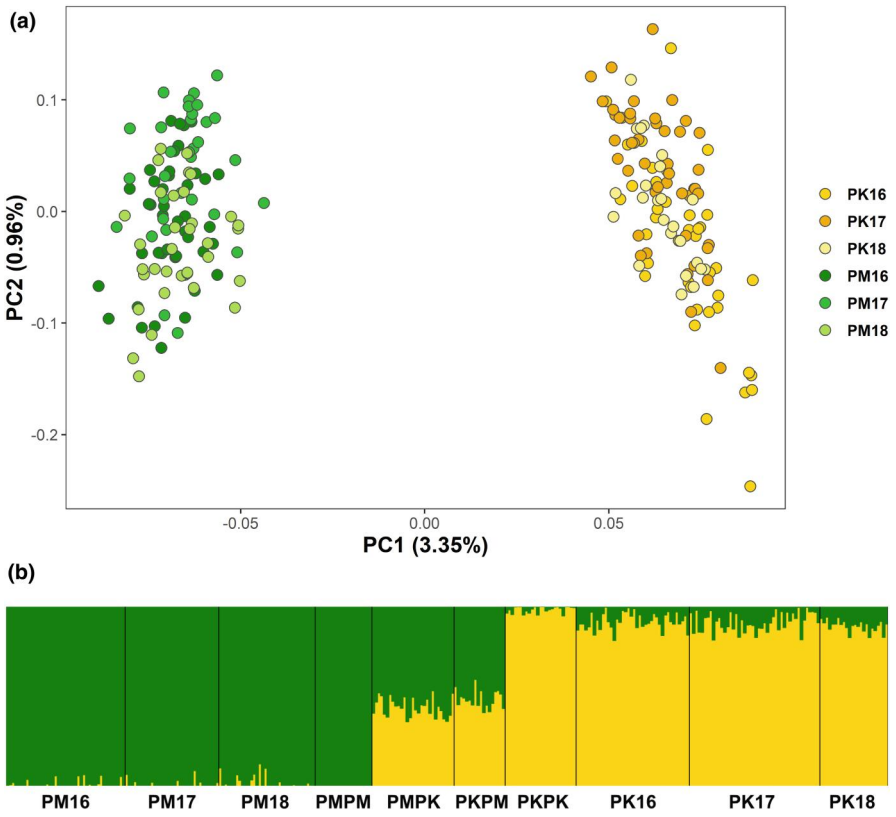

FIGURE 3 Genomic divergence between the ancestral Pod Kopište (PK) and the introduced Pod Mrčaru (PM) population: (a) principal component (PC) analysis of allele frequencies in native PK and PM populations sampled across 3 years (2016, 2017, 2018); (b) Bayesian inference of ancestral genomic components in PK and PM population and intra- (PKPK, PMPM) and inter-population (PKPM, PMPK) F1 crossings, computed with software *fastStructure* ($K=2$).

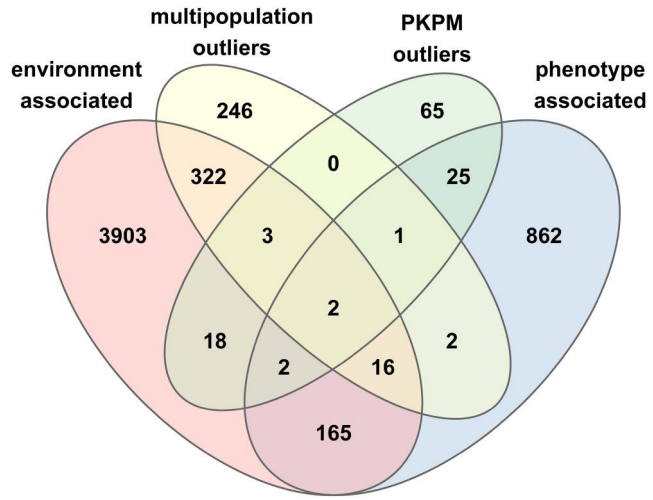

FIGURE 4 Adaptive nature of highly diverged loci between Pod Kopište and Pod Mrčaru populations: overlap of 116 'PKPM outlier' loci with the loci associated with diverged phenotypic traits in Pod Mrčaru and Pod Kopište *P. siculus* populations (phenotype associated), the loci identified as putatively under directional selection (multipopulation outliers) and the loci associated with the environmental variation (environment associated) across independent set of 12 other wild *P. siculus* populations. All pairwise overlaps are significant ($p<.0000001$).

loci associated with PK-PM diverged phenotypic traits (GPA), were higher than could be expected purely by chance ($p<.0000001$).

The role of ecological covariates in multi-population genomic differentiation was confirmed using multivariate redundancy analysis (RDA). Partitioning of genomic variance conducted using all 39,905 polymorphic loci in *P. siculus* dataset revealed that 18.89% of total genomic variance could be explained by ecological factors after controlling for spatial structure, while only 3.94% was explained by geographical distance after controlling for ecological variation among sampling sites (Table S19). The joint influence of ecological and geographical components was high and accounted for 36.21% of total genomic variance, which reflects correlations between spatial and ecological factors. Similarly, ecological factors explained 13.6% of male and 8.29% of female phenotypic variance after accounting for geographic distances, while partial RDA geographic model (after accounting for ecological covariates) explained only 1.73% of variance in males and was insignificant for females (Table S20).

3.4 | Diverged phenotypic traits have moderate heritability, but are plastic in the common garden

The patterns of phenotypic divergence between the ancestral PK and the transplanted PM population observed in 2004–2006 (Herrel et al., 2008) remained stable over the course of 11 years (Figures S17 and S18), with individuals from Pod Mrčaru islet having significantly larger heads and bodies than individuals from Pod Kopište (Figure 5a). Conversely, results of the intra- and inter-population crossing experiment show that this differentiation did not persist in the F1 and backcross offspring raised in the common garden (Figure 5b), indicating that phenotypic differences between PM and PK populations are largely driven by phenotypic plasticity and/or

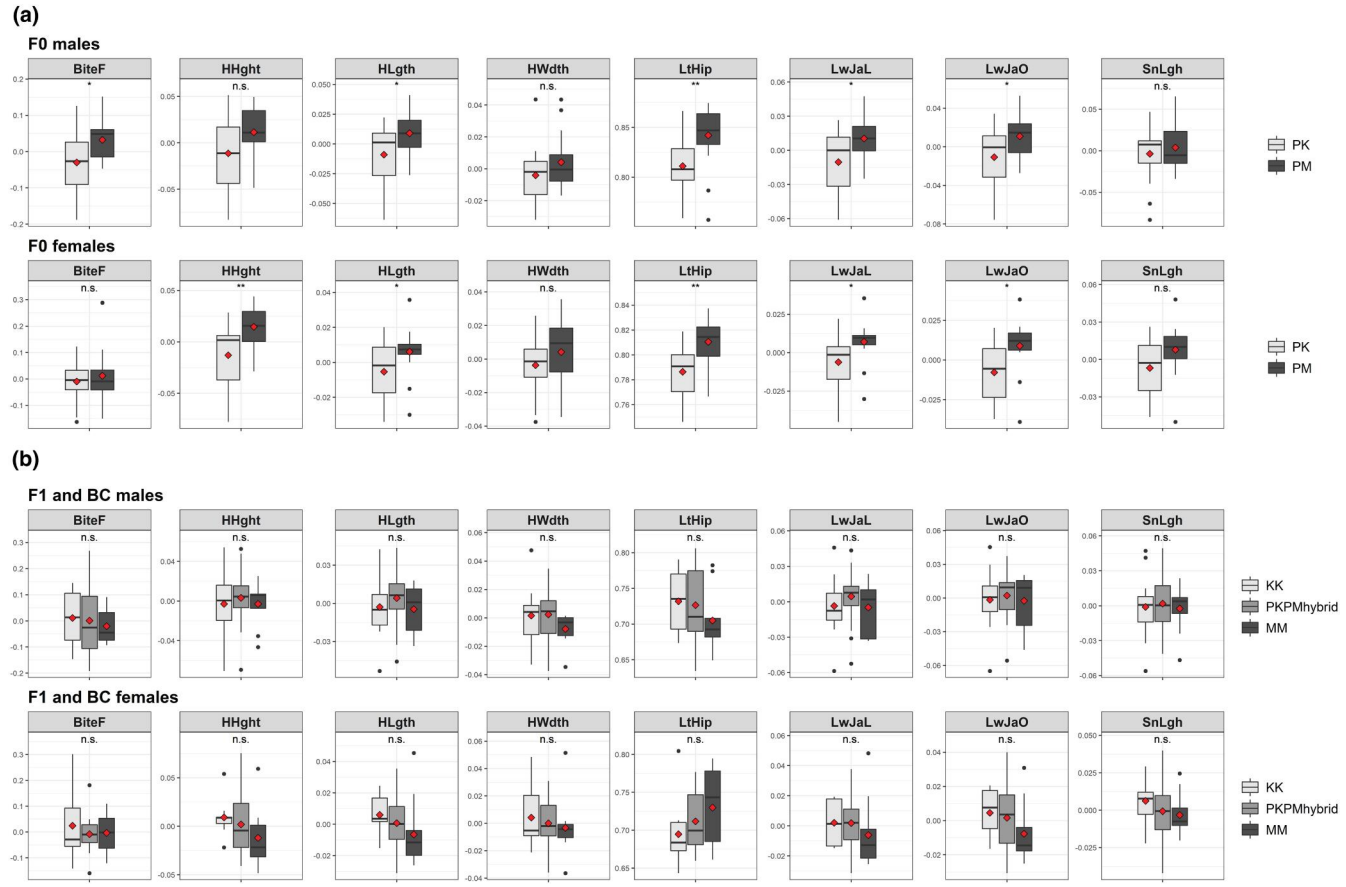

FIGURE 5 Phenotypic trait variability in male and female F0 individuals from Pod Kopište (PK) and Pod Mrčaru (PM), and F1 and BC individuals from common garden crossings: Crosses are denoted as KK = PK♂ + PK♀, MM = PM♂ + PM♀, PKPMhybrid = PK♂ + PM♀ or PM♂ + PK♀. Red rhombus indicates group mean, bold line stands for median, the box represents quartiles and whiskers stand for minimum and maximum recorded values. Pairwise *t*-test or ANOVA significance is indicated above boxplots (**<.01, *<.05, n.s. = not significant). Phenotypic trait codes are defined in Figure 2 and Table S1.

genotype by environment interactions. Nonetheless, quantitative genetic analysis pointed towards moderate heritability of bite force ($h^2 = 0.28$), morphometric traits related to lizard head size and shape ($h^2 = 0.42–0.51$), and body size ($h^2 = 0.35–0.37$) (Table 1). Likewise, the amount of estimated additive genetic variance in Pod Mrčaru and Pod Kopište genetic groups was not significantly different (posterior distribution of differences in variances is practically equivalent to zero), indicating the absence of bottleneck-related genetic erosion of additive genetic variance underlying the divergent traits in the PM population.

4 | DISCUSSION

Systems that are still in the early phases of ecotype formation are particularly well suited to investigate the genomic patterns underlying rapid adaptive evolution (Soria-Carrasco et al., 2014). In this study we leverage the relatively well-known colonization history and ecologically induced phenotypic divergence of *P. siculus* population on the island of Pod Mrčaru to study the evolutionary events driving rapid phenotypic shifts in populations encountering novel isolated environments. Perceiving this case study of contemporary adaptation within the multi-population framework further facilitated the comparison of the evolutionary shift in PM population induced by anthropogenic introduction with demographic and environmentally driven patterns among wild populations.

Genetic diversity of newly founded populations is a major factor contributing to its colonization success and is largely determined by the number of founders, genetic diversity of source population and the subsequent demographic trends (especially changes in population size and migration rates) (Crawford & Whitney, 2010; Forsman, 2014; Szűcs et al., 2017). The observed decrease in genetic diversity of PM population is modest in relation to average values reported for populations invading new habitats (Dlugosch & Parker, 2008). This implies that the founding event did not cause strong genome-wide genetic erosion, despite the very limited number of individuals contributing to the gene pool of the new population. Likewise, these results also suggest that the PM population did not experience any additional major bottlenecks. Various studies on newly founded populations report subsequent inflation of their genetic variance through introgressions or multiple introductions (e.g. Fuller et al., 2020; Kolbe et al., 2004). Our results show no

TABLE 1 Posterior mean estimates of variance components and heritability (h^2) for the two genetic groups (Pod Kopište = PK; Pod Mrčaru = PM).

	BiteF	HHgth	HLgth	HWdth	LwJaL	LwJaO	SnLgh	LtHip
$V_P \times 10^3$ [CI]								
PK	9.16 [6.35–12.41]	1.16 [0.8–1.57]	0.55 [0.38–0.74]	0.5 [0.36–0.67]	0.6 [0.42–0.81]	0.7 [0.49–0.94]	0.78 [0.55–1.05]	1.82 [1.25–2.44]
PM	9.25 [6.11–12.98]	1.04 [0.73–1.38]	0.52 [0.37–0.7]	0.49 [0.34–0.65]	0.58 [0.41–0.77]	0.64 [0.46–0.86]	0.68 [0.48–0.91]	1.9 [1.28–2.6]
$V_E \times 10^3$ [CI]	6.49 [4.19–8.99]	0.6 [0.38–0.83]	0.26 [0.18–0.35]	0.26 [0.17–0.34]	0.3 [0.2–0.41]	0.35 [0.23–0.47]	0.38 [0.25–0.51]	1.17 [0.79–1.57]
$V_A \times 10^3$ [CI]								
PK	2.66 [0.29–5.82]	0.56 [0.19–1.02]	0.29 [0.13–0.48]	0.25 [0.11–0.41]	0.3 [0.13–0.51]	0.35 [0.14–0.6]	0.4 [0.16–0.69]	0.65 [0.17–1.28]
PM	2.75 [0.2–6.57]	0.44 [0.15–0.77]	0.26 [0.12–0.44]	0.24 [0.11–0.4]	0.28 [0.12–0.45]	0.29 [0.12–0.48]	0.3 [0.13–0.51]	0.73 [0.18–1.43]
V_A [CI]								
PK-PM	-9.06e-05 [−0.0049–0.0049]	1.23e-04 [−0.0004–0.00066]	2.6e-05 [−0.00022–0.00028]	9.68e-06 [−0.00022–0.00023]	2.47e-05 [−0.00024–0.0003]	5.78e-05 [−0.00024–0.00038]	1.01e-04 [−0.00023–0.00045]	−7.4e-05 [−0.0011–0.00085]
h^2 [CI]								
PK	0.28 [0.05–0.54]	0.47 [0.24–0.71]	0.51 [0.33–0.71]	0.48 [0.3–0.67]	0.49 [0.29–0.69]	0.49 [0.29–0.7]	0.51 [0.3–0.71]	0.35 [0.13–0.58]
PM	0.28 [0.04–0.56]	0.42 [0.21–0.63]	0.49 [0.31–0.67]	0.47 [0.29–0.66]	0.47 [0.28–0.65]	0.45 [0.27–0.64]	0.44 [0.25–0.63]	0.37 [0.15–0.61]

Note: Total phenotypic variance (V_P) is partitioned into additive genetic (V_A), and environmental or residual (V_E) components. Environmental component estimates are the same for both genetic groups. V_A [CI] PK-PM marks the difference in posterior V_A distribution between genetic groups.

Abbreviations: BiteF, bite force; HHgth, head height; HLgth, head length; HWdth, head width; LtHop, length to hip; LwJaL – lower jaw length; LwJaO – lower jaw out-lever; SnLgh, snout length.

evidence that the gene flow was considerably replenishing the genetic diversity of PM population, as neither the estimates of recent migration rates nor the analyses of ancestral genomic components point to existence of immigrants or PM individuals of mixed ancestry. Nevertheless, *Podarcis* species are known for their propensity to hybridize in both their old and the more recent evolutionary history, and *P. siculus* is no exception (Capula, 2002; Gaczorek et al., 2023; Yang et al., 2021). Thus, due to our limited genomic insights, we cannot completely rule out the possibility of hybridization between the newly translocated *P. siculus* and native *P. melisellensis* populations in the short time of their coexistence on Pod Mrčaru island, but we consider this event to be unlikely.

The lack of correlation between genetic diversity indices and island area, along with ample amount of standing genomic variation observed in some populations on small islands, suggests that genetic diversity of insular *P. siculus* is less defined by the island size than by source population and prior evolutionary and demographic processes. Although the number of founders on Pod Mrčaru islet was particularly small – only 10 *P. siculus* individuals (Gorman et al., 1972), field surveys suggested higher population density of *P. siculus* on Pod Mrčaru than on Pod Kopište (Herrel et al., 2008; Vervust et al., 2009). In line with those observations on census population size, we obtained similar estimates of N_E on Pod Kopište as on the ~ three times smaller Pod Mrčaru islet. On the other hand (and unlike genetic diversity), effective population size was found to be limited by small islands area across multiple populations. This result suggests that the current PM population is relatively large and with high fitness. Comparatively large population size, modest loss of genetic variation, and swift competitive success, all point to rapid initial population growth of PM population after the founding event. It has been suggested that a fast increase in population size has a potential to limit the amount of genomic variation lost during a bottleneck (Allendorf, 1986; Kirkpatrick & Jarne, 2000; Murphy et al., 2015). A recent population expansion could also have led to an excess of rare variants (Keinan & Clark, 2012; Maruyama & Fuerst, 1985). This might likewise be an underlying cause of the smaller decrease in allelic richness than in heterozygosity observed in PM population, which deviates from common expectations of bottleneck effects on genetic diversity (Nei et al., 1975). Relatively high amount of retained genetic variance could be additionally driven by other subtle evolutionary mechanisms, such as associative overdominance that may promote the maintenance of neutral genetic variation in small populations experiencing bottleneck (Schou et al., 2017).

In <25 generations, the introduced PM population has diverged at the genome-wide level from the source population, reaching >60% of the differentiation observed between the long-term isolated insular populations on Pod Kopište and Kopište (the next closest island inhabited by *P. siculus*). While the widespread genomic divergence is consistent with the neutral expectation of genetic drift propelled by a small number of founders and lack of gene flow (Sendell-Price et al., 2021), both drift and selection are expected to contribute not only to genomic but also to phenotypic differentiation of small populations invading different habitats (Colautti & Lau, 2015; Keller &

Taylor, 2008; Kolbe et al., 2012). Even the good alignment between the phenotypic change detected in the PM population and the observed ecological shift of lizards on Pod Mrčaru (Herrel et al., 2008) cannot completely exclude the possible role of phenotypic drift, nor allow us to discriminate between adaptive genetic evolution and adaptive phenotypic plasticity.

Considering that none of the methods utilized to pinpoint 'PKPM outlier' loci was specifically designed to account for non-equilibrium conditions involved in the translocation experiment and bottleneck that PM population experienced at the time of its introduction (Excoffier et al., 2009; Foll & Gaggiotti, 2008), their putatively adaptive nature was inferred indirectly. Nonetheless, complementary insights into substantial number of 'PKPM outlier' loci being associated with ecologically pertinent diverged traits and found relevant for adaptive evolution across multiple populations indicate adaptive nature of their differentiation. Given that our methodology offers only limited and partial insights across the genome, it is impossible to infer if any of the adaptive signals stem from direct selective pressures on investigated loci, or whether those loci only reflect adaptive genomic responses in linked genomic regions through the hitchhiking effect (Nosil et al., 2009). Additionally, a large proportion of loci with above-average PK-PM F_{ST} values showing generally neutral patterns of allelic frequency change are also indicative of genetic drift contributing to genome-wide population divergence.

Our results support the arguments for partial genetic basis of the studied phenotypic traits. Moreover, they point to an evolutionary parallelism in genetic basis of adaptation in the introduced and wild populations and are thus unlikely to reflect merely stochastic genetic drift. Considerable environmental impact on phenotypic and genomic divergence across populations was additionally implied by ecology having higher explanatory power than geographic distances in RDA analyses. However, in such studies it is difficult to pinpoint the association between specific phenotypic traits and specific environmental factors. Firstly, the signal of ecological impact on populations' phenotypic (and genotypic) divergence might stem as well from natural selection on other, likely correlated, yet unanalysed phenotypic traits. Furthermore, the variances in climate factors, island area, and ecological isolation, utilized in genotype-environment association analysis, are not only expected to exert selective pressures on populations directly, but also through considerable modulation of biotic components of insular ecosystems (Mueller-Dombois, 1992; Novosolov et al., 2016; Veron et al., 2019), and thus the effects of unmeasured cofounding abiotic variables may be at play. Lizards translocated on Pod Mrčaru encountered an ecologically distinct habitat with a different vegetational composition and somewhat different prey availability. The vegetational cover is expected to influence microclimatic conditions, temperature, solar exposure, wind exposure, moist availability, but also shelter availability and predator exposure, prey variance and abundance, basking opportunities, etc. Among the employed environmental covariates, temperature has a particularly important influence on biology and life history of *P. siculus* (Senczuk et al., 2017) and is known to drive the thermal ecology of *Podarcis* lizards on small islands (Pafilis et al., 2019). Even though effective thermoregulation is achieved along *P. siculus* colonization range (Burke & Ner, 2005; Kapsalas et al., 2016), lizard thermoregulatory behaviour and performance can as well be the subject of natural selection (Logan et al., 2018).

Genome-wide distribution and number of loci associated with phenotypic variation or having putatively adaptive role in the novel lizard population on Pod Mrčaru are indicative of polygenic selection affecting allele frequency distribution across multiple loci underlying adaptive quantitative traits (Fuller et al., 2020; Perreault-Payette et al., 2017; Rellstab et al., 2015). These results are congruent with the scenario of adaptation from standing genetic variation, which is considered to be faster than adaptation from de novo mutations and more likely to ensue in early stages of population establishment (Barrett & Schluter, 2008; Crisci et al., 2016). Nevertheless, our reduced genomic approach did not allow to completely exclude the potential role of novel mutations.

The results of the common garden experiment point to moderate heritability of bite force and phenotypic traits related to head size and shape in lizards from Pod Mrčaru and Pod Kopište, confirming those traits show enough additive genetic variance to evolve under selection in both populations. This is in agreement with our recent work showing that not only intra- but also inter-specific patterns of head size and shape in insular *Podarcis* lizards are driven by variation in ecological conditions, and thus widely subjected to natural selection (Taverne et al., 2019). Moreover, no significant erosion of additive genetic component was observed in PM population. Both theory and experimental findings support that additive genetic variation for ecologically important traits does not necessarily follow a decrease in neutral genetic diversity in populations that have undergone bottleneck (Estoup et al., 2016), and can even increase if nonadditive genetic variance translates into additive, for example, due to epistasis or dominance (Santos et al., 2012; Van Buskirk & Willi, 2006). Additionally, head shape and size are considered to be under sexual selection in *P. siculus* (Taverne et al., 2020), which may further support the maintenance of genetic variance underlying those traits (Radwan et al., 2016).

Heritable nature of differentiated traits coupled with adaptive role of diverged loci is indicative of rapid evolutionary response to new ecological conditions encountered on Pod Mrčaru. Conversely, the crossing experiment revealed a lack of persistence of differences between populations in F1 generation, which confirms the ongoing plasticity of focal traits in PM population. However, heritability and plasticity are not necessarily mutually exclusive, and variance in most traits is the additive result of the combined effect of genetics and environment on the phenotype (Visscher et al., 2008). The lack of difference among phenotypic distributions in offspring groups raised in the common garden environment indicates that the part of variance which is evident as population phenotypic divergence is governed mainly by plasticity. The estimated heritability thus refers only to the part of the phenotypic variance among individuals that is explained by the genetic component (note that the traits are still variable in the common garden). Overall, our results indicate the alignment of genetic and plastic mechanisms across phenotypic

responses to ecological change. At this point we were unable to specifically test two important evolutionary questions: whether there are also genotype by environment interactions at play, and to what extent is such plastic response a feature of the ancestral PK population. Our study system could provide an opportunity to test for the plasticity-first hypothesis (Noble et al., 2019), but would demand another, up to 4 years long, reciprocal crossing experiments in quite challenging experimental conditions with lizards fed an omnivorous diet (with the plant material preferably resembling the one encountered on Pod Mrčaru islet). The epigenomic aspects of PM population differentiation also need to be addressed in future research – epigenomic responses are recognized as important driver of invasion success, can facilitate environmentally induced plastic effects or inflate genetic variation through modulations of transposons activity (Herrel et al., 2020; Marin et al., 2020; Pimpinelli & Piacentini, 2020). Regardless of the exact underlying mechanism, stability of phenotypic divergence between PK and PM population over the course of more than a decade suggests continuous environmental reinforcement. In the initial stage of the founder population settlement on Pod Mrčaru, plasticity could have boosted survival and population growth, at the same time empowering the competitive success of *P. siculus* over *P. melisellensis* through the exploration of alternative trophic resources. Our insights into concurrent plastic and genetic adaptive processes are in line with recent observations of early evolution in lizard cryptic coloration initiated by phenotypic plasticity and accompanied by genomic adaptation (Corl et al., 2018). Such plastic responses, well-adjusted to environmental challenge, have the potential to uncover previously hidden genetic variance and jump-start genomic adaptation (Noble et al., 2019). Studying this remarkable system in its evolutionary infancy demonstrates that additive genetic variance is not necessarily diminished in a population established by a small number of founders and further advances our understanding of intertwined plastic and genetic mechanisms underlying the successful colonization of novel habitats.

AUTHOR CONTRIBUTIONS

AŠ, AH and JS designed the research, AH, AŠ, DL, IS, ÓM and MG collected phenotypic data and samples on the field, ÓM, AŠ, DL, IS, IC and MG performed the crossing garden experiment and phenotyping, TH performed and analysed vegetational and floristic survey, AH performed survey on prey availability, ÓM and IS analysed phenotypic data and IS analysed heritability estimates. DYCB and RN assembled the genome, IS, ÓM, AŠ, MN, and RB performed population genomic analyses. AŠ, IS, AH, ÓM, JS, MEA, MT and MN interpreted the data, AŠ, IS and DYCB drafted the manuscript, and AH, JS, ÓM, MT, MN and MEA revised the draft.

ACKNOWLEDGEMENTS

We acknowledge the full on-site support by staff at the Nature Park Lastovo Islands, and dr. Anne-Claire Fabre, dr. Chloé Vigliotti, Nina King-Gillies, Maria Krajnović, Tomislav Gojak, Noa Dorotić Štambuk and Tonka Dorotić Štambuk for help with the fieldwork. We thank Ema Stanić, Luka Lelas, Mario Djura, Petra Baček, Mislav Orešković, Lucija Librenjak, Ana Dudas, Maja Kovačević, Paula Šašić, Mislav Brajković, Filip Sakoman and Lara Šafar-Godinić for help with common-garden crossing experiment and phenotyping of experimental individuals. We are appreciative of the inspiring discussions with dr. Patrik Nosil in all phases of our work on this system. The population genomic part of the research was performed using the resources of computer cluster Isabella based in SRCE – University of Zagreb University Computing Centre.

FUNDING INFORMATION

This research was funded by: Croatian Science Foundation grant HRZZ-IP-06-2016-9177 (AŠ, OM), National Geographic explorer grant – National Geographic Committee for Research and Exploration (AH), and 'Young researchers' career development project – training of doctoral students' DOK-2018-01-8879 of the Croatian Science Foundation funded by the European Union from the European Social Fund (IS).

CONFLICT OF INTEREST STATEMENT

The authors declare no competing interests.

DATA AVAILABILITY STATEMENT

All data needed to evaluate the conclusions in the paper are present in the paper and/or the Supporting Information. Individual genotypic and phenotypic data are available on DataDryad (https://doi.org/10.5061/dryad.zkh1893gh). Raw sequence reads are deposited in the SRA (BioProject PRJNA1032101). The assembly genome is stored in GenBank database (accession no. JAXCMG000000000, BioProject PRJNA1032059). Custom-made scripts are uploaded on Github (https://github.com/Stambuk-lab/Sabolic_et_al_2023).

ORCID

Anamaria Štambuk https://orcid.org/0000-0002-3177-7694

REFERENCES

Allendorf, F. W. (1986). Genetic drift and the loss of alleles versus heterozygosity. *Zoo Biology*, *5*(2), 181–190. https://doi.org/10.1002/zoo.1430050212

Allendorf, F. W., Luikart, G., & Aitken, S. N. (2013). *Conservation and the genetics of populations* (2nd ed.). Wiley-Blackwell.

Aubret, F., & Shine, R. (2009). Genetic assimilation and the postcolonization erosion of phenotypic plasticity in Island tiger snakes. *Current Biology*, *19*(22), 1932–1936. https://doi.org/10.1016/j.cub.2009.09.061

Barrett, R. D. H., & Schluter, D. (2008). Adaptation from standing genetic variation. *Trends in Ecology & Evolution*, *23*(1), 38–44. https://doi.org/10.1016/j.tree.2007.09.008

Burke, R. L., & Ner, S. E. (2005). Seasonal and diel activity patterns of Italian wall lizards, *Podarcis sicula campestris*, in New York. *Northeastern Naturalist*, *12*(3), 349–360. https://doi.org/10.1656/1092-6194(2005)012[0349:SADAPO]2.0.CO;2

Capula, M. (2002). Genetic evidence of natural hybridization between *Podarcis sicula* and *Podarcis tiliguerta* (Reptilia: Lacertidae). *Amphibia-Reptilia*, *23*(3), 313–321. https://doi.org/10.1163/15685380260449199

Carroll, S. P., Hendry, A. P., Reznick, D. N., & Fox, C. W. (2007). Evolution on ecological time-scales. *Functional Ecology*, *21*(3), 387–393. https://doi.org/10.1111/j.1365-2435.2007.01289.x

Cattau, C. E., Fletcher, R. J., Jr., Kimball, R. T., Miller, C. W., & Kitchens, W. M. (2018). Rapid morphological change of a top predator with the invasion of a novel prey. *Nature Ecology & Evolution*, *2*, 108–115. https://doi.org/10.1038/s41559-017-0378-1

Colautti, R. I., & Lau, J. A. (2015). Contemporary evolution during invasion: Evidence for differentiation, natural selection, and local adaptation. *Molecular Ecology*, *24*(9), 1999–2017. https://doi.org/10.1111/mec.13162

Corl, A., Bi, K., Luke, C., Challa, A. S., Stern, A. J., Sinervo, B., & Nielsen, R. (2018). The genetic basis of adaptation following plastic changes in coloration in a novel environment. *Current Biology*, *28*(18), 2970–2977. https://doi.org/10.1016/j.cub.2018.06.075

Crawford, K. M., & Whitney, K. D. (2010). Population genetic diversity influences colonization success. *Molecular Ecology*, *19*(6), 1253–1263. https://doi.org/10.1111/j.1365-294X.2010.04550.x

Crisci, J. L., Dean, M. D., & Ralph, P. (2016). Adaptation in isolated populations: When does it happen and when can we tell? *Molecular Ecology*, *25*(16), 3901–3911. https://doi.org/10.1111/mec.13729

D'Amico, M., Bastianelli, G., Faraone, F. P., & Lo Valvo, M. (2018). The spreading of the invasive Italian wall lizard on Vulcano, the last Island inhabited by the critically endangered Aeolian wall lizard. *Herpetological Conservation and Biology*, *13*(1), 146–157.

De Villemereuil, P., Gaggiotti, O. E., Mouterde, M., & Till-Bottraud, I. (2015). Common garden experiments in the genomic era: New perspectives and opportunities. *Heredity*, *116*, 249–254. https://doi.org/10.1038/hdy.2015.93

Dlugosch, K. M., & Parker, I. M. (2008). Founding events in species invasions: Genetic variation, adaptive evolution, and the role of multiple introductions. *Molecular Ecology*, *17*(1), 431–449. https://doi.org/10.1111/j.1365-294X.2007.03538.x

Endler, J. A. (1986). *Natural selection in the wild* (1st ed.). Princeton University Press.

Estoup, A., Ravigné, V., Hufbauer, R., Vitalis, R., Gautier, M., & Facon, B. (2016). Is there a genetic paradox of biological invasion? *Annual Review of Ecology, Evolution, and Systematics*, *47*(August 2016), 51–72. https://doi.org/10.1146/annurev-ecolsys-121415-032116

Excoffier, L., Hofer, T., & Foll, M. (2009). Detecting loci under selection in a hierarchically structured population. *Heredity*, *103*(4), 285–298. https://doi.org/10.1038/hdy.2009.74

Falconer, D. S., & Mackay, T. F. C. (1996). *Introduction to quantitative genetic. Longmans Green, Harlow, Essex, UK* (4th ed.). Longman.

Feiner, N., Stanley, E. L., Uller, T., Jackson, I. S. C., Stanley, E. L., & Uller, T. (2021). Evolution of the locomotor skeleton in *Anolis* lizards reflects the interplay between ecological. *Nature Communications*, *12*(1), 1–10. https://doi.org/10.1038/s41467-021-21757-5

Foll, M., & Gaggiotti, O. (2008). A genome-scan method to identify selected loci appropriate for both dominant and codominant markers: a Bayesian perspective. *Genetics*, *180*(2), 977–993. https://doi.org/10.1534/genetics.108.092221

Forsman, A. (2014). Effects of genotypic and phenotypic variation on establishment are important for conservation, invasion, and infection biology. *Proceedings of the National Academy of Sciences of the United States of America*, *111*(1), 302–307. https://doi.org/10.1073/pnas.1317745111

Fuller, J., Ferchaud, A. L., Laporte, M., Le Luyer, J., Davis, T. B., Côté, S. D., & Bernatchez, L. (2020). Absence of founder effect and evidence for adaptive divergence in a recently introduced insular population of white-tailed deer (*Odocoileus virginianus*). *Molecular Ecology*, *29*(1), 86–104. https://doi.org/10.1111/mec.15317

Gaczorek, T. S., Chechetkin, M., Dudek, K., Caeiro-Dias, G., Crochet, P. A., Geniez, P., Pinho, C., & Babik, W. (2023). Widespread introgression of MHC genes in Iberian *Podarcis* lizards. *Molecular Ecology*, *32*(14), 1–15. https://doi.org/10.1111/mec.16974

Ghalambor, C. K., McKay, J. K., Carroll, S. P., & Reznick, D. N. (2007). Adaptive versus non-adaptive phenotypic plasticity and the potential for contemporary adaptation in new environments. *Functional Ecology*, *21*(3), 394–407. https://doi.org/10.1111/j.1365-2435.2007.01283.x

Gienapp, P., Fior, S., Guillaume, F., Lasky, J. R., Sork, V. L., & Csilléry, K. (2017). Genomic quantitative genetics to study evolution in the wild. *Trends in Ecology & Evolution*, *32*(12), 897–908. https://doi.org/10.1016/j.tree.2017.09.004

Gorman, G., Clover, R., Nevo, E., Gorman, G., Soulé, M., Yang, S. Y., Clover, R., & Jovanović, V. (1972). Competitive exclusion between insular *Lacerta* species (Sauria, Lacertidae) – Notes on experimental introductions. *Oecologia*, *10*(2), 183–190. https://doi.org/10.1007/BF00347990

Hendry, A. (2013). Key questions in the genetics and genomics of eco-evolutionary dynamics. *Heredity*, *111*(6), 456–466. https://doi.org/10.1038/hdy.2013.75

Herrel, A. (2007). Herbivory and foraging mode in lizards. In S. M. Reilly, L. D. McBrayer, & D. B. Miles (Eds.), *Lizard ecology: The evolutionary consequences of foraging mode* (pp. 209–236). Cambridge University Press. https://doi.org/10.1017/CBO9780511752438.009

Herrel, A., Huyghe, K., Vanhooydonck, B., Backeljau, T., Breugelmans, K., Grbac, I., Damme, R. V., & Irschick, D. J. (2008). Rapid large-scale evolutionary divergence in morphology and performance associated with exploitation of a different dietary resource. *Proceedings of the National Academy of Sciences of the United States of America*, *105*(12), 4792–4795. https://doi.org/10.1073/pnas.0711998105

Herrel, A., Joly, D., & Danchin, E. (2020). Epigenetics in ecology and evolution. *Functional Ecology*, *34*(2), 381–384. https://doi.org/10.1111/1365-2435.13494

Herrel, A., Spithoven, L., Van Damme, R., & De Vree, F. (1999). Sexual dimorphism of head size in *Gallotia galloti*: Testing the niche divergence hypothesis by functional analyses. *Functional Ecology*, *13*(3), 289–297. https://doi.org/10.1046/j.1365-2435.1999.00305.x

Herrel, A., Vanhooydonck, B., & Van Damme, R. (2004). Omnivory in lacertid lizards: Adaptive evolution or constraint? *Journal of Evolutionary Biology*, *17*(5), 974–984. https://doi.org/10.1111/j.1420-9101.2004.00758.x

Hoffmann, A. A., Sgrò, C. M., & Kristensen, T. N. (2017). Revisiting adaptive potential, population size, and conservation. *Trends in Ecology & Evolution*, *32*(7), 506–517. https://doi.org/10.1016/j.tree.2017.03.012

Kapsalas, G., Gavriilidi, I., Adamopoulou, C., Foufopoulos, J., & Pafilis, P. (2016). Effective thermoregulation in a newly established population of *Podarcis siculus* in Greece: A possible advantage for a successful invader. *Acta Herpetologica*, *11*(2), 111–118. https://doi.org/10.13128/Acta_Herpetol-18075

Keinan, A., & Clark, A. G. (2012). Recent explosive human population growth has resulted in an excess of rare genetic variants. *Science*, *336*, 740–743. https://doi.org/10.1126/science.1217283

Keller, S. R., & Taylor, D. R. (2008). History, chance and adaptation during biological invasion: Separating stochastic phenotypic evolution from response to selection. *Ecology Letters*, *11*(8), 852–866. https://doi.org/10.1111/j.1461-0248.2008.01188.x

Kirkpatrick, M., & Jarne, P. (2000). The effects of a bottleneck on inbreeding depression and the genetic load. *American Naturalist*, *155*(2), 154–167. https://doi.org/10.1086/303312

Kolbe, J. J., Glor, R. E., Rodríguez Schettino, L., Lara, A. C., Larson, A., & Losos, J. B. (2004). Genetic variation increases during biological invasion by a Cuban lizard. *Nature*, *431*(7005), 177–181. https://doi.org/10.1038/nature02807

Kolbe, J. J., Leal, M., Schoener, T. W., Spiller, D. A., & Losos, J. B. (2012). Founder effects persist despite adaptive differentiation: A field

experiment with lizards. *Science*, *335*(6072), 1086–1089. https://doi.org/10.1126/science.1209566

Lande, R. (2009). Adaptation to an extraordinary environment by evolution of phenotypic plasticity and genetic assimilation. *Journal of Evolutionary Biology*, *22*(7), 1435–1446. https://doi.org/10.1111/j.1420-9101.2009.01754.x

Lande, R. (2015). Evolution of phenotypic plasticity in colonizing species. *Molecular Ecology*, *24*(9), 2038–2045. https://doi.org/10.1111/mec.13037

Levis, N. A., Isdaner, A. J., & Pfennig, D. W. (2018). Morphological novelty emerges from pre-existing phenotypic plasticity. *Nature Ecology & Evolution*, *2*(8), 1289–1297. https://doi.org/10.1038/s41559-018-0601-8

Logan, M. L., Curlis, J. D., Gilbert, A. L., Miles, D. B., Chung, A. K., McGlothlin, J. W., & Cox, R. M. (2018). Thermal physiology and thermoregulatory behaviour exhibit low heritability despite genetic divergence between lizard populations. *Proceedings of the Royal Society B: Biological Sciences*, *285*(1878), 20180697. https://doi.org/10.1098/rspb.2018.0697

Marin, P., Genitoni, J., Barloy, D., Maury, S., Gibert, P., Ghalambor, C. K., & Vieira, C. (2020). Biological invasion: The influence of the hidden side of the (epi)genome. *Functional Ecology*, *34*(2), 385–400. https://doi.org/10.1111/1365-2435.13317

Marques, D. A., Jones, F. C., Di Palma, F., Kingsley, D. M., & Reimchen, T. E. (2018). Adaptation to a new niche in an adaptive radiation. *Nature Ecology & Evolution*, *2*, 1128–1138. https://doi.org/10.1038/s41559-018-0581-8

Maruyama, T., & Fuerst, P. A. (1985). Population bottlenecks and nonequilibrium models in population genetics. II. Number of alleles in a small population that was formed by a recent bottleneck. *Genetics*, *111*(3), 675–689. https://doi.org/10.1093/genetics/111.3.675

Mayr, E., & Provine, W. B. (1980). *The evolutionary synthesis: Perspectives on the unification of biology* (1st ed.). Harvard University Press. https://doi.org/10.2307/2408142

Moran, E. V., & Alexander, J. M. (2014). Evolutionary responses to global change: Lessons from invasive species. *Ecology Letters*, *17*(5), 637–649. https://doi.org/10.1111/ele.12262

Mueller-Dombois, D. (1992). The formation of Island ecosystems. *GeoJournal*, *28*(2), 293–296. https://doi.org/10.1007/BF00177244

Murphy, S. M., Cox, J. J., Clark, J. D., Augustine, B. C., Hast, J. T., Gibbs, D., Strunk, M., & Dobey, S. (2015). Rapid growth and genetic diversity retention in an isolated reintroduced black bear population in the Central Appalachians. *Journal of Wildlife Management*, *79*(5), 807–818. https://doi.org/10.1002/jwmg.886

Nei, M., Maruyama, T., & Chakraborty, R. (1975). The bottleneck effect and genetic variability in populations. *Evolution*, *29*(1), 1. https://doi.org/10.2307/2407137

Noble, D. W. A., Radersma, R., & Uller, T. (2019). Plastic responses to novel environments are biased towards phenotype dimensions with high additive genetic variation. *Proceedings of the National Academy of Sciences of the United States of America*, *116*(27), 13452–13461. https://doi.org/10.1073/pnas.1821066116

Nosil, P., Funk, D. J., & Ortiz-Barrientos, D. (2009). Divergent selection and heterogeneous genomic divergence. *Molecular Ecology*, *18*(3), 375–402. https://doi.org/10.1111/j.1365-294X.2008.03946.x

Novosolov, M., Rodda, G. H., Feldman, A., Kadison, A. E., Dor, R., & Meiri, S. (2016). Power in numbers. Drivers of high population density in insular lizards. *Global Ecology and Biogeography*, *25*(1), 87–95. https://doi.org/10.1111/geb.12390

Oostra, V., Saastamoinen, M., Zwaan, B. J., & Wheat, C. W. (2018). Strong phenotypic plasticity limits potential for evolutionary responses to climate change. *Nature Communications*, *9*(1), 1005. https://doi.org/10.1038/s41467-018-03384-9

Pafilis, P., Herrel, A., Kapsalas, G., Vasilopoulou-Kampitsi, M., Fabre, A. C., Foufopoulos, J., & Donihue, C. M. (2019). Habitat shapes the thermoregulation of Mediterranean lizards introduced to replicate experimental islets. *Journal of Thermal Biology*, *84*(July), 368–374. https://doi.org/10.1016/j.jtherbio.2019.07.032

Pardo-Diaz, C., Salazar, C., & Jiggins, C. D. (2015). Towards the identification of the loci of adaptive evolution. *Methods in Ecology and Evolution*, *6*(4), 445–464. https://doi.org/10.1111/2041-210X.12324

Perreault-Payette, A., Muir, A. M., Goetz, F., Perrier, C., Normandeau, E., Sirois, P., & Bernatchez, L. (2017). Investigating the extent of parallelism in morphological and genomic divergence among lake trout ecotypes in Lake Superior. *Molecular Ecology*, *26*(6), 1477–1497. https://doi.org/10.1111/mec.14018

Pimpinelli, S., & Piacentini, L. (2020). Environmental change and the evolution of genomes: Transposable elements as translators of phenotypic plasticity into genotypic variability. *Functional Ecology*, *34*(2), 428–441. https://doi.org/10.1111/1365-2435.13497

Pritchard, J. K., & Di Rienzo, A. (2010). Adaptation – Not by sweeps alone. *Nature Reviews Genetics*, *11*(10), 665–667. https://doi.org/10.1038/nrg2880

Putman, B. J., Pauly, G. B., & Blumstein, D. T. (2020). Urban invaders are not bold risk-takers: A study of three invasive lizards in Southern California. *Current Zoology*, *66*(6), 657–665. https://doi.org/10.1093/cz/zoaa015

Radersma, R., Noble, D. W. A., & Uller, T. (2020). Plasticity leaves a phenotypic signature during local adaptation. *Evolution Letters*, *4*(4), 360–370. https://doi.org/10.1002/evl3.185

Radwan, J., Engqvist, L., & Reinhold, K. (2016). A paradox of genetic variance in epigamic traits: Beyond "good genes" view of sexual selection. *Evolutionary Biology*, *43*(2), 267–275. https://doi.org/10.1007/s11692-015-9359-y

Rellstab, C., Gugerli, F., Eckert, A. J., Hancock, A. M., & Holderegger, R. (2015). A practical guide to environmental association analysis in landscape genomics. *Molecular Ecology*, *24*(17), 4348–4370. https://doi.org/10.1111/mec.13322

Roman, J., & Darling, J. A. (2007). Paradox lost: Genetic diversity and the success of aquatic invasions. *Trends in Ecology & Evolution*, *22*(9), 454–464. https://doi.org/10.1016/j.tree.2007.07.002

Santos, J., Pascual, M., Simões, P., Fragata, I., Lima, M., Kellen, B., Santos, M., Marques, A., Rose, M. R., & Matos, M. (2012). From nature to the laboratory: The impact of founder effects on adaptation. *Journal of Evolutionary Biology*, *25*(12), 2607–2622. https://doi.org/10.1111/jeb.12008

Schlötterer, C., Kofler, R., Versace, E., Tobler, R., & Franssen, S. U. (2015). Combining experimental evolution with next-generation sequencing: A powerful tool to study adaptation from standing genetic variation. *Heredity*, *114*(5), 431–440. https://doi.org/10.1038/hdy.2014.86

Schou, M. F., Loeschcke, V., Bechsgaard, J., Schlötterer, C., & Kristensen, T. N. (2017). Unexpected high genetic diversity in small populations suggests maintenance by associative overdominance. *Molecular Ecology*, *26*(23), 6510–6523. https://doi.org/10.1111/mec.14262

Senczuk, G., Colangelo, P., De Simone, E., Aloise, G., Castiglia, R., De Simone, E., Aloise, G., & Castiglia, R. (2017). A combination of long term fragmentation and glacial persistence drove the evolutionary history of the Italian wall lizard *Podarcis siculus*. *BMC Evolutionary Biology*, *17*(1), 1–15. https://doi.org/10.1186/s12862-016-0847-1

Sendell-Price, A. T., Ruegg, K. C., Robertson, B. C., & Clegg, S. M. (2021). An Island-hopping bird reveals how founder events shape genome-wide divergence. *Molecular Ecology*, *30*(11), 2495–2510. https://doi.org/10.1111/mec.15898

Soria-Carrasco, V., Gompert, Z., Comeault, A. A., Farkas, T. E., Parchman, T. L., Johnston, J. S., Buerkle, C. A., Feder, J. L., Bast, J., Schwander, T., Egan, S. P., Crespi, B. J., & Nosil, P. (2014). Stick insect genomes reveal natural selection's role in parallel speciation. *Science*, *344*(6185), 738–742. https://doi.org/10.1126/science.1252136

Stuart, Y. E., Campbell, T. S., Hohenlohe, P. A., Reynolds, R. G., Revell, L. J., & Losos, J. B. (2014). Rapid evolution of a native species following

invasion by a congener. *Science*, *346*(6208), 463–466. https://doi.org/10.1126/science.1257008

Szűcs, M., Melbourne, B. A., Tuff, T., Weiss-Lehman, C., & Hufbauer, R. A. (2017). Genetic and demographic founder effects have long-term fitness consequences for colonising populations. *Ecology Letters*, *20*(4), 436–444. https://doi.org/10.1111/ele.12743

Taverne, M., Dutel, H., Fagan, M., Štambuk, A., Lisičić, D., Tadić, Z., Fabre, A.-C., & Herrel, A. (2021). From micro to macroevolution: Drivers of shape variation in an Island radiation of *Podarcis* lizards. *Evolution*, *75*, 2685–2707. https://doi.org/10.1111/evo.14326

Taverne, M., Fabre, A. C., King-Gillies, N., Krajnović, M., Lisičić, D., Martin, L., Michal, L., Petricioli, D., Štambuk, A., Tadić, Z., Vigliotti, C., Wehrle, B. A., & Herrel, A. (2019). Diet variability among insular populations of *Podarcis* lizards reveals diverse strategies to face resource – Limited environments. *Ecology and Evolution*, *9*(22), 12408–12420. https://doi.org/10.1002/ece3.5626

Taverne, M., King-Gillies, N., Krajnović, M., Lisičić, D., Mira, Ó., Petricioli, D., Sabolić, I., Štambuk, A., Tadić, Z., Vigliotti, C., Wehrle, B., & Herrel, A. (2020). Proximate and ultimate drivers of variation in bite force in the insular lizards *Podarcis melisellensis* and *Podarcis sicula*. *Biological Journal of the Linnean Society*, *131*(1), 88–108. https://doi.org/10.1093/biolinnean/blaa091

Taverne, M., Watson, P. J., Dutel, H., Boistel, R., Lisicic, D., Tadic, Z., Fabre, A. C., Fagan, M. J., & Herrel, A. (2023). Form-function relationships underlie rapid dietary changes in a lizard. *Proceedings of the Royal Society B: Biological Sciences*, *290*(2000), 20230582. https://doi.org/10.1098/rspb.2023.0582

Van Buskirk, J., & Willi, Y. (2006). The change in quantitative genetic variation with inbreeding. *Evolution*, *60*(12), 2428–2434. https://doi.org/10.1554/06-485.1

Veron, S., Mouchet, M., Govaerts, R., Haevermans, T., & Pellens, R. (2019). Vulnerability to climate change of islands worldwide and its impact on the tree of life. *Scientific Reports*, *9*(1), 1–14. https://doi.org/10.1038/s41598-019-51107-x

Vervust, B., Grbac, I., & Van Damme, R. (2007). Differences in morphology, performance and behaviour between recently diverged populations of *Podarcis sicula* mirror differences in predation pressure. *Oikos*, *116*(8), 1343–1352. https://doi.org/10.1111/j.2007.0030-1299.15989.x

Vervust, B., Pafilis, P., Valakos, E. D., & Van Damme, R. (2010). Anatomical and physiological changes associated with a recent dietary shift in the lizard *Podarcis sicula*. *Physiological and Biochemical Zoology*, *83*(4), 632–642. https://doi.org/10.1086/651704

Vervust, B., Van Dongen, S., Grbac, I., & Van Damme, R. (2009). The mystery of the missing toes: Extreme levels of natural mutilation in Island lizard populations. *Functional Ecology*, *23*(5), 996–1003. https://doi.org/10.1111/j.1365-2435.2009.01580.x

Visscher, P. M., Hill, W. G., & Wray, N. R. (2008). Heritability in the genomics era – Concepts and misconceptions. *Nature Reviews Genetics*, *9*(4), 255–266. https://doi.org/10.1038/nrg2322

Wang, S. P., & Althoff, D. M. (2019). Phenotypic plasticity facilitates initial colonization of a novel environment. *Evolution*, *73*(2), 303–3016. https://doi.org/10.1111/evo.13676

Warren, B. H., Simberloff, D., Ricklefs, R. E., Aguilée, R., Condamine, F. L., Gravel, D., Morlon, H., Mouquet, N., Rosindell, J., Casquet, J., Conti, E., Cornuault, J., Fernández-Palacios, J. M., Hengl, T., Norder, S. J., Rijsdijk, K. F., Sanmartín, I., Strasberg, D., Triantis, K. A., … Thébaud, C. (2015). Islands as model systems in ecology and evolution: Prospects fifty years after MacArthur-Wilson. *Ecology Letters*, *18*(2), 200–217. https://doi.org/10.1111/ele.12398

Wehrle, B. A., Herrel, A., Nguyen-Phuc, B.-Q., Maldonado, S. J., Dang, R. K., Agnihotri, R., Tadić, Z., & German, D. P. (2020). Rapid dietary shift in *Podarcis siculus* resulted in localized changes in gut function. *Physiological and Biochemical Zoology*, *93*(5), 396–415. https://doi.org/10.1086/709848

Wolak, M. E., & Reid, J. M. (2017). Accounting for genetic differences among unknown parents in microevolutionary studies: How to include genetic groups in quantitative genetic animal models. *Journal of Animal Ecology*, *86*(1), 7–20. https://doi.org/10.1111/1365-2656.12597

Yang, W., Feiner, N., Pinho, C., While, G. M., Kaliontzopoulou, A., Harris, D. J., Salvi, D., & Uller, T. (2021). Extensive introgression and mosaic genomes of Mediterranean endemic lizards. *Nature Communications*, *12*(1), 2762. https://doi.org/10.1038/s41467-021-22949-9

SUPPORTING INFORMATION

Additional supporting information can be found online in the Supporting Information section at the end of this article.

How to cite this article: Sabolić, I., Mira, Ó., Brandt, D. Y. C., Lisičić, D., Stapley, J., Novosolov, M., Bakarić, R., Cizelj, I., Glogoški, M., Hudina, T., Taverne, M., Allentoft, M. E., Nielsen, R., Herrel, A., & Štambuk, A. (2023). Plastic and genomic change of a newly established lizard population following a founder event. *Molecular Ecology*, *00*, e17255. https://doi.org/10.1111/mec.17255

MOLECULAR ECOLOGY

Supplemental Information for:

Plastic and genomic change of a newly established lizard population following a founder event

Iva Sabolić, Óscar Mira, Débora Y.C. Brandt, Duje Lisičić, Jessica Stapley, Maria Novosolov, Robert Bakarić, Ivan Cizelj, Marko Glogoški, Tomislav Hudina, Maxime Taverne, Morten E. Allentoft, Rasmus Nielsen, Anthony Herrel, Anamaria Štambuk*
*Corresponding author email: astambuk@biol.pmf.hr

Table of Contents:

Supplementary Materials and Methods Page 2
Figures S1 to S10
Tables S1 to S8

Supplementary Results Page 28
Figures S11 to S18
Tables S9 to S20

Supplementary References Page 45

Supplementary Materials and Methods

Multipopulation framework

DNA sample and phenotypic data collection from wild populations

During the summer of 2016 and 2019, we sampled 14 *P. siculus* populations (13 insular and one mainland) from the Croatian coast of Adriatic Sea, including Pod Kopište and Pod Mrčaru (Figs. 1, S1 and S2). Lizards were caught using a pole with a noose or by hand, sexed and weighed with a spring balance scale (Pesola). Body and head measurements for each individual were taken *in situ* with a digital caliper (Powerfix Profi+; accuracy limit of 0.01 mm). In addition, we measured bite force using a Kistler force transducer set in a custom-built holder and connected to a Kistler charge amplifier. Bite force was measured 5 times and the highest recorded value was multiplied by 0.67 to correct for lever arms. In total, 14 phenotypic measurements were obtained for 421 individuals (201 females and 220 males) (Table S1). Finally, the tail tip was clipped and stored in 96% ethanol before releasing the lizards back into their natural habitat.

Figure S1. Island of Pod Mrčaru.

Figure S2. Island of Pod Kopište.

Table S1. Phenotypic measurements performed *in situ* on wild populations.

Code	Measurement	Description
BHgth	body height	measured at the highest part of the body (mm)
BiteF	bite force	maximum bite force from five measurements * 0.67 to compensate lever arms (n)
BMs	body mass	scale accuracy limit of 0.1 mg
BWdth	body width	measured in the widest part of the body (mm)
FLLgh	front limb length	added length of left front limb humerus, radius, metatarsus, and 3rd front toe (mm)
HHgth	head height	measured behind the orbits at the tallest part of the head (mm)
HLgth	head length	distance from the extreme of the upper jaw to the back of the parietal bone (mm)
HLLgh	hind limb length	added length of left rear limb humerus, radius, metatarsus, and 4th hind toe (mm)
HWdth	head width	measured approximately at the level of the jugal bones at the widest part of the head (mm)
ILLgh	inter limb length	distance between the point of insertion of left front and hind limbs
LwJaL	lower jaw length	distance from the anterior tip of the lower jaw to the back of the retroarticular process (near the posterior edge of the ear opening) (mm)
LwJaO	lower jaw out-lever	distance from the anterior tip of the lower jaw to the posterior edge of the quadrate (near the anterior edge of the ear opening) (mm)
SnLgh	snout length	distance from the anterior tip of the lower jaw to the posterior edge of the jugal (mm)
SVLgh	snout-vent length	distance from the tip of the snout to the posterior edge of the anal scale (mm)

Ecological variables

We obtained a set of environmental variables for each sampled site from a historical climate (1970-2000) dataset available in WorldClim (Fick, 2017). The dataset was chosen because of the high resolution available (30 seconds; ~1 km^2), which was critical due to the small area of some the sampled islets (Table S2). We extracted over 18 environmental variables related to climate for each island using QGIS (QGIS Development Team, 2015) – however, after analyzing their correlation and relevance, we retained only 6 of them for subsequent analyses: mean annual temperature, maximum temperature of the warmest month, minimum temperature of the coldest month, mean annual precipitation, mean annual solar radiation, and mean annual wind speed. Using QGIS we additionally calculated minimum distance to the nearest large island or to the mainland. We also obtained the area of each sampled island from the previous surveys of Croatian coast (Drenovec, 2012; Duplačić Leder, Ujević, & Čala, 2004). For the population sampled on mainland (ST; Split) we set area to an extremely high value (10,000,000) to better reflect its mainland status in comparison with the limited areas of the islands. We considered area and distance to the nearest large island as ecological variables because they largely determine the abiotic and biotic conditions on the islands, and directly affect predator abundance, as well as the probability of invasion, anthropological influence, and/or flora dispersal.
We standardized all eight ecological variables (Table S2) to zero mean and unit variance. To account for correlation among environmental factors, we further performed a principal component analysis (PCA) on standardized variables. Environmental data for 12 sites was used

for genotype-environment association (Fig. S3), and environmental data for 14 sites/populations was used for RDA (Fig. S4). We used the scores from first 5 principal components which explained more than 99.6% variance as environmental input for subsequent genotype-phenotype-environment analyses. We modeled geographic variation among populations using distance-based Moran's eigenvector maps (dbMEMs), a spatial eigenfunction method that decomposes physical distances into a new set of independent variables appropriate for subsequent RDA analyses. Raw geographic latitude and longitude values were transformed to Cartesian coordinates, and dbMEMs variables were obtained through a Euclidian distance matrix using R packages *SoDA* (Chambers, 2013) and *adespatial* (Dray et al., 2020). Only positive Moran's eigenvectors (first two dbMEMs) were retained for subsequent analyses.

Table S2. Ecological variables obtained for all sampled *P. siculus* populations.

Code	Description	Source
TemperatureMean	mean annual temperature (°C)	Worldclim (BIO1)
TemperatureMax	maximum temperature of the warmest month (°C)	Wordclim (BIO5)
TemperatureMin	minimum temperature of the coldest month (°C)	Wordclim (BIO6)
PrecipitationMean	mean annual precipitation (mm)	calculated from Worldclim monthly averages
SolarRadiationMean	annual mean solar radiation (kJ m^{-2} day^{-1})	calculated from Worldclim monthly averages
WindSpeedMean	annual mean wind speed (m s^{-1})	calculated from Worldclim monthly averages
Area	island surface area (m^2)	(Drenovec, 2012; Duplačić Leder et al., 2004)
DistanceToLargeIsland	minimum distance to the nearest large island or to mainland (m)	calculated in QGIS

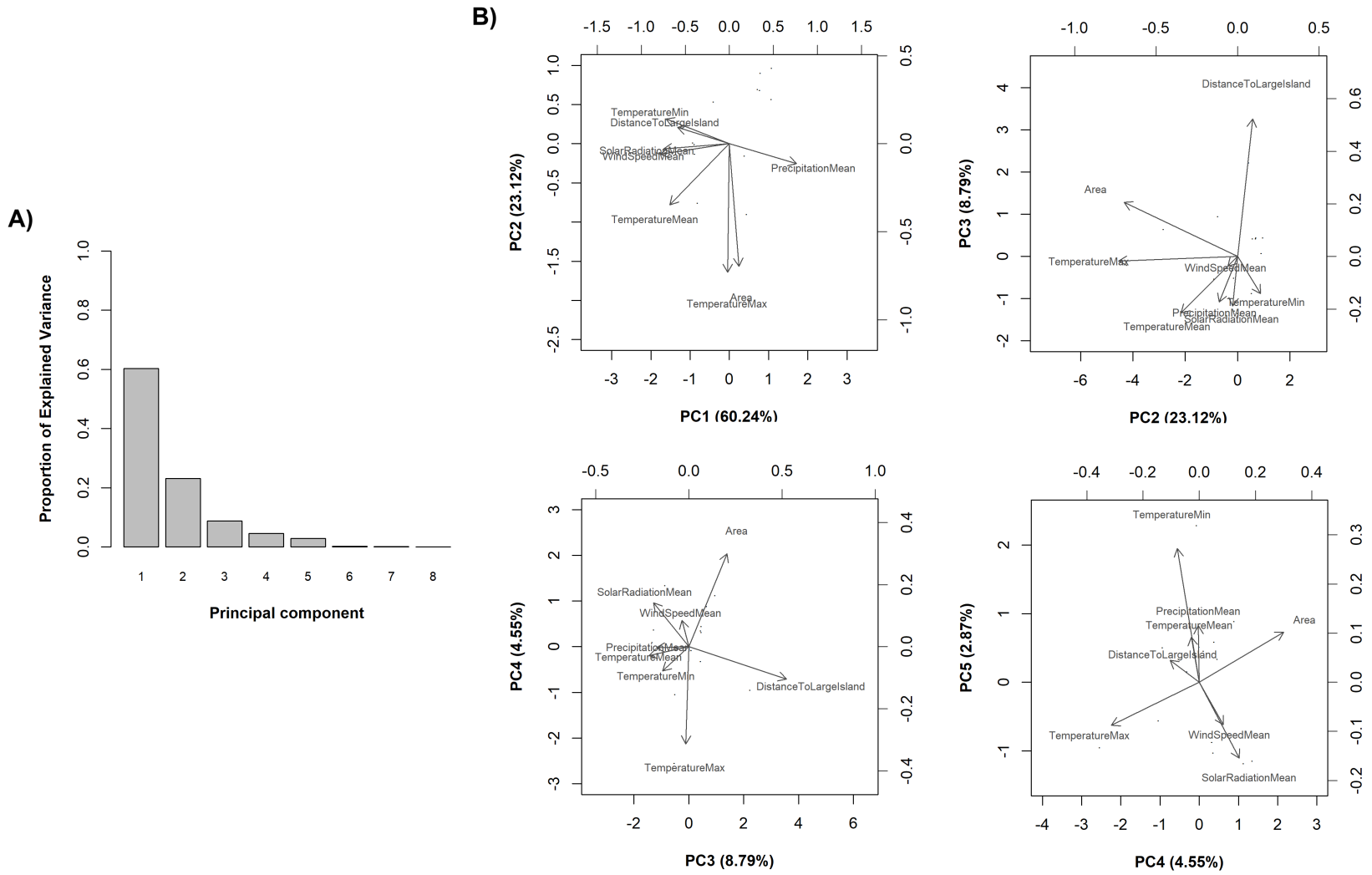

Figure S3. Results from principal component analysis (PCA) on standardized ecological variables for 12 wild *P. siculus* populations (excluding PK and PM) used in genotype-environment association analysis: **A)** proportion of explained variance for all 8 principal components, and **B)** biplots showing loadings of each ecological variable to first five principal components.

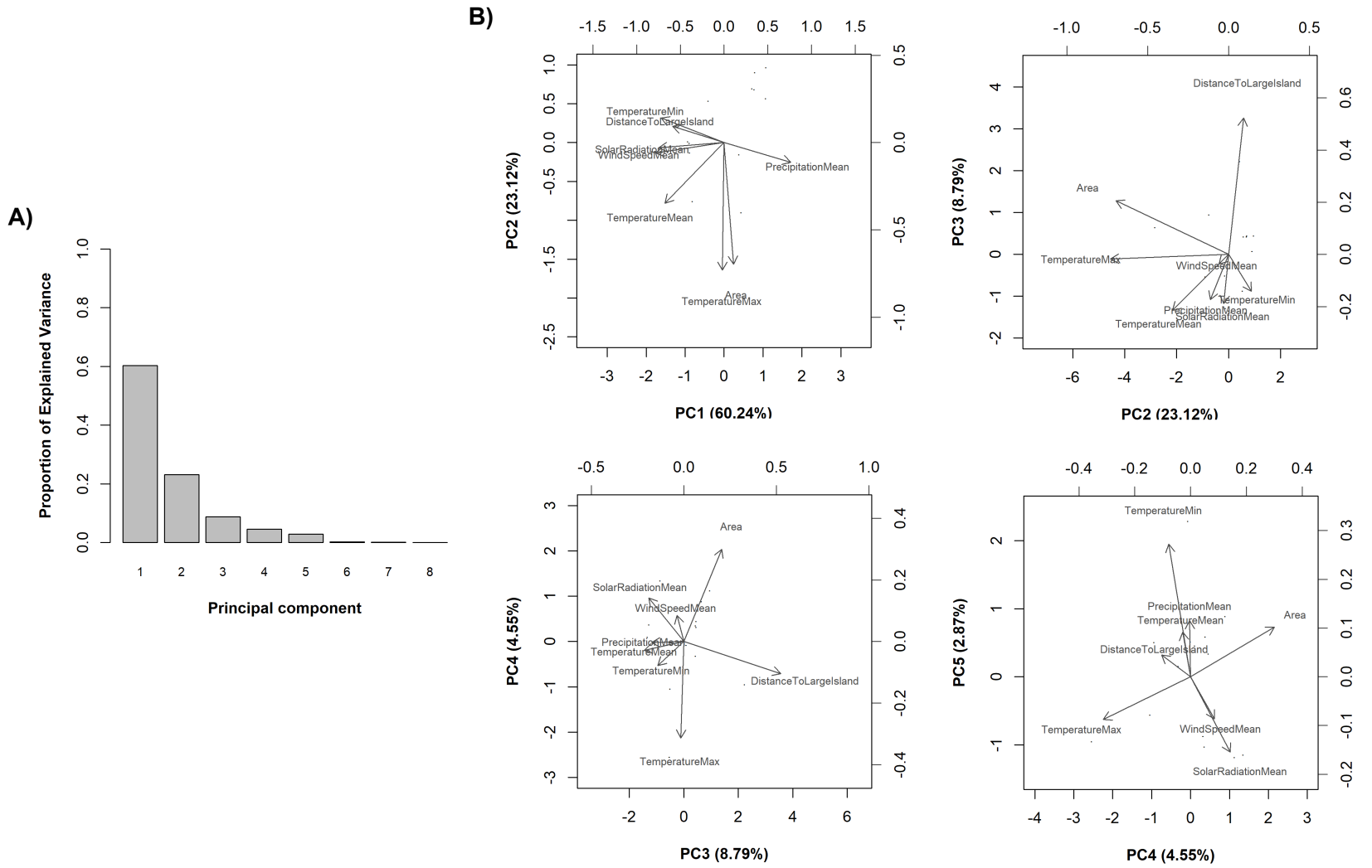

Figure S4. Results from principal component analysis (PCA) on standardized ecological variables for 14 wild *P. siculus* populations used in redundancy analysis: **A)** proportion of explained variance for all 8 principal components, and **B)** biplots showing loadings of each ecological variable to first five principal components.

Floristic and vegetation survey of Pod Kopište and Pod Mrčaru islands

To better characterize ecological divergence of habitats on two focal islands, floristic and vegetational survey was conducted in May 2017. Habitats on both islands are opened i.e. without forest or macchia. Ongoing presence of app. 10 sheep on Pod Kopište and sporadic presence of 1-2 goats on Pod Mrčaru affects the vegetational succession on both islands. Presence of herbivores and gull colonies causes permanent inflow of nutrients, especially nitrates. Vegetation was surveyed using the standard Braun-Blanquet method. Plots for the vegetation surveys were chosen to be representative for the present habitat types and a 50 m^2 plot positioned in each habitat type (two plots on Pod Kopište, one on Pod Mrčaru). For each plant that was observed on the plot the area cover percentage was determined using the Braun-Blanquet scale of 9 categories (Table S3) (Mueller-Dombois & Ellenberg, 1974).

Table S3. Braun-Blanquet vegetation survey categories for determination of area covered with each plant species.

Category	Description
r	Individual plant on the plot, (species also scares on the surrounding area)
+	2 - 5 individuals on the plot, coverage < 5%
1	6 - 50 individuals on the plot, coverage < 5%
2m	> 50 individuals on the plot, coverage < 5%
2a	coverage 5 - 15%, regardless on number of individuals
2b	coverage 16 - 25%, regardless on number of individuals
3	coverage 26 - 50%, regardless on number of individuals
4	coverage 51 - 75%, regardless on number of individuals
5	coverage 76 - 100%, regardless on number of individuals

Invertebrate availability on islands Kopište, Pod Popište and Ppd Mrčaru

Invertebrate availability was censused in June of 2004 and April of 2006 on three islands (Pod Kopiste, Pod Mrcaru and Kopiste) using timed sweep netting (40 samples of one minute of vigorously sampling the vegetation on the island including all vegetation types) and by setting 20 pitfalls of 15 cm in diameter and 10 cm of depth filled with 5cm of a water and formaldehyde solution with some soap. Pitfalls were left for 48 hours. Contents of sweep netting were transferred to plastic bags, frozen, sorted and preserved in a 5% aqueous formaldehyde solution. All invertebrates were sorted to the taxonomical level of order (or family), counted and weighed using a precision balance (+/- 0.0001mg).

Phenotype-environment associations

We partitioned the phenotypic variance between ecological and geographical components using a redundancy analysis (RDA) implemented in R package *vegan* (Oksanen et al., 2019). RDA is a constrained linear ordination method in which multiple regressions are fitted between response (individual genotype) and explanatory variables (environment). PCA is then performed on the fitted values to extract the RDA axes, which represent linear combinations of explanatory variables that best explain the variation in the response matrix. Phenotypic measurements collected for 421 individuals (201 females and 220 males) from 14 wild *P. siculus* populations (Fig. 1, Table S1) were $\log_{10}$-transformed and size corrected by linear regression of each variable against the snout-vent length (SVLgh). To account for the sexual dimorphism of the species, regressions were calculated independently for each sex. All phenotypic variables were further standardized to zero mean and unit variance.

To avoid using collinear variables that could lead to overrepresentation, a principal component analysis (PCA) was implemented on both phenotypic and ecological variables using *prcomp()* function from R package *stats* (R Core Team, 2017). First five principal components from PCA of phenotypic variables (explaining 75% or more of the total variance) were selected as RDA response matrix, and first five principal components from the PCA of ecological variables (explaining more than 99.6% of variance; Fig. S4) were selected as RDA ecological explanatory matrix. Finally, first two dbMEMs were used as RDA geographical explanatory matrix.

We performed the RDA separately for male and female individuals. Three different types of RDA analyses were performed using functions available in R package *vegan* v.2.5.6 (Oksanen et al., 2019): full RDA analysis with both ecological and geographical data as explanatory variables, partial RDA analysis with ecology as explanatory and dbMEMs as conditioning variables, and partial RDA with dbMEMs as explanatory and ecological data as conditioning variables. Variance partitioning between ecological and/or spatial distance components was based on adjusted R^2 values from the respective RDA analyses and *varpart()* function from the *vegan* package. Significance of the models and marginal effects of explanatory variables were tested using ANOVA permutation test for constrained correspondence analysis with 999 replicates.

***P. siculus* genome assembly**

We extracted the DNA for the genome assembly from a female *P. siculus* individual sampled on Pod Mrčaru in 2017. The individual was anesthetized with 5% isoflurane, and a small cut made on the ventral surface of its body to expose the heart. We nicked the heart with a pair of small scissors and submerged the lizard in a 50 mL conical tube filled with cold 0.9X saline sodium citrate buffer (SSC, Sigma-Aldrich), allowing the heart to pump the circulating blood into the collection tube. Once we collected the blood, lizard was removed from the tube, the tube capped and centrifuged at 4°C, 1500 RPM for 9 min. We decanted most of the supernatant, leaving only around ~3.5 mL of liquid in the tube, and resuspended the blood cells in the remaining supernatant by vortexing. We then added 12 mL of lysis buffer (1% SDS, 20 mM EDTA, 100 mM NaCl, 20 mM Tris; pH 7.5-8.0) and mixed the contents carefully by inverting the tube. We added 0,003g of proteinase K to the suspension to achieve a final concentration of 200 $\mu g\ mL^{-1}$, and incubated the mixture for 20 minutes at 55°C and then overnight at 30°C. The next day, we added 3.75 mL of 10M ammonium acetate (NH4OAc) to the tube, and mixed thoroughly by inverting. We followed this by adding 9 mL of isopropanol and mixing the tube again. The resulting condensed DNA was spooled on a clean Pasteur pipet (which was previously flamed to close the ends), and scraped into a clean

15 mL conical tube filled with 10 mL of 70% ethanol. The DNA was allowed to agitate for two hours, after which we decanted the ethanol and let the pellet dry completely. DNA was resuspended in 1 mL of TE buffer (Tris-EDTA; pH 8.0) overnight at room temperature. Extracted DNA was stored at -20 °C.
The *P. siculus* genome was assembled *de novo* using 10X Genomics linked-reads technology. After DNA extraction pulse field electrophoresis confirmed high molecular weight DNA fragment sizes (>50kb) were present. Sequencing libraries were generated using the 10X Genomics Chromium Library Preparation, and traces were verified using Fragment AnalyzerTM. Libraries were sequenced on an Illumina HiSeq 4000 sequencer. Illumina BCL files were converted to FASTQ files using supernova *mkfastq* v.2.0.0 (Weisenfeld, Kumar, Shah, Church, & Jaffe, 2017), and genomes were assembled using supernova run v.2.0.0 (Weisenfeld et al., 2017). A total of 614.05 million reads were provided as input, with mean read length of 138.5 bases, raw coverage of 59.68 X and mean molecule size was 60.71 kb. The output had 1170 scaffolds larger than 10 kb, a N50 contig size of 75.56 kb, a N50 scaffold size of 37.45 Mb and only 3.57% of bases in the assembly were in scaffolds smaller than 10 kb. Total assembly size in scaffolds larger than 10 kb was 1.33 Gb. Fasta files in the ph format were generated with supernova *mkoutput* v.2.0.1 (Weisenfeld et al., 2017).
We used BUSCO v.3.0.2 (Simão, Waterhouse, Ioannidis, Kriventseva, & Zdobnov, 2015) to evaluate the completeness of our genome assembly. BUSCO searches for a list of conserved single copy ortholog genes that would be expected to be found in any tetrapod genome. We used the tetrapoda_odb9 gene dataset and found a high level of genome completeness: 93.7% complete BUSCOs (with 92.4% single-copy BUSCOs and 1.3% duplicated), 3.5% fragmented BUSCOs and 2.8% missing BUSCOs.
To remove any scaffolds with possible contaminants, we ran BLAST (Altschul, Gish, Miller, Myers, & Lipman, 1990) with all assembly scaffolds as queries against the NCBI database. We used parameters -max_hsps 1 -max_target_seqs 3 and output results in tabular format (-outfmt 6) including taxon IDs. R package *taxonomizr* (Sherrill-Mix, 2021) was used to assign taxonomy to each alignment hit. We removed from the final assembly all scaffolds that did not find a BLAST hit to Squamata. In total, 175112 scaffolds were removed, adding up to 70.75 Mb. Of those, 170218 scaffolds (46 Mb) did not have any blast hits and are probably composed of repetitive sequences. We further removed 1533 scaffolds whose sequences were composed only of Ns, probably due to some error in the supernova pipeline. After these filters, the genome was reduced from 209378 scaffolds to 32733 scaffolds, but only lost 70 Mb out of 1.5 Gb.

Genotyping by sequencing (GBS) library preparation and sequencing

A total of 370 DNA samples (18-47 per population) from 14 wild *P. siculus* populations sampled in 2016 and 2019, and 235 additional samples from lizards collected in the 2017-2018 from Pod Kopište and Pod Mrčaru and used in the common garden experiment (including the F1 crosses), were processed in the laboratory for population genomic analyses. Approximately 15mg of sampled tail tissue was flash frozen in liquid nitrogen to improve mechanical disruption and extraction efficiency, and then minced with scissors. Genomic DNA was extracted with commercial kits (Sigma Aldrich-GenElute Mammalian Genomic DNA Miniprep Kit), using the provided protocol. The quality and quantity of extracted DNA was checked by agarose electrophoresis and spectrophotometric measurement on a Nanodrop (NanoDrop 2000c Thermo Scientific). Extracted DNA was preserved at -20 °C.
GBS sequencing libraries were prepared according to customized protocols published in 2012 (Parchman et al., 2012; Peterson, Weber, Kay, Fisher, & Hoekstra, 2012), which were

adapted for pair-end sequencing. Seven µl (150-550 ng) of extracted genomic DNA was first digested by incubation at 37 °C for 8 hours with 3 µl of reaction mix containing 1.15 µl of 10X T4 buffer, 0.25 µl of nuclease free water (nfH2O), 0.6 µl of 1 M NaCl, 0.6 µl of1 mg/mL BSA, and 0.28 µl of EcoR1 and 0.12 µl MseI restriction endonuclease enzymes (New England BioLabs). Second, custom made EcoR1 adaptors containing 8-10 bp long barcodes that differed by a minimum of 4 bases, and a Y-shaped MseI adaptor (Table S4), were ligated on the digested DNA. In order to get the annealed, double-stranded adaptors, 100 µM stocks of single-stranded oligonucleotides were first mixed with nfH2O, heated to 95 °C for 5 minutes and slowly cooled down to room temperature. Digestion product was then incubated at 16 °C for 6 hours with 2.4 µl of ligation mix containing 1 µl of each adaptor working stock (EcoR1 final concentration 1 µM and MseI final concentration 10 µM), 0.072 µl of nfH2O, 0.1 µl of 10X T4 buffer, 0.05 µl of 1M NaCl, 0.05 µl of 1 mg/mL BSA, and 0.1675 µl of 400 U/µl T4 DNA ligase (New England BioLabs). Lastly, the digestion-ligation products were diluted up to 100 µL with 0.1X TE, and 4 µl of diluted product amplified in a 20.15 µl reaction containing 4 µl of 5× Iproof buffer, 9.67 µl of nfH20, 0.4 µl of 50 mM MgCl2, 0.4 µl of 10 mM dNTP, 0.15 µl of DMSO, 1.33 µl of primer working stock (2.5 µM of each Illumina PCR compatible primer; Table S4), and 0.2 µl of 2 U/µl iProof Polymerase (Bio-Rad). PCR conditions included 98 °C for 30 s, followed by 16 PCR cycles (98 °C for 20 s; 60 °C for 30 s; 72 °C for 40 s) and a final extension at 72 °C for 10 min. The quality of PCR products was checked on agarose gel, after which the samples were pooled together to be sequenced per lane.

The prepared libraries were sent to the BGI sequencing company in Hong-Kong for further processing. BGI provided services of library quality control (using Agilent 2100 Bioanalyzer and Real-time Quantitative PCR), gel size selection of DNA fragments from 250 to 450 bp, and 150 bp pair-end GBS sequencing on Illumina HiSeq X Ten platform with 40% PhiX. The company also provided services of initial quality control, de-phixing and demultiplexing of obtained reads. Obtained data were delivered in FASTQ format.

Table S4. Sequences of adaptors and primers used in the library preparations. Barcodes imbedded in EcoR1 adaptor are marked with red X. The asterisks between the first three bases in PCR1 primer mark phosphothiolate modifications.

Oligo name	5’ Sequence 3’
EcoR1_1	AATTGXXXXXXXXXAGATCGGAAGAGCGTCGTGTAGGGAAAGAGTGT
EcoR1_2	CTCTTTCCCTACACGACGCTCTTCCGATCTXXXXXXXXXC
Mse1_1	GTGACTGGAGTTCAGACGTGTGCTCTTCCGATCT
Mse1_2	TAAGATCGGAAGAGCGAGAACAA
PCR1	A*A*TGATACGGCGACCACCGAGATCTACACTCTTTCCCTACACGACGCTCTTCCGATCT
PCR2	CAAGCAGAAGACGGCATACGAGATCGTGATGTGACTGGAGTTCAGACGTGTGC

Quality control and variant detection

Raw reads ranged in length from 98 to 150 bp. All raw reads were checked, trimmed of residual adaptor and/or barcode contamination, and standardized to 98 bp for forward reads and 100 bp length for reverse reads using custom made Perl scripts. Reads with uncalled bases and/or cut sites containing more than one mismatch were removed, and those with an average Phred quality score bellow 20 were discarded (default sliding window size of 0.15) using *process_radtags* program in Stacks v.2.2 (Catchen, Hohenlohe, Bassham, Amores, &

Cresko, 2013; Rochette, Rivera-Colón, & Catchen, 2019). Raw and processed read quality was checked using FastQC v.0.11.8 (Andrews, Krueger, Seconds-Pichon, Biggins, & Wingett, 2010) and MultiQC v.1.0 software (Ewels, Magnusson, Lundin, & Käller, 2016). We mapped filtered reads on the assembled *P. siculus* reference genome using Bowtie2 software, a short read aligner program that enables alignment of large sets of short DNA sequence reads to large genomes (Langmead & Salzberg, 2012). Reference genome was first indexed, and reads then mapped to it using the end-to-end alignment mode. Aligned reads were transformed to BAM format using Samtools v.1.9 (Li et al., 2009).
Variant sites were called following the *ref_map* pipeline from Stacks v.2.53 (Catchen et al., 2013; Rochette et al., 2019). Stacks *gstacks* was run using a maximum-likelihood „marukilow" model which accounts for statistical uncertainties associated with sequencing errors during variant (alpha threshold = 0.01) and genotype (alpha threshold = 0.05) calling. Default settings were applied for all other *gstacks* parameters, apart for the minimum mapping quality to consider a read, which was set to more conservative value of 20. Stacks *populations* was used to filter single nucleotide polymorphisms (SNPs) according to population-wise parameters: minimum allele frequency was set to 0.05; minimum ratio of individuals in a population in which a locus must be present in order to process was set to 0.6; minimum number of populations a locus must be present in order to process that locus was set equal to the number of populations (no missing populations allowed); ratio of individuals across populations in which a locus must be present in order to process that locus was set to 0.7; maximum observed heterozygosity required to process a nucleotide site at a locus was set to 0.6; and SNP calling restricted to only the first SNP found on locus.
Variant call format (VCF) file produced by populations program was checked using custom made Perl script in order to identify samples containing more than 25% of missing values. The Stacks *ref_map* pipeline was then repeated using the same parameters specified above, but excluding 14 samples that did not pass the missing values threshold. This ensured that SNPs included in the final dataset were called only for the high quality samples. The final VCF file was filtered using custom made Perl scripts in several steps to reduce the number of missing values. First, we filtered out variant sites with mean coverage depth lower than 4X and larger than 20X. Second, we removed loci with more than 25% of missing data and then imputed population's most frequent known genotype for any remaining missing values (if two or more genotypes present in the population had the same highest frequency, one was assigned at random). The median percentage of loci imputed in each sample was 4.75% in the full dataset (585 individuals, 39905 SNPs) and 5.22 % in PKPM dataset (219 individuals, 12381 SNPs). For 116 "PKPM outlier" loci, median percentage of loci imputed in each sample was 7.76% both in the full dataset and in the PK-PM dataset. Per sample missing rate for 116 "PKPM outlier" loci thus followed the missing rate across all loci in individuals in both the full dataset (adjusted $R^2 = 0.654$, p value = < 2.2e-16) and in PK-PM dataset (adjusted $R^2 = 0.895$, p value = < 2.2e-16). Before proceeding with any further analyses we additionally performed a principal component analysis (PCA) on allele frequencies using R package *adegenet* (T Jombart, 2008). We examined the PCA scatterplots and further removed six additional outlier samples from subsequent analysis. The final datasets consisted of 39905 SNPs genotyped across 585 *P. siculus* individuals, of which 12381 were polymorphic in Pod Mrčaru and Pod Kopište populations sampled across three years (Table S5).
PGDSpider v.2.1.1.5 (Lischer & Excoffier, 2012) was used to convert genotype datasets from VCF format to all other program-specific input files, apart from conversion of Bayscan/Geste format to BayPass file format, for which Python script *geste2baypass.py* was used (available at: https://github.com/CoBiG2/RAD_Tools /blob/master/geste2baypass.py).

Table S5. Codes, island area, year sampled and the number of samples for *P. siculus* populations used in genomic analyses (total 585 individuals). Asterisk marks the population sampled from the mainland.

Code	Origin	Area (m^2)	Year sampled	Samples (N)
RK	Rakita	4001	2019	25
OB	Obrovanj	40002	2019	25
VC	Visovac	17376	2019	25
DU	Veliki Dupinić	16075	2019	25
OS	Oštrica	20648	2019	25
KL	Kluda	78407	2019	22
ST*	Split	10000000	2016	18
PJ	Pijavica	11037	2016	20
PG	Palagruža	26510	2016	20
SC	Sušac	4025460	2016	19
BJ	Bijelac	5530	2016	20
KP	Kopište	738726	2016	30
PK16	Pod Kopište	35835	2016	40
PK17	Pod Kopište		2017	46
PK18	Pod Kopište		2018	24
PM16	Pod Mrčaru	13514	2016	42
PM17	Pod Mrčaru		2017	33
PM18	Pod Mrčaru		2018	34
PKPK	PK♂ – PK♀ F1	NA	crossing experiment 2017+2018	25
PKPM	PK♂ – PM♀ F1	NA	crossing experiment 2017+2018	18
PMPK	PM♂ – PK♀ F1	NA	crossing experiment 2017+2018	29
PMPM	PM♂ – PM♀ F1	NA	crossing experiment 2017+2018	20

Genomic diversity and population divergence

Before proceeding with the analysis of genomic diversity and divergence in wild populations, we filtered the full genomic dataset (585 individuals, 39905 SNPs), and removed loci in linkage disequilibrium (LD) and out of Hardy-Weinberg equilibrium (HWe). LD was determined by employing a sliding window method implemented in Plink v1.9 (Purcell et al., 2007), using the *indep-pairwise* command with a window size of 50 SNPs, step size of 5, and r^2 threshold of 0.5. With this method, 18829 SNPs in LD ($r^2 < 0.5$) were removed from the full genomic dataset. Next, we performed a HWe test using R packages *pegas* (Paradis, 2010) and *dartR* (Gruber, Unmack, Berry, & Georges, 2018), with 99 replicates for each population. Only 2 loci significantly out of HWe ($p < 0.05$) in 60% or more of populations were removed, resulting in dataset consisting of 21074 SNPs (of which 9740 SNPs were polymorphic in Pod Kopište and Pod Mrčaru populations sampled across three years).

For estimation of genomic diversity indices and effective population size, the dataset was further randomly subsampled to a maximum of 19 samples per population using custom-made Perl script.

We inferred genetic diversity in all analyzed populations by estimating allelic richness (A_R), and observed and expected heterozygosity (Ho and He respectively), using the R package *diveRsity* (Keenan, Mcginnity, Cross, Crozier, & Prodöhl, 2013) with 999 bootstrap replicates

to infer A_R confidence intervals. We further computed per locus nucleotide diversity (π) using VCFtools (Danecek et al., 2011) software, and then averaged the per locus values in R (R Core Team, 2017) to obtain mean population π value. The inbreeding coefficient (F_{IS}) was estimated using Arlequin software (Excoffier & Lischer, 2010) with 1023 permutations. Effective population size (N_E) for each sampled site was calculated using the LD method with random mating in NeEstimator v.2.1 (Do et al., 2014). Singleton loci were excluded from analysis. N_E was calculated as arithmetic mean and standard deviation of three random subsets of 19 individuals per population. Average N_E estimates for the F1 from the crossing experiment were compared with the average number of parents for each of the three random subsets.

We determined genomic distances between all pairs of 14 wild populations sampled in 2016 and 2019 by calculating pair-wise F_{ST} index, using R package *StAMPP* (Pembleton, Cogan, & Forster, 2013) with 9999 bootstrap iterations. We further performed PCA on a scaled matrix of allele frequencies using functions available in R packages *stats* and *adegenet* (Thibaut Jombart & Ahmed, 2011) in order to assess the genomic divergence and distribution of the samples. PCA was performed on both genomic dataset with 14 wild *P. siculus* populations sampled in 2016 and 2019, and the genomic dataset with Pod Mrčaru and Pod Kopište individuals sampled in 2016, 2017 and 2018.

Next, we used software fastSTRUCTURE (Raj, Stephens, & Pritchard, 2014) to infer the number of observed genomic clusters in our datasets. The analysis was performed on genomic dataset with 14 wild populations sampled in 2016 and 2019, as well as the genomic dataset with all wild and experimental Pod Mrčaru and Pod Kopište individuals and their offspring. We ran fastSTRUCTURE analysis with the simple algorithm, and tested K values (number of model components) ranging from 1 to 14 for the dataset with 14 wild populations, and from 1 to 10 for dataset with all genotyped Pod Mrčaru and Pod Kopište individuals and their offspring. The analysis was run four times independently for each tested K value. Ideal number of clusters was chosen based on model complexity that maximizes marginal likelihood, or the number of components used to explain structure in the data. For both datasets we choose the model with the lowest ideal K value estimated in order to not overestimate the population structure. Software *distruct* v.2 (Chhatre, 2018; Rosenberg, 2004) was used to graphically display individual membership coefficients to each of the cluster.

We used BA3-SNPs (Mussmann, Douglas, Chafin, & Douglas, 2019) software to estimate recent migration rates between sampled populations. We performed several pilot runs in order to adjust prior acceptance rates of inbreeding coefficient, allele frequency, and migration rate. Priors were finally set to 0.02, 0.27, and 0.11 for each parameter respectively in order to achieve an acceptance rate of ~0.3 as recommended in the BayesAss v.3.0 manual (Wilson & Rannala, 2003). The analysis was run four times independently with 3,000,000 iterations and 1,000,000 burn-in. Convergence within and between replicate runs was checked using the package *CODA* (Plummer, Best, Cowles, & Vines, 2005) in R.

"PK-PM outlier" loci identification

We used three genome scan methods to pinpoint outlier loci in Pod Mrčaru and Pod Kopište populations, and analyses were run on Pod Kopište and Pod Mrčaru data for each sampled year independently. The data for each year consisted of: PKPM2016 = 82 individuals, 10859 polymorphic SNPs; PKPM2017 = 79 individuals, 10171 polymorphic SNPs; and PKPM2018 = 58 individuals, 9867 polymorphic SNPs. By the term "outlier" we refer here to loci that deviate from general distribution, without assuming their neutrality or adaptive nature.

We first employed a multivariate PCA approach implemented in R package *PCAdapt* (Luu, Bazin, & Blum, 2017) which uses a Mahalanobis distance test to detect outliers that do not follow the distribution of the main bulk loci, without assuming membership of samples to populations or groups. The optimal number of principal components (K) for the analysis was chosen by running analysis with K = 1-10, and assessing score plots for explained levels of population structure. Only the first principal component (K = 1) was retained as it was the only one contributing to differentiation between two islands. *PCAdapt* significant loci were considered those with p-value lower than 0.05.
Next, we used genome scan method implemented in BayeScan (Foll & Gaggiotti, 2008), a Bayesian software that relays on logistic regression to separate F_{ST} coefficients into population-specific (neutral or demographic variation) and locus-specific component (adaptive variation). BayeScan settings included 20 pilot runs of 5,000 iterations, followed by 100,000 iterations with 50,000 burn-in, and a thinning interval of 10. Prior odds for the neutral model were set to 10:1. Statistical significance was assessed based on obtained loci-specific q-value – a false discovery rate (FDR) analogue of the p-value. Loci were considered outliers if they showed q-value lower than 0.05 threshold.
Finally, a coalescent simulation implemented in Arlequin (Excoffier & Lischer, 2010) was performed to obtain the null distribution of locus-specific F-statistics conditioned on observed heterozygosities. Arlequin analysis was performed using a non-hierarchical finite island model, testing 10,000 simulations with 100 demes. Loci with positive F_{ST} higher than 95% confidence interval limits of the distribution were considered as putative outliers.
We then investigated the adaptive nature of these highly diverged loci by examining their representation in loci associated with diverged phenotypic traits in Pod Mrčaru and Pod Kopište populations, and/or loci associated with environmental variance, or loci detected as outlier loci putatively under selection across 14 wild *P. siculus* populations.

Identification of loci putatively under selection in wild populations

We used a genome scan method implemented in BayPass (Gautier, 2015), to pinpoint loci putatively under selection in 12 *P. siculus* populations sampled in the wild in 2016 and 2019, excluding Pod Mrčaru and Pod Kopište (274 individuals, 39883 SNPs). Samples from Pod Mrčaru and Pod Kopište populations have been excluded from this analysis to ensure statistical independence. BayPass is an extension of previously widely used Bayenv2 method (Günther & Coop, 2013), which refines the covariance matrix calculation through the use of a hierarchical Bayesian model and implements a calibration procedure for XtX statistics to identify SNPs putatively under selection. BayPass analysis was run in several successive steps. First, we analyzed the data under the core model in order to obtain the population covariance matrix and estimate the XtX statistics for outlier loci detection. Next, we simulated pseudo-observed datasets (PODs) with 10,000 SNPs using *simulate.baypass()* function available in *baypass_utils* R source package, and the mean covariance matrix and beta parameters calculated under the core model in the previous step. Simulated PODs were then analyzed under the core model in the same way as the real data, and 0.01 and 0.99 quantiles of the XtX distribution from the POD analyses were calculated in order to provide a cut-off value to discriminate between neutral and outlier loci for XtX statistics obtained on the real dataset. Loci with mean XtX values lower or higher than the obtained 1% and 99% POD threshold were considered outliers putatively under balancing or directional selection, respectively (Fig. S5).
Five replicate analyses were run for each Baypass step. MCMC parameters across all of them included 30 pilot runs with 5,000 iterations each, followed by 50,000 steps of burn-in, and

100,000 post burn-in iterations with a thinning interval of 25. Convergence of the algorithm was confirmed by assessing correlations of estimated parameters among runs, and mean values across replicate runs were taken as the final result. Similarity between covariance matrices obtained for empirical and simulated datasets was verified using Förstner and Moonen distance (FMD < 1) statistics from R function *fmd.dist()* included in the *baypass_utils* R source package. We further assessed the similarity between estimated BayPass covariance matrices and population-pairwise F_{ST} values obtained from the full dataset with 39883 SNPs using the R package *StAMPP* (Pembleton et al., 2013) with 9999 bootstrap iterations. For this purpose, we transformed the covariance to a correlation matrix and compared it with population-pairwise F_{ST} values using the Mantel test available in *ecodist* package in R (Goslee & Urban, 2007).

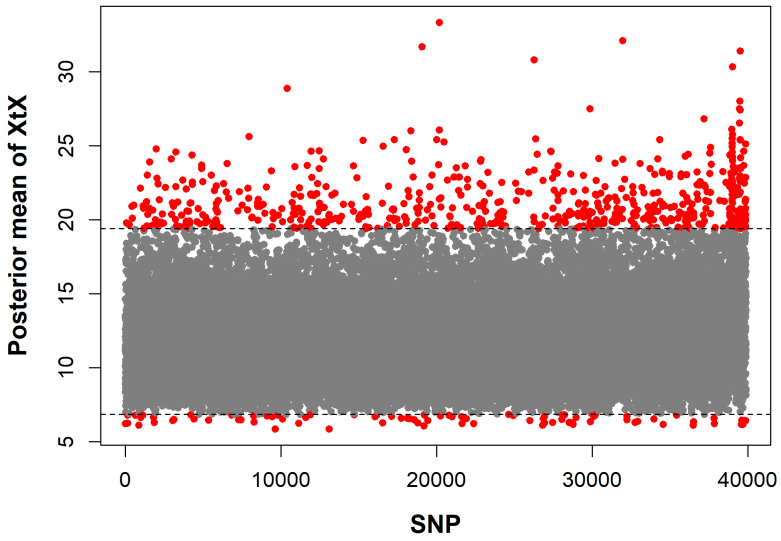

Figure S5. Manhattan plot of posterior mean XtX values obtained in BayPass core model analysis of 12 wild *P. siculus* populations. Red color denotes outlier SNPs under balancing (low XtX values) or directional (high XtX values) selection based on the thresholds obtained from analysis preformed on simulated pseudo-observed datasets (PODs).

Genotype-environment association

Genotype-environment associations (GEA) were assessed using the *P. siculus* genomic dataset with 12 wild populations sampled in 2016 and 2019 (274 individuals, 39883 SNPs) and previously mentioned BayPass software (Gautier, 2015). First, we filtered the full genomic dataset to exclude loci identified as putatively under selection (both directional and balancing) in previous BayPass runs. We then ran the BayPass core model again on the neutral dataset in order to obtain neutral population covariance matrix. The full dataset was then analyzed under BayPass auxiliary model (AUX), with the neutral covariance matrix acquired in the previous step. To account for the correlation among explanatory factors, we performed a PCA on standardized ecological variables (Table S2) and used the scores from first five principal components (explaining more than 99.7% variance) as environmental input for the BayPass GEA analysis. SNPs considered strongly associated with the ecological variables were those with Bayes factor values > 20 dB (deciban units) (Fig. S6). We performed all BayPass analyses five times independently, and confirmed convergence by assessing correlations between estimated parameters among runs. We used mean values of

parameters estimated across replicate runs as the final result. BayPass MCMC parameters consisted of 30 pilot runs with 5,000 iterations each, followed by 50,000 steps of burn-in, and 100,000 post burn-in iterations with a thinning interval of 25.

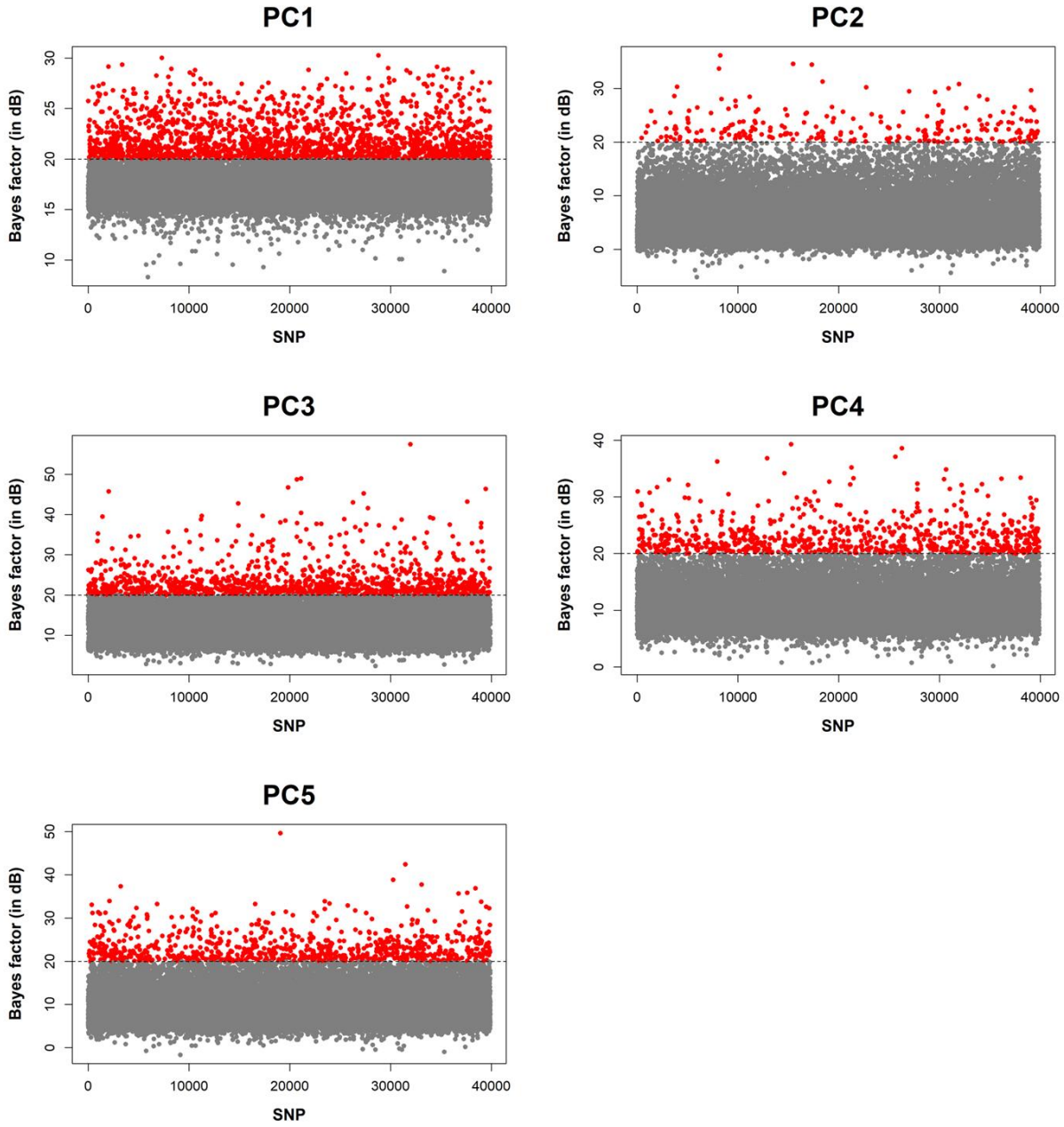

Figure S6. Manhattan plots of Bayes factor (BF) values in deciban units obtained from BayPass auxiliary model analysis of 12 wild *P. siculus* populations using the first five principal components (PC1-PC5) from PCA of ecological variables. Red color denotes SNPs with significant association to analyzed ecological variables (BF > 20 dB).

Genotypic variance was then partitioned between spatial (neutral) and ecological (adaptive) component using a multivariate redundancy analysis (RDA) approach. RDA was performed on genomic dataset with all 14 wild *P. siculus* populations sampled in 2016 and 2019, including Pod Mrčaru and Pod Kopište (356 individuals, 39905 SNPs). Ecological variation among populations was modeled using scores from the first five principal components in the PCA of ecological variables (Fig. S3), and geographical variation using first two dbMEM vectors obtained from distance-based Moran's eigenvector analysis. Genotype data was expressed as a matrix of population allele frequencies. As with the phenotype-environment analysis, we performed three different types of RDA analyses using the R package *vegan* v.2.5.6 (Oksanen et al., 2019): full RDA analysis, partial RDA with ecology as explanatory and dbMEMs as conditioning variables, and partial RDA with dbMEMs as explanatory and ecological data as conditioning variables. Variance partitioning between ecological and geographical components was based on adjusted R^2 values from the RDA analyses and *varpart()* function from *vegan*. Significance of the model, RDA canonical axes, and marginal effects of explanatory variables were tested using ANOVA after 999 permutations.

Significance of loci overlap

We analyzed whether the number of overlaps among lists of outlier loci obtained using different analyses was significantly higher than expected by chance through calculation of hypergeometric probabilities using *phyper()* function in *stats* package in R v.4.0.0 (R Core Team, 2017).

Genotype-phenotype association

We used individual allele counts from 2016 Pod Mrčaru and Pod Kopište dataset (53 males, 10094 polymorphic SNPs and 29 females, 9592 polymorhic SNPs) and latent factor mixed models (LFMM) analysis to explore genotype-phenotype associations (GPA) in our two focal populations. The LFMM approach is similar to a mixed model regression often used in GWAS, which test associations between a multidimensional set of response variables (genotypes) and a set of variables of interest (phenotypic traits or environmental variation). However, unlike standard mixed models that employ a kinship matrix or principal components, LFMM corrects for confounding effects due to population structure and other hidden causes by including random unobserved variables K (called latent factors). Although phenotype is usually considered a response and genotype an explanatory variable in a biological sense, LFMM corrects for the confounding effects of latent factors by modeling them together with the response variables. Consequently, the LFMM genotype-phenotype association test used in this study was performed with genotypes modeled as a response and phenotype as explanatory variable.

Phenotypic variables (Table S1) obtained for 2016 Pod Mrčaru and Pod Kopište individuals were size corrected prior to GPA analysis to eliminate variation resulting from allometric growth. All measures were $\log_{10}$-transformed and size-corrected using linear regression to snout-vent length (SVLgh). Regression residuals were used in posterior GPA analyses (apart from the SVLgh itself, which was processed raw). All phenotypic variables were additionally scaled to zero mean and unit variance. We further assessed phenotypic divergence in male and female individuals from Pod Kopište and Pod Mrčaru using a PCA implemented in R function *prcomp()* prior to the GPA analysis itself.

We ran LFMM analysis separately for male and female individuals using the ridge analytical method from R package *lfmm* (Caye, Jumentier, Lepeule, & François, 2019), fitted with two latent factors (K = 2) identified by PCA analysis of genomic data from Pod Mrčaru and Pod

Kopište populations. We recalibrated obtained z -scores with modified genomic inflation factors (GIFs; Table S6) following the procedure described by Frichot and François (Frichot & François, 2015), in order to obtain a uniform p-value distribution which is expected under the null-hypothesis (Figs. S7, S8, S9 and S10). Loci showing significant association with analyzed phenotypic variables were determined by Benjamini-Hochberg procedure on adjusted p-values with false discovery rate (FDR) = 0.05.
We avoided including the phenotypic data collected for Pod Mrčaru and Pod Kopište individuals in 2017 and 2018 along with those obtained in 2016 for the GPA analysis, due to the difference in phenotyping methods used (image processing vs. caliper measurement, respectively).

Table S6. Genomic inflation factors (GIFs) obtained during model fitting and modified GIFs used to adjust p-values in LFMM analyses.

	2016 PKPM ♀		2016 PKPM ♂	
trait	**GIF default**	**GIF modified**	**GIF default**	**GIF modified**
HHgth	0.894	0.62	1.014	0.75
HLgth	1.388	0.86	0.824	0.71
HWdth	1.344	0.86	1.034	0.69
LwJaL	1.418	0.81	0.944	0.74
LwJaO	1.288	0.87	0.876	0.71
SnLgh	1.194	0.78	0.796	0.69
ILLgh	1.309	0.95	1.224	0.93
HLLgh	1.520	0.92	1.253	0.87
FLLgh	1.296	0.83	1.275	0.96
BHgth	1.264	0.82	0.955	0.73
BWdth	1.036	0.78	0.968	0.72
BiteF	1.048	0.70	0.942	0.70
BMs	1.081	0.73	1.037	0.75
SVLgh	1.668	0.96	1.590	1.08

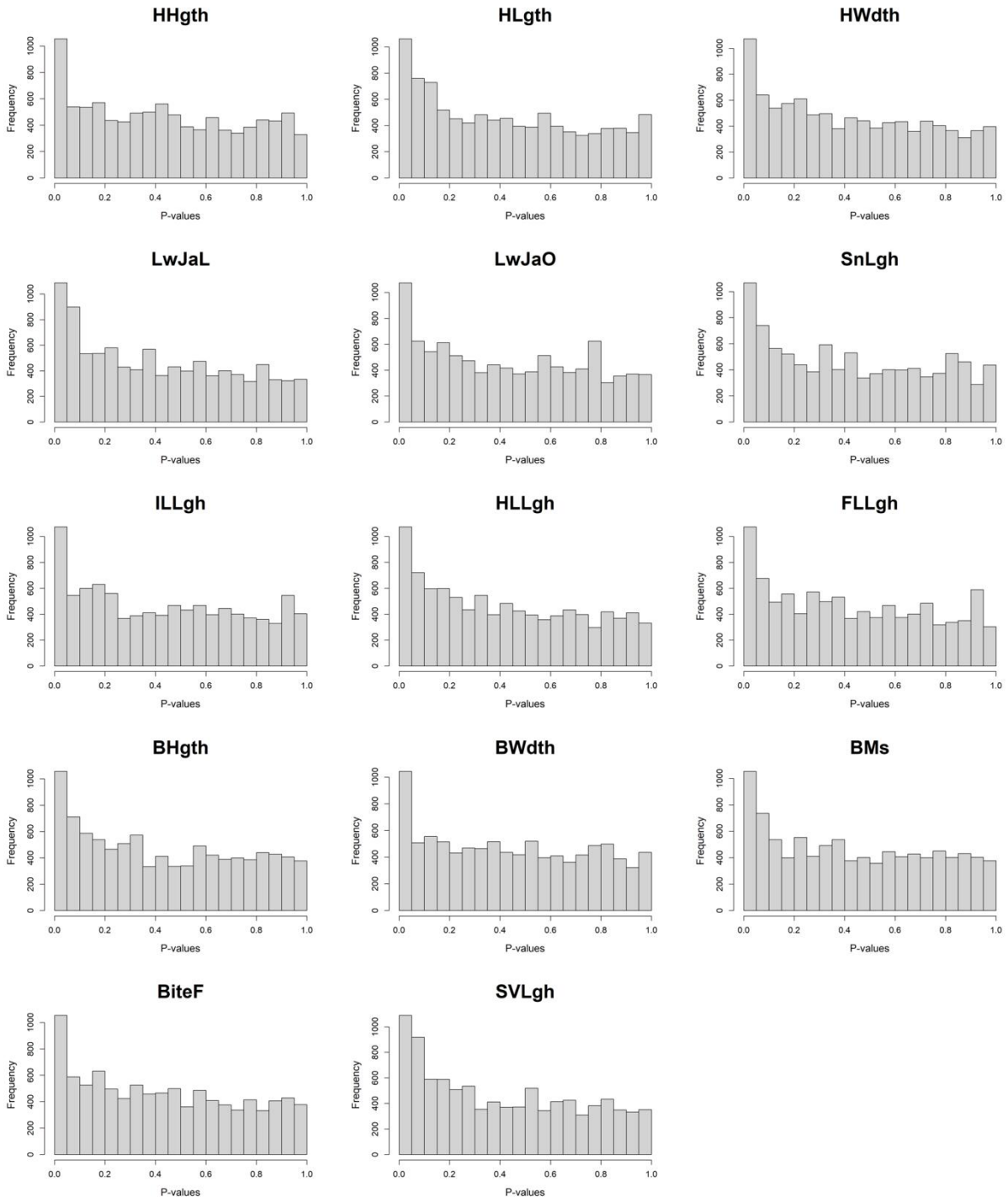

Figure S7. Histograms of adjusted p-values for all loci found in LFMM analysis of female *P. siculus* individuals from Pod Mrčaru and Pod Kopište islands. Phenotypic trait abbreviations are defined in Table S1.

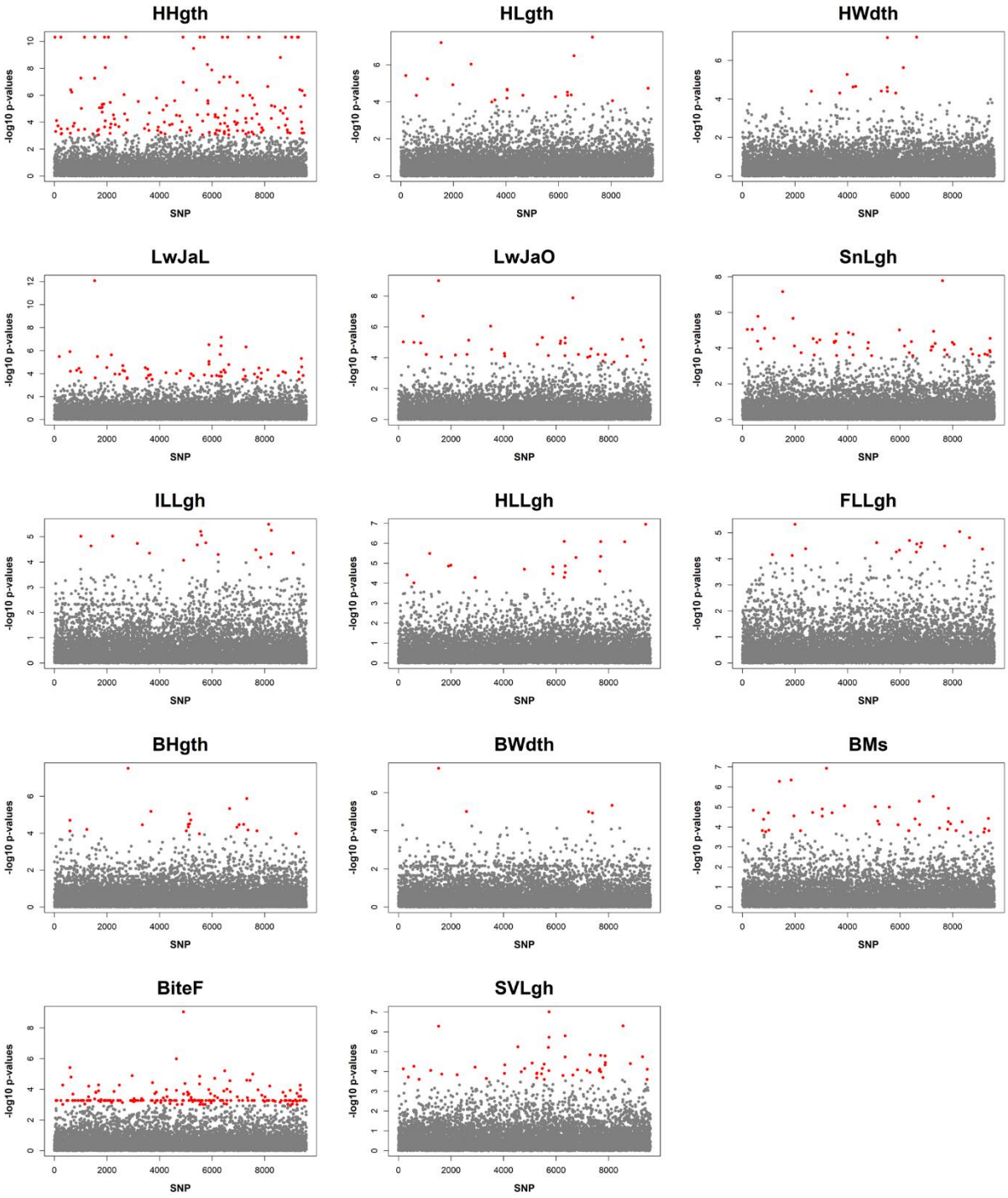

Figure S8. Manhattan plots of adjusted p-values obtained from LFMM analysis of female *P. siculus* individuals from Pod Mrčaru and Pod Kopište islands. Red color denotes SNPs with significant association to analyzed phenotypic variables (Benjamini-Hochberg FDR <0.05). Phenotypic trait abbreviations are defined in Table S1.

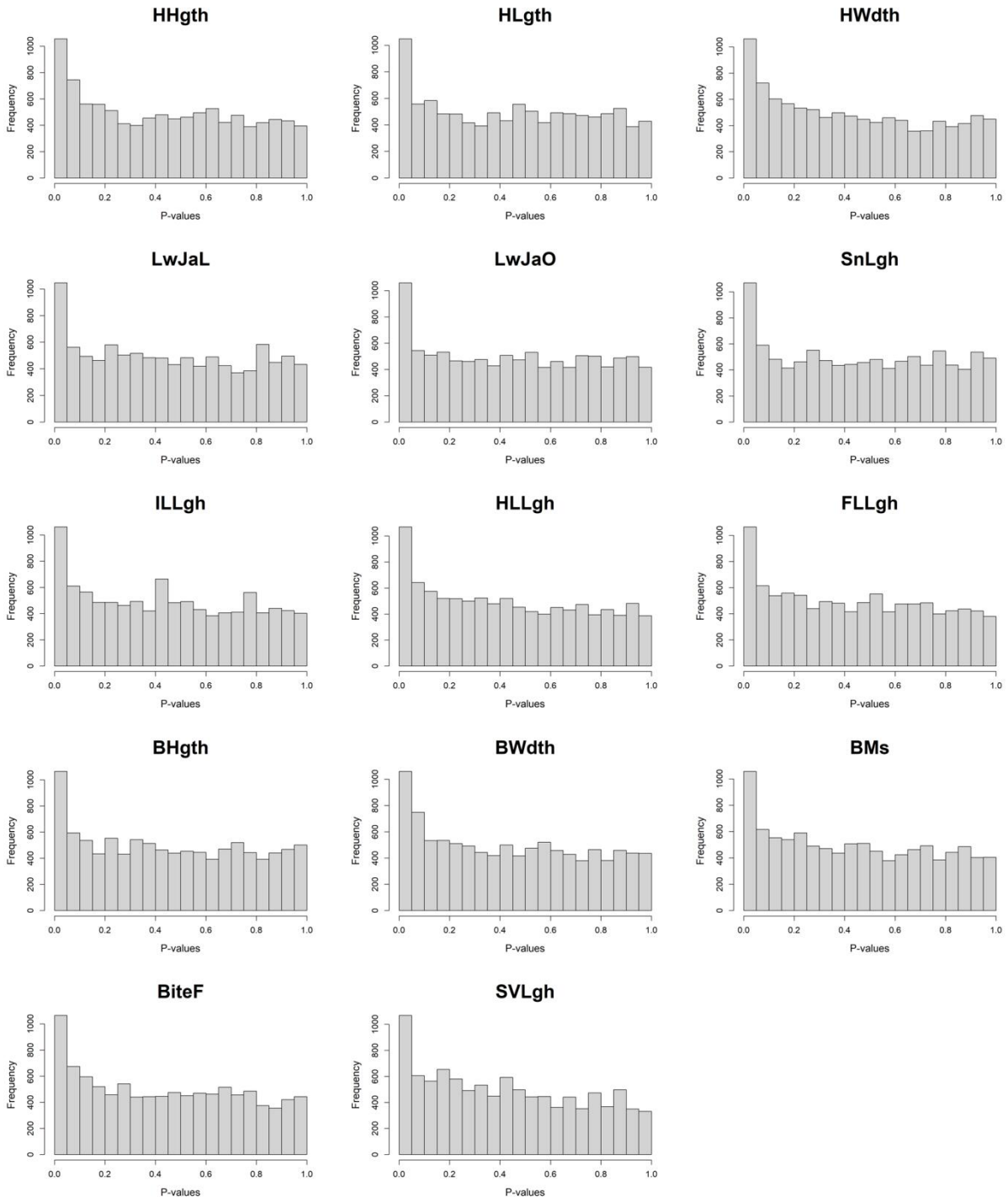

Figure S9. Histograms of adjusted p-values for all loci found in LFMM analysis of male *P. siculus* individuals from Pod Mrčaru and Pod Kopište islands. Phenotypic trait abbreviations are defined in Table S1.

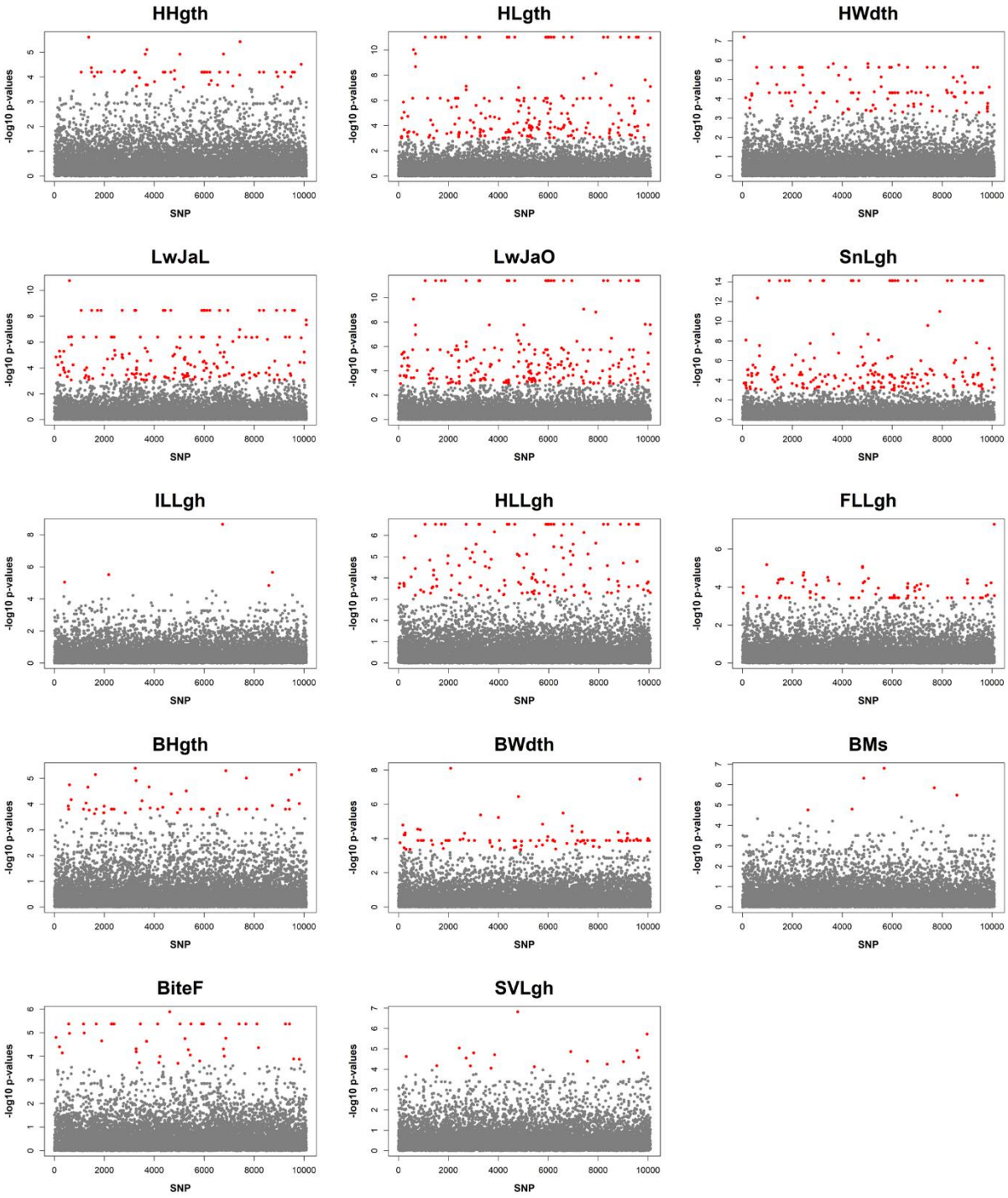

Figure S10. Manhattan plots of adjusted p-values obtained from LFMM analysis of male *P. siculus* individuals from Pod Mrčaru and Pod Kopište islands. Red color denotes SNPs with significant association to analyzed phenotypic variables (Benjamini-Hochberg FDR <0.05). Phenotypic trait abbreviations are defined in Table S1.

Crossing experiment in the common garden

Sampling and experimental design

We conducted a crossing experiment in the common garden in three consecutive years between 2017 and 2019. In order to serve as a parental generation in the experiment, we sampled *P. siculus* individuals in their natural environment on islets of Pod Mrčaru and Pod Kopište in March of 2017 and 2018. The exact dates of sampling were chosen according to weather conditions and the onset of activity on islands in the given year. Across both years, a total of 50 adult lizards were caught on each islet by use of a pole and a noose or by hand. Animals were sexed and transferred to the Zoological Garden of Zagreb in individual bags. Upon arrival to the zoo, male and female individuals were placed in separate terrariums for 4 weeks, with the aim of acclimatization and in order to make sure that caught females were not gravid. After the acclimatization period, we set up controlled crossings within and between ancestral (Pod Kopište) and transplanted population (Pod Mrčaru) for each pair of island combinations (PK male - PK female, PK male - PM female, PM male - PK female, and PM male - PM female).

The pairs in the crossing experiment were kept in glass or plastic terrariums (60x30x30 cm) equipped with UV lamps (Arcadia T5 6% UVB Forest), small infra-red lamps, peat moss, rocks for perching and basking, dried bark, and plastic containers with vermiculite for hiding and laying eggs. Terrariums containing within and between island crosses were distributed randomly in the breeding facility. Terrariums were sprayed with water daily, and a small Petri dish containing drinking water was checked and refilled according to consumption. The room was subjected to the same light regime (12L:12D) and constant temperature (23–24 °C diurnal, 20 °C nocturnal). During daylight period lizards were able to thermo-regulate by repositioning themselves respectively to the infra-red light. Individuals were kept on the same cricket-based diet – 1 or 2 small to medium sized crickets (*Gryllus assimilis*), periodically covered in calcium supplement (fine dust JBL MicroCalcium), were given to each individual depending on its size three times a week. In mid-December, temperature was gradually decreased to ~12 °C, light regime modified to 9L:15D, and feeding interrupted to induce hibernation which lasted approximately three months (until mid-March). In this period all activities were paused to be resumed once the feeding, light, and temperature regimes were re-established.

Female abdomens and terrariums were checked daily during mating season and weekly out of mating season for mating scars and laid eggs. When an egg was found, it was placed separately from the parents in a closed plastic container (100 ml; 2/3 filled with moist vermiculite), and kept in an incubator at constant temperature of 28–29 °C. After hatching, offspring were placed in individual terrariums distributed randomly through the room. Offspring were raised under the same conditions their parents were kept in and fed with the same cricket species, though much smaller in size.

All individuals were marked with color-coded visible implant fluorescent elastomer tags (Northwest Marine Technologies) for their reliable identification. New F0 individuals added to experiment in 2018 to increase the number of reared families and offspring. The substrate used for egg incubation was also changed to larger grain vermiculite in 2018 to improve egg hatching success.

A piece of tail tissue was taken from all individuals in common garden experiment and stored in 96% ethanol for genomic analyses.

Common garden phenotypic data collection

We phenotyped the parental generation after the mating period in each respective year in order to not disturb the premating behavior, and the offspring the day after they hatched and every two months afterwards until reaching approximately 18 months of age. We collected phenotypic data by photographing individuals from the dorsal side of the body and left lateral side of the head. During the photographing, lizards were placed as flat as possible on a horizontal surface with a graph paper in the background in order to ensure proper scaling. All pictures were taken with the camera (Canon EOS 450D, with Canon EF-S 18-55mm f lens) placed perpendicular to the paper, at the same distance from the object (16 cm), and using the same camera settings (automatic mode with zoom set to 18 mm for dorsal and to 35 mm for lateral pictures of the head).

The images were analyzed with image analysis software ImageJ (Schneider, Rasband, & Eliceiri, 2012) to obtain morphological measures of interest. First, eight landmarks were placed at the specific points on the left lateral pictures of the head (Fig. 2A). The coordinates of those landmarks were then exported and analyzed with custom made script in R v.4.0.0 (R Core Team, 2017) in order to measure the exact distance between them. Five morphometric measurements were obtained from the eight landmark coordinates: head height (measured at the highest part of the head at the level of orbits), head length (measured from the tip from tip of the snout to anterior edge of the ear opening), snout length (measured from the tip of the snout to the posterior end of the temporal scale), lower jaw length (measured from the tip of the lower jaw to the posterior edge of the ear opening), and lower jaw outlever (measured from the tip of the lower jaw to the anterior edge of the ear opening) (Fig. 2A). This process was repeated three times independently, the three values for each measurement were averaged, and the averaged value was used in all subsequent analysis. Dorsal images of lizards and tools available in ImageJ software were used to calculate phenotypic measures of head width (measured at the widest part of the head at the level of jugal bones) and body length to the hip (measured from the tip of the snout to the beginning of the tail) (Fig. 2B). Each measure was taken three times independently and averaged. The averaged value was used in all posterior analysis.

Using this approach we measured 7 phenotypic traits of the head and body across 68 F0, 85 F1 and 5 backcross (BC) individuals in total. We also measured bite force for a subset of individuals from the crossing experiment (54 F0 and 75 F1 individuals), using a Kistler force transducer set in a custom-built holder and connected to a Kistler charge amplifier. The bite force of F0 individuals was measured in the time outside of the breeding period and of F1 juveniles when they were approximately four-months old. Bite force was measured 3 times and only the maximum recorded value (expressed in newtons, N) was retained. This maximum value was additionally multiplied by 0.67 before further analysis in order to correct for the lever arm length.

Repeatability of the phenotyping method

To assess repeatability of the employed image analysis method we analyzed the raw values obtained across three replicate measurements of each experimental individual (68 F0, 85 F1, 5 BC). Repeatability of the image analysis method was estimated using an analysis of variance (ANOVA) approach described by Arnqvist and Mårtensson (Arnqvist & Mårtensson, 1998). Repeatability (R) was estimated as $R = S^2_A/(S^2_W+S^2_A)$, where the within-individual variation S^2_W is given by $MS_{Residual}$ and among-individual variation S^2_A is calculated as $S^2_A = (MS_{Individual}-MS_{Residual})/n$, where n is the number of replicates per individual. We further

estimated the repeatability after averaging the three replicate measures for subsequent analysis (R_n) as $R_n = n*R/(1+(n-1)*R)$. Repeatability estimates obtained using this method range from 0 to 1 where, for instance, repeatability of 0.8 indicates that 80% of the total phenotypic variation is attributable to variation that is naturally present between analyzed individuals, while the remaining 20% of phenotypic variation is attributable to differences among replicates.

To examine the repeatability of the entire phenotyping process (both photographing and image analysis), we further re-phenotyped 21 F1 individuals in October 2020. Three separate photographs were taken for each individual and each photograph was in turn analyzed three times independently, obtaining nine replicate measures for each phenotypic trait. These were analyzed using the same ANOVA approach as previously employed on full dataset. The same 21 F1 individuals were additionally measured three times independently with a digital caliper (Powerfix Profi+; ±0.01 mm), in to in order to test the difference between our image analysis and a more 'traditional' caliper-based approach. Correlations between values obtained using a caliper-based approach and those obtained using image analysis were explored using Pearson's product-moment correlation.

Repeatability analyses were conducted in R v.4.0.0 (R Core Team, 2017) using *aov()* and *cor.test()* functions from package *stats*.

The repeatability of the phenotyping procedure was deemed sufficient for all analyzed traits across both image analysis (R_n = 0.99-1 for the dataset with all 158 F0 and F1 experimental individuals) and photographing (R = 0.85-0.97 for the dataset with 21 F1 individuals re-phenotyped in October 2020) (Table S7). Furthermore, measures obtained using image analysis were found to be significantly correlated with measures obtained using traditional caliper-based phenotyping approach (21 F1 individuals; Pearson's r = 0.87-0.95) (Table S8).

Table S7. Repeatability (R) of the phenotyping procedure (extracting phenotypic measures based on landmark data) estimated from: 3 replicates per picture obtained for all 158 individuals included in the 2017-2019 common garden crossing experiment; and 9 replicates (3 pictures * 3 replicates per picture) obtained for 21 F1 individuals re-phenotyped in October 2020.

	158 individuals			**21 individuals**	
trait	***R***	***R_n***	**p-value**	***R***	**p-value**
HHgth	0.98	0.993	<2e-16 ***	0.908	<2e-16 ***
HLgth	0.997	0.999	<2e-16 ***	0.907	<2e-16 ***
HWdth	0.996	0.999	<2e-16 ***	0.885	<2e-16 ***
LwJaL	0.984	0.994	<2e-16 ***	0.908	<2e-16 ***
LwJaO	0.962	0.987	<2e-16 ***	0.914	<2e-16 ***
SnLgh	0.994	0.998	<2e-16 ***	0.850	<2e-16 ***
LtHip	0.959	0.986	<2e-16 ***	0.765	<2e-16 ***

Table S8. Correlation between measures obtained using geometric morphometry based on landmark data and measures obtained using traditional caliper-based phenotypisation approach estimated from 3 technical replicates obtained for 21 F1 individuals re-phenotyped in October 2020.

trait	Pearson's *r* [95% CI]	p-value
HHgth	0.902 [0.771 - 0.96]	2.276e-08
HLgth	0.892 [0.749 - 0.956]	5.603e-08
HWdth	0.952 [0.884 - 0.981]	3.154e-11
LwJaL	0.919 [0.808 - 0.967]	3.932e-09
LwJaO	0.907 [0.782 - 0.962]	1.414e-08
SnLgh	0.874 [0.711 - 0.948]	2.199e-07
LtHip	0.874 [0.71 - 0.948]	2.319e-07

Data transformation

Average phenotypic values obtained from the three replicate measurements of each experimental individual (apart from bite force, for which only the maximum value was considered) were size-corrected before further analyses to eliminate variation resulting from allometric growth. Size-correction was done separately per sex and generation (F0/F1), as both sex and age are known to have significant effect on lizard's growth trajectories, and our F1 individuals were phenotyped while still in the sub-adult stage. All measures were $\log_{10}$-transformed and size-corrected by linear regression on length to hip (LtHip). Regression residuals were used in all posterior analyses (apart from LtHip, which was processed raw). Obtained data for all traits was either normally distributed, or showed close to normal distribution as judged by Shapiro-Wilk test and the empirical distribution observed in a skewness-kurtosis plot (Cullen & Frey, 1999) from the package *fitdistrplus* (Delignette-Muller & Dutang, 2015).

Phenotypic differentiation in F0 and F1 individuals

A pairwise t-test was used to examine the variability in parental phenotype, and variability in offspring phenotype was examined using a one-way analysis of variance (ANOVA). Both analyses were conducted using functions available in R package *stats* (R Core Team, 2017). We further assessed whether the pattern of phenotypic differentiation in Pod Kopište and Pod Mrčaru F0 individuals resembled the one reported in 2008 (Herrel et al., 2008). To that end, we visually compared raw values and standard deviations obtained for male and female individuals in 2004-2006 (Herrel et al., 2008) to those obtained for F0 individuals in 2017 and 2018 by us.

Quantitative genetic analyses

Univariate animal model, as implemented in Bayesian *MCMCglmm* R package (Hadfield, 2010), was used to assess additive genetic variance underlying phenotypic traits connected to head size and shape in our two focal populations. To that end, we implemented an animal model with genetic group specific additive variance (Muff, Niskanen, Saatoglu, Keller, & Jensen, 2019). We derived the T^{-1} and D^{-1} components from the Cholesky decomposition of inverse A^{-1} relatedness matrix directly from the pedigree, and then scaled them by the

respective group-proportions to obtain group-specific A^{-1} relatedness matrices for each genetic group. We also included a matrix with genetic group proportions for each individual (Q) as fixed effect in the model to account for potential differences in mean breeding values between individuals from different genetic groups (Wolak & Reid, 2017). Inbreeding coefficient was not included in the model as only one individual in the pedigree was inbred, and we strived to keep the models as simple as possible. For LtHip, we additionally included sex and generation as fixed effects in the model; for all other traits the effect of those two factors was accounted for by separate size-correction of variables on LtHip before the MCMCglmm analysis itself.

We used a default normal prior with zero mean and large variance ($mu = 0$, $V = 10^8$) to model fixed effects. For additive genetic and residual variance we used a weakly informative inverse gamma prior ($V = 1$, $nu = 0.002$), as it provided better mixing properties of the chains than suggested parameter expanded priors (Muff et al., 2019; Wolak & Reid, 2017). The total number of iterations was set to 2,500,000, with a burn-in period of 500,000 and a thinning interval of 100. We visually inspected trace plots and used Heidelberger and Welch's convergence diagnostic test (Heidelberger & Welch, 1983) available with *heidel.diag()* function from R package *CODA* (Plummer et al., 2005) to ensure good mixing qualities of MCMC chains and model convergence. All models were further checked for inadequate effective sample sizes and high levels of autocorrelation.

Heritability (h^2) was calculated from posterior estimates as the ratio of additive genetic variance component to total phenotypic variance. Although we attempted to approximate narrow-sense heritability and estimate additive genetic variance component with as much precision as possible, a disproportionally large number of offspring in our pedigree came from full-sib families. Thus, we cannot completely exclude that dominance effect could have a significant influence on estimates obtained in the animal model analysis conducted in this study. Due to the limitations of the obtained pedigree it was further impossible to estimate the influence of other environmental and/or non-additive factors (e.g. maternal or permanent environment effects), which may also contribute to phenotypic variation in our analyzed traits of interest.

It has been proposed that heritability may not be the most suitable measure to approximate the evolutionary potential of a trait, i.e. its evolvability (Garcia-Gonzalez, Simmons, Tomkins, Kotiaho, & Evans, 2012; Houle, 1992). However, due to the use of residuals in our animal model analyses, we were likewise unable to calculate alternative measures of additive genetic variation standardized by the trait mean (Garcia-Gonzalez et al., 2012), such as the coefficient of additive genetic variation (CV_A) and its square (I_A).

Supplementary Results

Floristic and vegetation survey of Pod Kopište and Pod Mrčaru islands

A total of 36 plant species was recorded on Pod Kopište and only 13 plant species on Pod Mrčaru (Table S9), which is in accordance with habitat diversity and islands area. Species composition is indicative for nutrient rich soil, especially on Pod Kopište. Dominant habitat type for central part of Pod Kopište is Wall Barley (*Hordeum murinum* ssp. *leporinum*) community (As. *Hordeetum leporine* Br.-Bl. 1936), for coastal part of Pod Kopište is *Limonium anfractum* rock cliff community (As. *Limonietum anfracti* Ilijanić 1982), which is also dominant habitat on Pod Mrčaru. The most frequent plant species on Pod Mrčaru, *Crithmum maritimum* and *Lavatera arborea,* are either rare or absent on Pod Kopište. Most dominant species in central part of Pod Kopište are *Bromus madritensis* and *Hordeum murinum* ssp. *leporinum,* that are resistant to permanent overgrazing, and which are rare or absent on Pod Mrčaru.

Table S9. Cover percentage of plant species on Pod Kopište and Pod Mrčaru expressed with Braun-Blanquet vegetation survey categories

Location Species	Pod Kopište -central part	Pod Kopište - coast	Pod Mrčaru
Hordeum murinum L. ssp. *leporinum*	5	2a	r
Lotus cytisoides L.	+	1	2b
Atriplex prostrata Boucher ex DC. in Lam. et DC.	r	r	1
Asparagus acutifolius L.	r	r	r
Lagurus ovatus L.	2m	+	
Geranium molle L.	1	r	
Medicago minima (L.) Bartal.	1	r	
Melilotus indica (L.) All.	1	1	
Desmazeria marina (L.) Druce	+	2m	
Desmazeria rigida (L.) Tutin	+	r	
Parapholis incurva (L.) C.E.Hubb.	+	2a	
Valantia muralis L.	+	2m	
Sisymbrium officinale (L.) Scop.	r	r	
Malva neglecta Wallr.	r	r	
Fumaria officinalis L.	r	r	
Amaranthus deflexus L.	r	r	
Cynodon dactylon (L.) Pers.	1		+
Chenopodium vulvaria L.	r		1
Bromus madritensis L.	4		
Brachypodium distachyon (L.) P.Beauv.	1		
Erodium cicutarium (L.) Ľ Hér.	1		
Herniaria glabra L.	+		
Erodium malacoides (L.) Ľ Hér.	r		
Juniperus phoenicea L.	r		
Marrubium incanum Desr.	r		
Olea europaea L.	r		
Crithmum maritimum L.		r	3
Allium ampeloprasum L.		r	2b
Limonium dictyophorum (Tausch) Degen		r	1
Silene vulgaris (Moench) Garcke ssp. *angustifolia* Hayek		r	+
Sonchus asper (L.) Hill		r	r
Spergularia salina J. Presl et C. Presl		2a	
Chenopodium murale L.		1	
Bromus rigidus Roth		+	
Arenaria leptoclados (Rchb.) Guss.		r	
Parietaria judaica L.		r	
Lavatera arborea L.			3
Arthrocnemum macrostachyum (Moric.) C. Koch			r

Table S10. Availability of invertebrates on three islands, Kopište, Pod Kopište, and Pod Mrčaru based on 12 pitfall traps left for 48h. Mass is expressed in mg.

	Kopište (KP)				Pod Kopište (PK)				Pod Mrčaru (PM)			
taxon	**number**	**mass**	**%mass**	**%number**	**number**	**mass**	**%mass**	**%number**	**number**	**mass**	**%mass**	**%number**
Acarina	3	0.7	0.1	0.7								
Aphididae	2	0.5	0.1	0.5	2	0.8	0.00	0.8				
Aranea	6	239.9	32.8	1.5	28.00	314.8	19.0	10.7	45	19.53	0.58	3.74
Chilopoda	1	14.4	2.0	0.2								
Coleoptera	2	2.5	0.3	0.5	8.00	32.7	2.0	3.1	21	39.62	1.18	1.75
Collembola	325	230.8	31.6	80.4	102	70.4	4.3	38.9	25	7.80	0.23	2.08
Crustacea									1	8.08	0.24	0.08
Dermoptera									2	134.88	4.00	0.17
Dictyoptera	1	8.2	1.1	0.2								
Diplopoda	2	47.8	6.5	0.5								
Diptera	22	62.3	8.5	5.4	29	48.0	2.9	11.1	31	44.06	1.31	2.58
Gastropoda	1	0.2	0.0	0.2					9	251.48	7.46	0.75
Hemiptera	1	0.2	0.0	0.2	5	318.0	19.2	1.9	4	3.60	0.11	0.33
Homoptera					2	1.1	0.1	0.8	5	13.30	0.39	0.42
Hymenoptera (Formicidae)	6	2.6	0.4	1.5	12	8.8	0.5	4.6	12	12.08	0.36	1.00
Hymenoptera (wasps)					4	1.5	0.1	1.5				
Isopoda	1	28.4	3.9	0.2	13	800.0	48.4	5.0	32	2636.44	78.21	2.66
Lepidoptera									1	3.65	0.11	0.08
Opiliones	17	48.9	6.7	4.2								
Peudoscorpionidae	4	1.5	0.2	1.0					1	0.71	0.02	0.08
Thysanoptera					55	52.6	3.2	21.0	3	0.31	0.01	0.25
Thysanura	10	42.3	5.8	2.5								
larvae					2.00	5.5	0.3	0.8	1011	195.61	5.80	84.04

Table S11. Availability of invertebrates on three islands, Kopište, Pod Kopište, and Pod Mrčaru based on 40 minutes of sweep sampling covering all vegetation types on the islands. Mass is expressed in mg.

	Kopište (KP)				**Pod Kopište (PK)**				**Pod Mrčaru (PM)**			
taxon	number	mass	%mass	%number	number	mass	%mass	%number	number	mass	%mass	%number
Aphididae					40	32.3	0.6	2.1				
Aranea	31	67.4	5.2	13.4	6	14.8	0.3	0.3	9	22.4	0.4	1.8
Coleoptera	48	128.5	10.0	20.7	16	5.8	0.1	0.8	1	0.4	0.01	0.2
Dermoptera					1	0.2	0.00	0.1				
Diptera	72	111.1	8.6	31.0	644	1635.7	32.5	33.7	268	488.2	8.2	53.7
Gastropoda	3	98.3	7.6	1.3	1	3.4	0.1	0.1	1	11.5	0.2	0.2
Hemiptera	9	112.3	8.7	3.9	61	80.8	1.6	3.2	27	32.1	0.5	5.4
Homoptera	18	86.4	6.7	7.8	603	909.7	18.1	31.6	81	157.3	2.6	16.2
Hymenoptera - bees	2	520.3	40.4	0.9	4	1091.9	21.7	0.2	11	5097.8	85.4	2.2
Hymenoptera - Formicidae	12	13.2	1.0	5.2	2	2.2	0.04	0.1	10	3.5	0.1	2.0
Hymenoptera - wasps	25	50.2	3.9	10.8	486	406.5	8.1	25.5	24	11.9	0.2	4.8
Lepidoptera	3	18.2	1.4	1.3	13	327.9	6.5	0.7	1	19.0	0.3	0.2
Orthoptera	4	20.8	1.6	1.7								
Peudoscorpionidae									2	0.8	0.01	0.4
Thysanoptera					3	1.0	0.02	0.2	46	7.5	0.1	9.2
larvae	5	62.0	4.8	2.2	26	520.1	10.3	1.4	18	115.5	1.9	3.6
unidentified					3	0.4	0.01	0.2				

Table S12. Shannon diversity (H) and evenness (E_H) indices for the invertebrate fauna of the three islands sampled based on proportions in total mass and number of taxa and for two sampling methods (sweep netting and pitfall traps)

	Kopište (KP)		**Pod Kopiste(PK)**		**Pod Mrcaru (PM)**	
	mass	**number**	**mass**	**number**	**mass**	**number**
			Sweep netting			
H	2.00	1.98	1.76	1.47	0.62	1.57
E_H	0.71	0.70	0.62	0.52	0.22	0.55
			Pitfalls			
H	1.79	0.92	1.47	1.83	0.91	0.78
E_H	0.57	0.29	0.47	0.58	0.29	0.25

Table S13. *Podarcis siculus* genome assembly characteristics.

Genome feature	Value
Number of scaffolds >= 10 kb	1.17 K
N50 edge size	13.46 Kb
N50 contig size	75.56 Kb
N50 phase block size	1.11 Mb
N50 scaffold size	37.45 Mb
% of base assembly missing from scaffolds >= 10 kb	3.57 %
Assembly size (only scaffolds >= 10 kb)	1.33 Gb

Table S14. Pairwise F_{ST} between fourteen wild *P. siculus* populations (all values are significant at $p<0.0001$). Population codes are defined in Fig. 1.

	OB	**VC**	**DU**	**OS**	**ST**	**KL**	**PJ**	**PG**	**SC**	**BJ**	**KP**	**PK**	**PM**
RK	0.185	0.321	0.370	0.332	0.234	0.434	0.447	0.446	0.446	0.528	0.475	0.508	0.528
OB		0.277	0.340	0.300	0.196	0.404	0.418	0.418	0.417	0.499	0.448	0.484	0.503
VC			0.437	0.398	0.310	0.502	0.523	0.523	0.526	0.602	0.552	0.579	0.597
DU				0.278	0.376	0.532	0.549	0.544	0.547	0.622	0.570	0.596	0.613
OS					0.340	0.507	0.523	0.518	0.522	0.593	0.550	0.579	0.596
ST						0.424	0.444	0.445	0.444	0.548	0.473	0.507	0.529
KL							0.168	0.383	0.326	0.482	0.351	0.388	0.414
PJ								0.356	0.273	0.463	0.293	0.334	0.362
PG									0.213	0.425	0.236	0.275	0.306
SC										0.307	0.071	0.119	0.153
BJ											0.266	0.300	0.330
KP												0.077	0.110
PK													0.045

Table S15. Recent migration rates in fourteen wild *P. siculus* populations. Population codes are defined in Fig 1.

		Population of origin													
Migration rate per population (m)		**RK**	**OB**	**VC**	**DU**	**OS**	**ST**	**KL**	**PJ**	**PG**	**SC**	**BJ**	**KP**	**PK**	**PM**
RK	mean	0.889	0.009	0.008	0.008	0.009	0.009	0.009	0.009	0.009	0.009	0.009	0.008	0.009	0.009
	95% CI	0.840; 0.937	-0.008; 0.025	-0.007; 0.024	-0.008; 0.024	-0.008; 0.025	-0.008; 0.025	-0.008; 0.025	-0.008; 0.025	-0.008; 0.025	-0.008; 0.025	-0.008; 0.025	-0.008; 0.025	-0.008; 0.025	-0.008; 0.025
OB	mean	0.009	0.889	0.009	0.009	0.009	0.009	0.009	0.009	0.009	0.009	0.009	0.009	0.008	0.008
	95% CI	-0.008; 0.025	0.840; 0.938	-0.008; 0.025	-0.007; 0.025	-0.008; 0.025	-0.008; 0.025	-0.008; 0.025	-0.008; 0.025	-0.007; 0.024	-0.008; 0.025	-0.008; 0.025	-0.008; 0.025	-0.008; 0.025	-0.008; 0.025
VC	mean	0.009	0.009	0.889	0.008	0.009	0.008	0.009	0.009	0.009	0.008	0.008	0.008	0.009	0.009
	95% CI	-0.008; 0.025	-0.008; 0.025	0.840; 0.937	-0.008; 0.024	-0.008; 0.025	-0.008; 0.025	-0.008; 0.025	-0.008; 0.025	-0.008; 0.025	-0.008; 0.025	-0.008; 0.025	-0.008; 0.025	-0.008; 0.025	-0.008; 0.025
DU	mean	0.008	0.009	0.009	0.889	0.009	0.009	0.008	0.008	0.009	0.009	0.009	0.009	0.008	0.009
	95% CI	-0.007; 0.024	-0.008; 0.025	-0.008; 0.025	0.840; 0.938	-0.008; 0.025	-0.008; 0.025	-0.008; 0.024	-0.008; 0.025	-0.008; 0.025	-0.008; 0.025	-0.008; 0.025	-0.008; 0.025	-0.008; 0.024	-0.008; 0.025
OS	mean	0.009	0.008	0.008	0.009	0.889	0.008	0.009	0.008	0.009	0.008	0.009	0.009	0.009	0.009
	95% CI	-0.008; 0.025	-0.008; 0.025	-0.008; 0.025	-0.008; 0.025	0.840; 0.938	-0.008; 0.025	-0.008; 0.026	-0.008; 0.024	-0.008; 0.026	-0.008; 0.024	-0.008; 0.025	-0.008; 0.025	-0.007; 0.025	-0.008; 0.025
ST	mean	0.010	0.011	0.010	0.011	0.010	0.865	0.011	0.010	0.010	0.010	0.011	0.010	0.010	0.010
	95% CI	-0.009; 0.030	-0.010; 0.031	-0.009; 0.030	-0.009; 0.030	-0.009; 0.030	0.809; 0.920	-0.009; 0.030	-0.009; 0.030	-0.010; 0.030	-0.010; 0.031	-0.009; 0.030	-0.010; 0.030	-0.009; 0.030	-0.009; 0.030
KL	mean	0.009	0.009	0.009	0.009	0.009	0.009	0.880	0.009	0.009	0.009	0.009	0.009	0.009	0.009
	95% CI	-0.008; 0.027	-0.009; 0.027	-0.009; 0.028	-0.009; 0.027	-0.008; 0.027	-0.008; 0.027	0.829; 0.931	-0.008; 0.027	-0.008; 0.027	-0.008; 0.026	-0.008; 0.027	-0.008; 0.026	-0.008; 0.027	-0.008; 0.027
PJ	mean	0.010	0.010	0.010	0.010	0.010	0.010	0.010	0.872	0.010	0.010	0.010	0.010	0.010	0.010
	95% CI	-0.009; 0.028	-0.009; 0.029	-0.009; 0.029	-0.009; 0.028	-0.009; 0.028	-0.009; 0.029	-0.009; 0.029	0.819; 0.926	-0.008; 0.028	-0.009; 0.028	-0.009; 0.029	-0.009; 0.029	-0.009; 0.028	-0.009; 0.029
PG	mean	0.010	0.010	0.010	0.010	0.010	0.010	0.010	0.010	0.873	0.010	0.010	0.010	0.010	0.010
	95% CI	-0.008; 0.027	-0.009; 0.028	-0.009; 0.028	-0.009; 0.029	-0.008; 0.028	-0.009; 0.029	-0.009; 0.029	-0.009; 0.029	0.819; 0.927	-0.008; 0.028	-0.009; 0.028	-0.009; 0.028	-0.009; 0.028	-0.009; 0.029
SC	mean	0.010	0.010	0.010	0.010	0.010	0.010	0.010	0.010	0.010	0.869	0.010	0.010	0.010	0.010
	95% CI	-0.009; 0.030	-0.009; 0.029	-0.009; 0.029	-0.009; 0.030	-0.009; 0.029	-0.009; 0.030	-0.009; 0.029	-0.009; 0.029	-0.009; 0.030	0.814; 0.924	-0.009; 0.029	-0.009; 0.029	-0.009; 0.029	-0.009; 0.029
BJ	mean	0.010	0.010	0.010	0.010	0.010	0.010	0.010	0.010	0.010	0.010	0.873	0.010	0.010	0.010
	95% CI	-0.009; 0.028	-0.009; 0.029	-0.009; 0.028	-0.008; 0.028	-0.009; 0.028	-0.009; 0.028	-0.009; 0.028	-0.009; 0.028	-0.009; 0.029	-0.008; 0.028	0.819; 0.926	-0.009; 0.029	-0.009; 0.029	-0.009; 0.028
KP	mean	0.008	0.008	0.008	0.007	0.008	0.007	0.007	0.008	0.008	0.008	0.008	0.902	0.007	0.008
	95% CI	-0.007; 0.022	-0.007; 0.022	-0.007; 0.022	-0.007; 0.022	-0.006; 0.022	-0.007; 0.022	-0.007; 0.022	-0.007; 0.022	-0.007; 0.022	-0.007; 0.022	-0.007; 0.022	0.857; 0.946	-0.007; 0.022	-0.007; 0.022
PK	mean	0.006	0.006	0.006	0.006	0.006	0.006	0.006	0.006	0.006	0.006	0.006	0.006	0.919	0.006
	95% CI	-0.006; 0.018	-0.006; 0.018	-0.006; 0.018	-0.006; 0.018	-0.006; 0.018	-0.006; 0.019	-0.006; 0.018	-0.006; 0.018	-0.006; 0.018	-0.006; 0.018	-0.006; 0.018	-0.006; 0.018	0.881; 0.958	-0.006; 0.019
PM	mean	0.006	0.006	0.006	0.006	0.006	0.006	0.006	0.006	0.006	0.006	0.006	0.006	0.006	0.922
	95% CI	-0.005; 0.017	-0.005; 0.017	-0.006; 0.018	-0.005; 0.017	-0.005; 0.017	-0.006; 0.018	-0.006; 0.018	-0.005; 0.018	-0.005; 0.017	-0.006; 0.018	-0.005; 0.018	-0.005; 0.017	-0.006; 0.018	0.886; 0.959

Table S16. Allelic diversity indices and effective population size (N_E) in fourteen wild *P. siculus* populations, and inter- and intra-population Pod Kopište (PK) and Pod Mrčaru (PM) crosses (population codes are defined in Fig. 1 and Table S5).

ID	N	AR		Ho	He	π		FIS	N_E	
		Mean	95% CI			Mean	SD		Mean	SD
RK	19	1.65	[1.63, 1.67]	0.192	0.217	0.327	0.144	0.140****	127.5	2.3
OB	19	1.70	[1.68, 1.72]	0.196	0.229	0.321	0.144	0.170****	308.2	12.9
VC	19	1.60	[1.58, 1.62]	0.179	0.202	0.327	0.150	0.136****	662.6	66.2
DU	19	1.53	[1.52, 1.54]	0.174	0.189	0.352	0.143	0.107***	139.7	3.7
OS	19	1.60	[1.59, 1.61]	0.205	0.222	0.368	0.141	0.104**	235.6	12.3
ST	18	1.67	[1.64, 1.70]	0.165	0.200	0.285	0.151	0.203****	566.8	45.9
KL	19	1.40	[1.38, 1.41]	0.119	0.126	0.307	0.151	0.081*	736.3	131.2
PJ	19	1.37	[1.35, 1.39]	0.089	0.100	0.251	0.152	0.131****	377.0	36.8
PG	19	1.37	[1.34, 1.39]	0.105	0.109	0.281	0.160	0.066	552.7	83.1
SC	19	1.38	[1.36, 1.40]	0.100	0.105	0.262	0.154	0.079**	281.5	19.6
BJ	19	1.16	[1.15, 1.17]	0.044	0.046	0.265	0.164	0.054	168.6	19.1
KP	19	1.39	[1.36, 1.40]	0.106	0.110	0.271	0.153	0.057	216.9	12.2
PK16	19	1.35	[1.34, 1.36]	0.105	0.105	0.291	0.148	0.033	220.0	18.3
PM16	19	1.32	[1.30, 1.33]	0.093	0.095	0.287	0.151	0.042	318.9	31.5
PK17	19	1.34	[1.33, 1.35]	0.102	0.100	0.284	0.147	0.012	365.3	40.7
PM17	19	1.31	[1.30, 1.32]	0.093	0.090	0.275	0.151	-0.014	230.3	16.3
PK18	19	1.34	[1.33, 1.35]	0.102	0.102	0.287	0.149	0.024	618.6	132.2
PM18	19	1.32	[1.31, 1.33]	0.098	0.097	0.292	0.152	0.013	306.0	44.2
PKPK	19	1.33	[1.32, 1.35]	0.105	0.102	0.296	0.151	-0.003	19.7[a]	0.2
PKPM	18	1.33	[1.32, 1.34]	0.108	0.101	0.298	0.150	-0.038	13.4[b]	0.0
PMPK	19	1.34	[1.32, 1.35]	0.104	0.101	0.290	0.149	-0.006	25.6[c]	0.3
PMPM	19	1.31	[1.30, 1.32]	0.099	0.096	0.301	0.151	-0.005	13.7[d]	0.2

ID, population code; N, number of samples (all values calculated on max. 19 random samples); AR, average allelic richness and 95% confidence intervals; Ho, observed heterozygosity; He, expected heterozygosity; π, average nucleotide diversity and standard deviation; F_{IS}, Inbreeding coefficient: * significant at $p < 0.05$; ** significant at $p < 0.01$; *** significant at $p < 0.001$; **** significant at $p < 0.0001$; N_E, average effective population size. Average number of parents (F0) in dataset: [a] 16 [b]13 [c]18.3 [d]15.3

Table S17. Loci associated with principal components (PC) of environmental covariates in BayPass analysis (GEA), and their overlap with loci putatively under directional selection across twelve *P. siculus* populations (XtX), and 116 PK-PM outlier loci ("PKPM outliers").

	GEA	**GEA ∩ XtX**	**GEA ∩ "PKPM outliers"**	**GEA ∩ XtX ∩ "PKPM outliers"**
PC1	1940	102	12	2
PC2	244	50	0	0
PC3	1142	124	8	3
PC4	738	106	7	1
PC5	83	104	2	1
UNIQUE LOCI	4431	343	25	5

Table S18. Loci associated with phenotypic traits in LFMM analysis (GPA) of male and female PK and PM individuals, and their overlap with 116 PK-PM outlier loci (PKPM "outliers"). Phenotypic trait codes are defined in Table S1.

trait	♀	♀ ∩ "**PKPM outliers**"	♂	♂ ∩ "**PKPM outliers**"
HHgth	168	-	53	-
HLgth	21	1	213	1
HWdth	12	-	109	-
LwJaL	67	3	182	3
LwJaO	37	1	233	3
SnLgh	51	3	205	1
ILLgh	17	2	5	1
HLLgh	19	5	134	7
FLLgh	16	1	76	5
BHgth	21	2	48	-
BWdth	5	-	90	2
BiteF	209	1	42	-
BMs	40	-	6	-
SVLgh	49	6	18	3
UNIQUE LOCI	590	16	514	16

Table S19. Genomic RDA variance partitioning results for fourteen wild *P. siculus* populations. Model significance was determined using ANOVA after 999 permutations.

Mode	Predictors/effect	Adj. R^2 (total variance)	Model significance
RDA full	Ecology + geography	0.5903	p=0.001
pRDA ecology	Ecology | geography	0.1889	p=0.012
pRDA geography	Geography | ecology	0.0394	p=0.185
NA	Ecology ∩ geography	0.3621	NA

Table S20. Phenotypic RDA variance partitioning results for male and female individuals from fourteen wild *P. siculus* populations. Model significance was determined using ANOVA after 999 permutations.

	Model	Predictors/effect	Adj. R^2 (total variance)	Model significance
Males	RDA full	Ecology + geography	0.1423	p=0.001
	pRDA ecology	Ecology | geography	0.1360	p=0.001
	pRDA geography	Geography | ecology	0.0173	p=0.002
	NA	Ecology ∩ geography	-0.0111	NA
Females	RDA full	Ecology + geography	0.099	p=0.001
	pRDA ecology	Ecology | geography	0.0829	p=0.001
	pRDA geography	Geography | ecology	-0.0003	p=0.462
	NA	Ecology ∩ geography	0.0163	NA

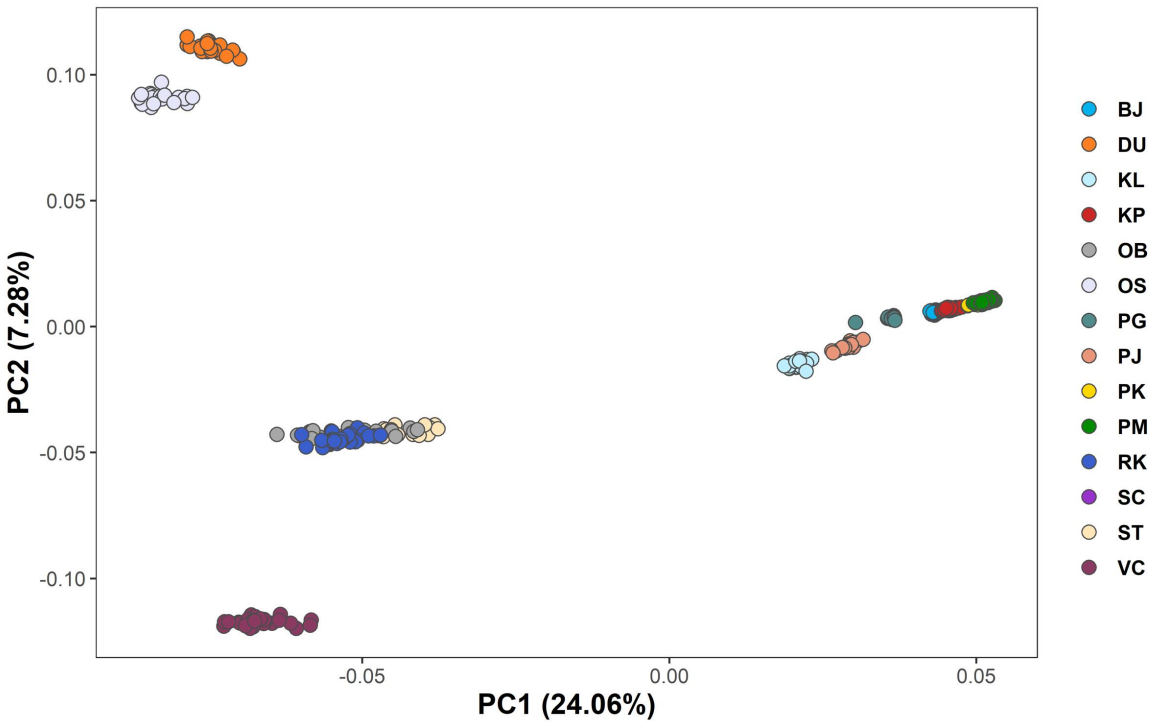

Figure S11. Principal component (PC) analysis of allele frequencies in fourteen wild *P. siculus* populations. Population codes are defined in Fig. 1.

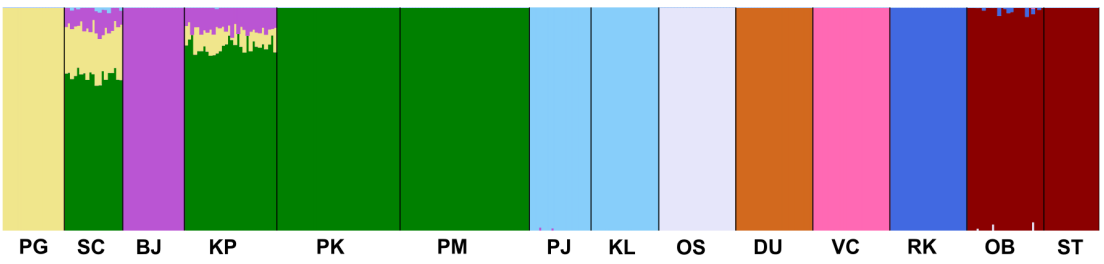

Figure S12. Bayesian inference of ancestral genomic components in fourteen wild *P. siculus* populations, computed in software *fastStructure* (K=9). Population codes are defined in Fig. 1.

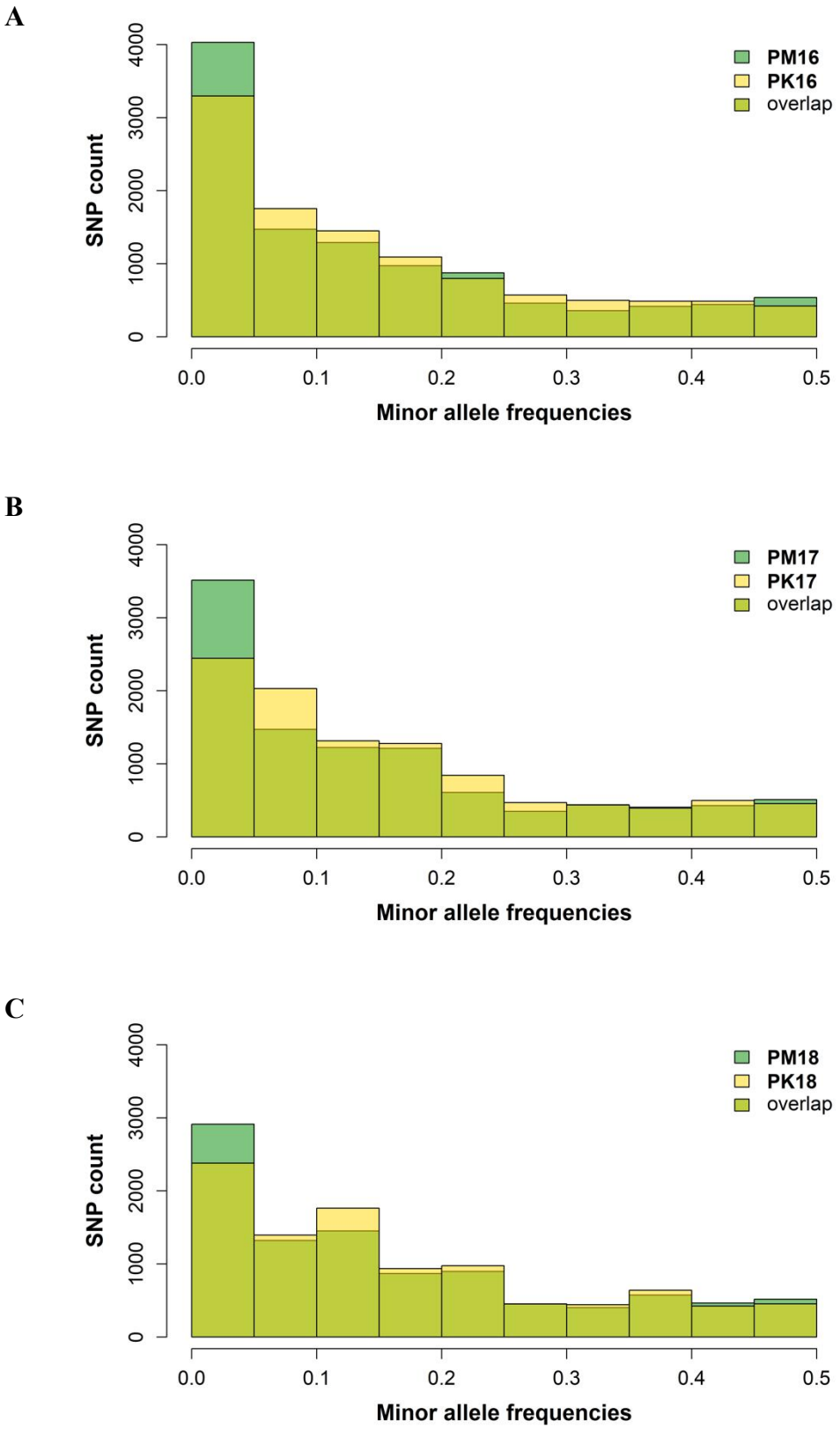

Figure S13. Distribution of minor allele frequencies (MAF) in Pod Kopište (PK) and Pod Mrčaru (PM) populations in A) 2016, B) 2017, C) 2018.

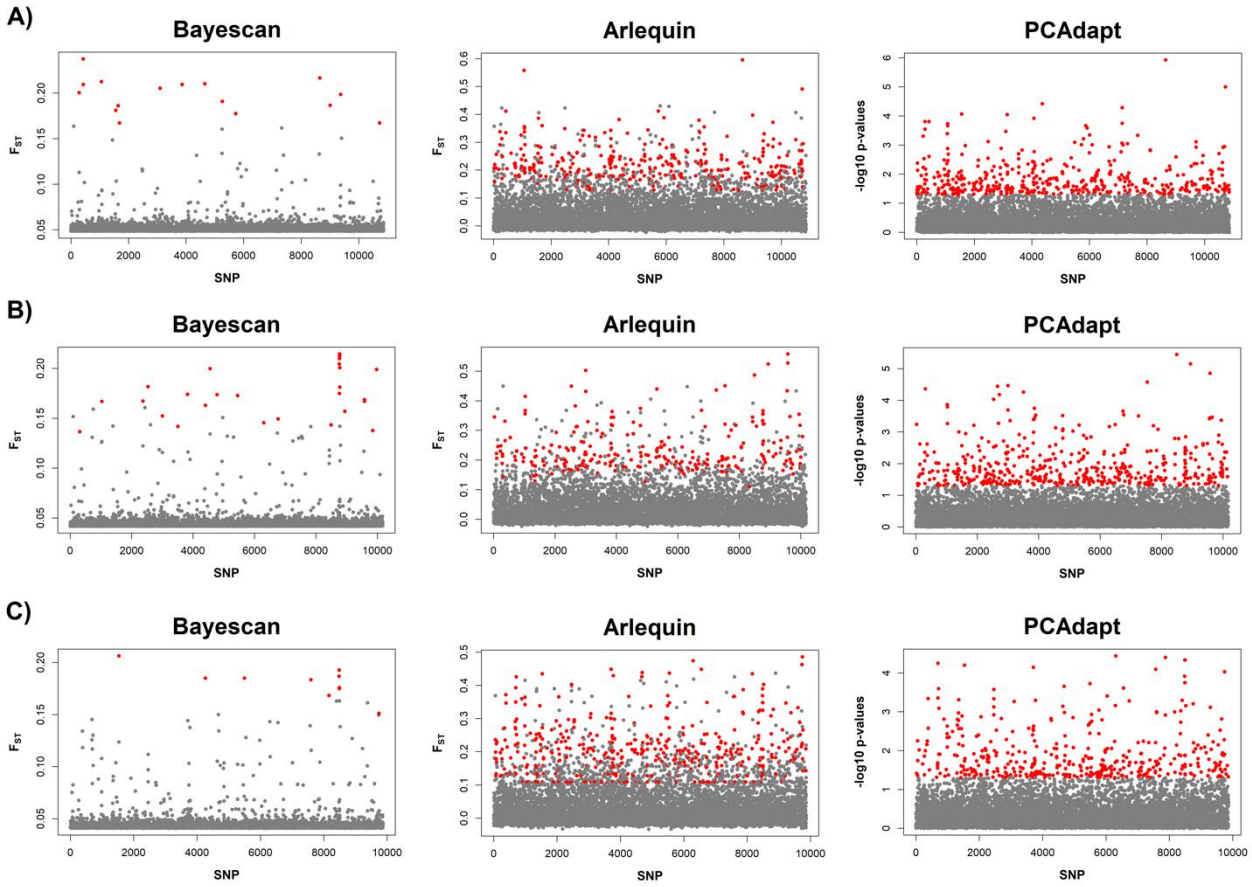

Figure S14. Manhattan plot for loci detected in PM and PK populations across each analyzed year and each genome scan method used **A)** 2016, **B)** 2017, **C)** 2018.

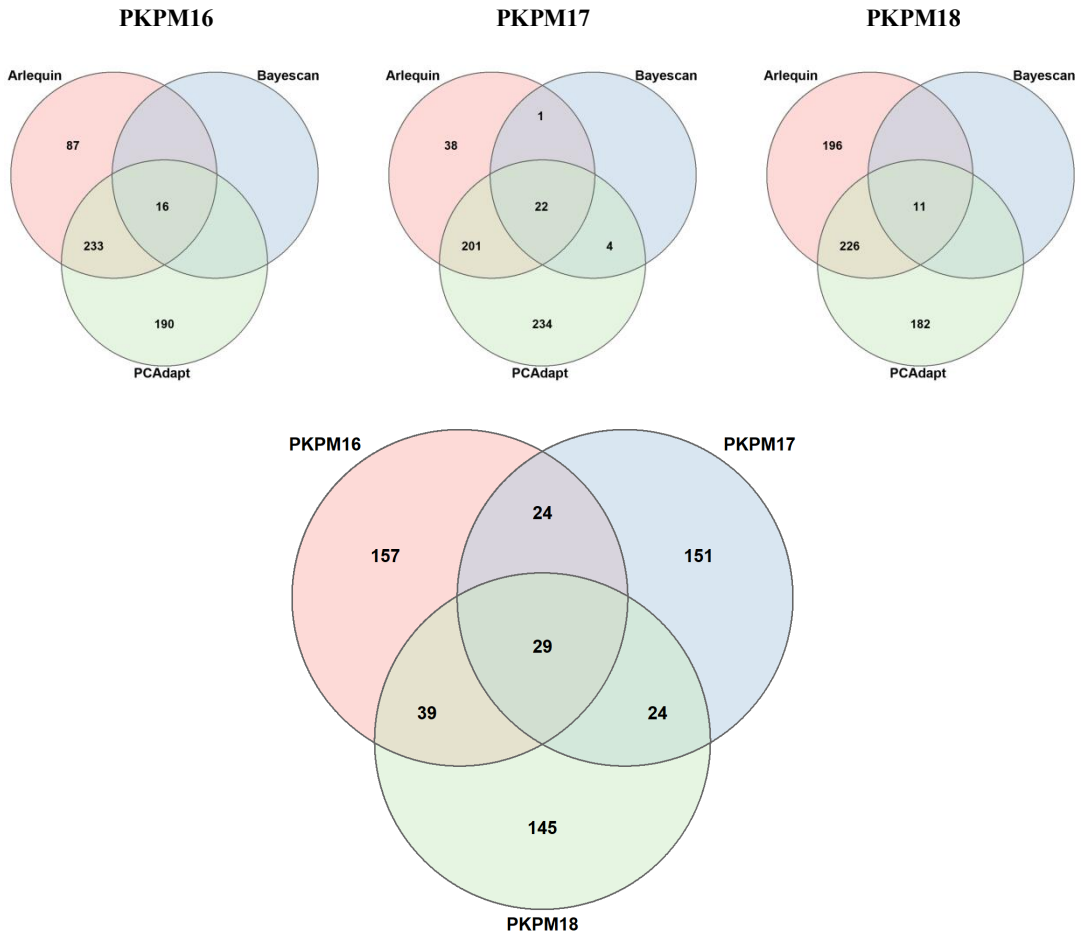

Figure S15. Venn diagram showing overlaps among outlier loci identified in Arlequin, Bayescan and *PCAdapt* genome scan analyses of Pod Kopište (PK) and Pod Mrčaru (PM) populations in three yearly sampling comparisons (2016, 2017, 2018) on top, and the overlap among outliers pinpointed in at least two out of three genome scans in each respective sampling year on the bottom. 116 loci in total were repeatably identified in at least two of three yearly comparisons.

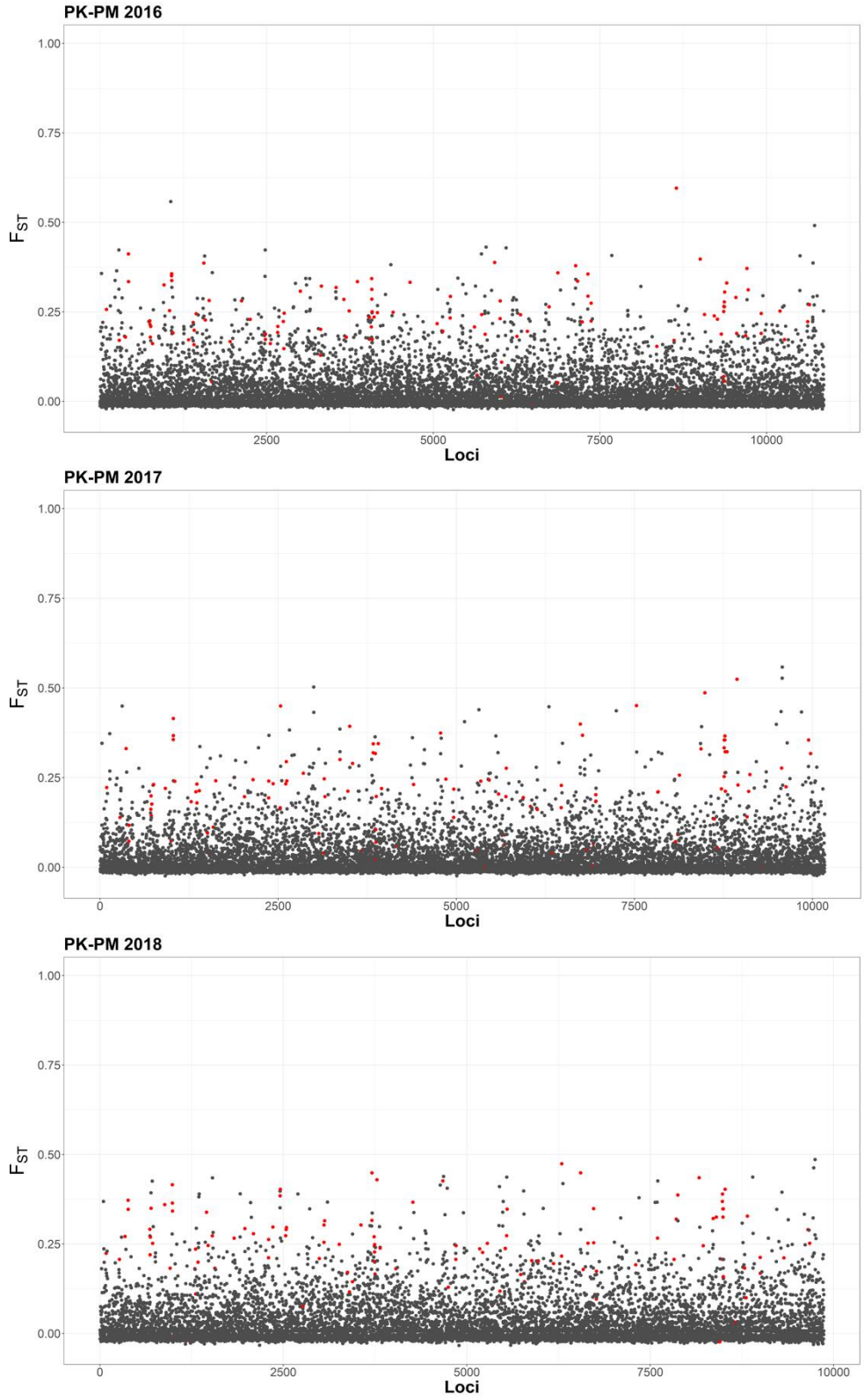

Figure S16. Manhattan plots of locus specific pairwise F_{ST} between Pod Kopište (PK) and Pod Mrčaru (PM) populations in three yearly sampling comparisons (2016, 2017, 2018). Red dots denote 116 "PKPM outlier" loci. Number of individuals analysed (N) and polymorphic SNP loci per year: 10859 in 2016 (N=82), 10171 in 2017 (N=79) and 9867 in 2018 (N=58).

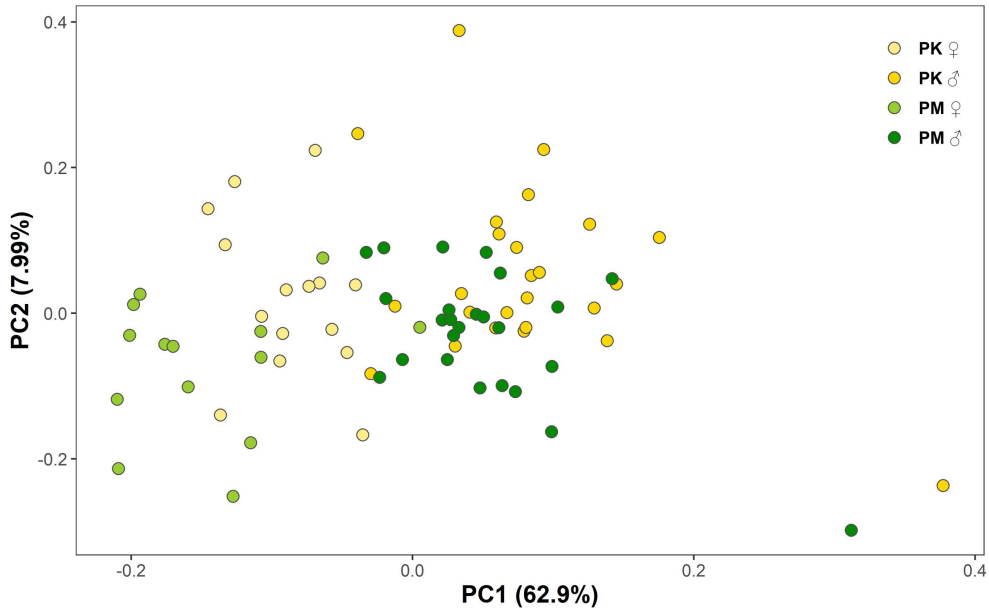

Figure S17. Principal component (PC) analysis of fourteen phenotypic traits in male and female Pod Kopište (PK) and Pod Mrčaru (PM) *P. siculus* individuals sampled in 2016. Generalized linear model (GLM) fitted in ANOVA on PC1 scores underlined significant separation according to analyzed groups (p = <2e-16 ***).

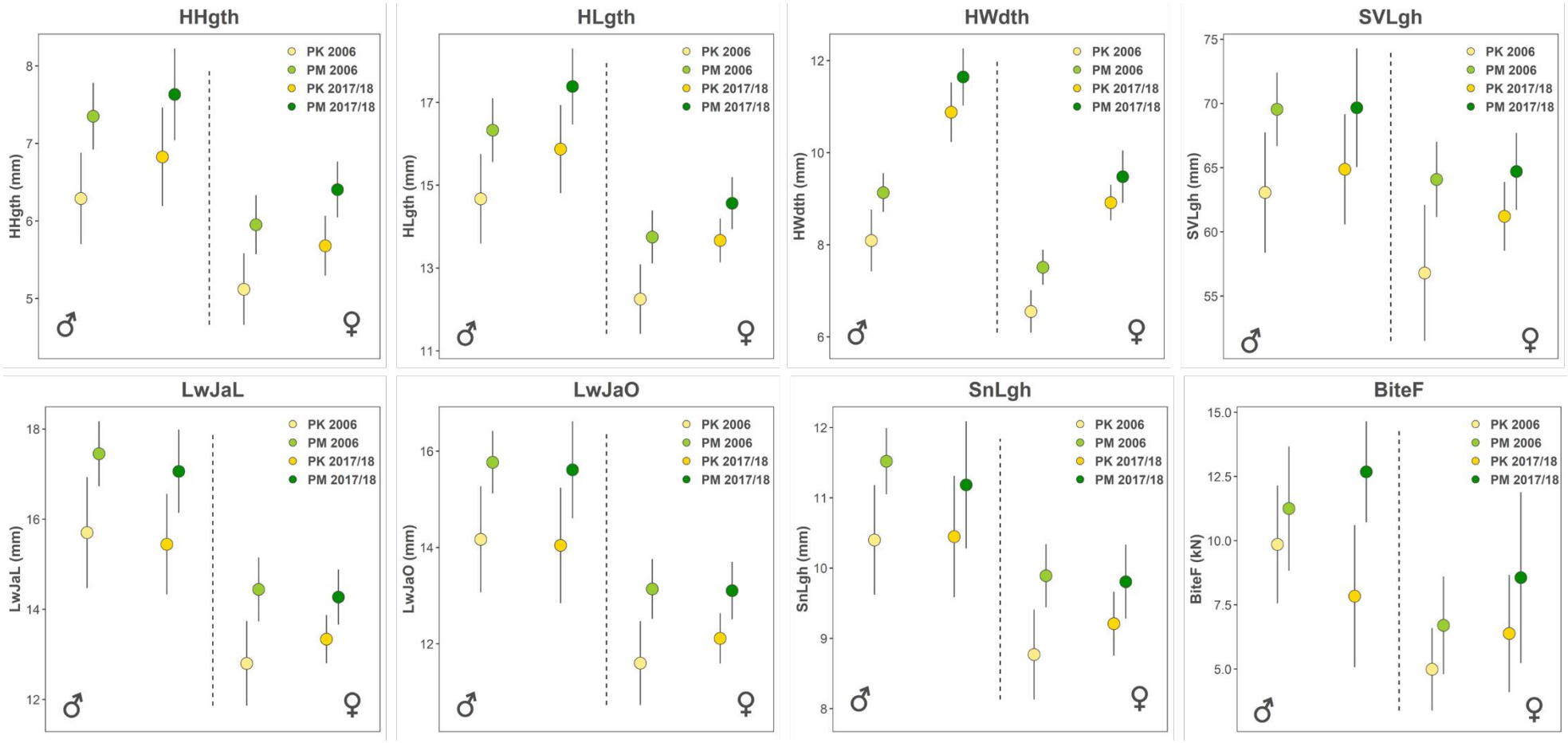

Figure S18. Raw population mean and standard deviation values for 8 traits recorded for male and female *P. siculus* individuals from Pod Kopište (PK) and Pod Mrčaru (PM) populations in 2006 (Herrel et al., 2008), and for experimental F0 individuals sampled for this study in 2017 and 2018. Individuals in 2006 were measured using a caliper, and individuals in 2017/18 using image processing. Bite force was measured using the same method in 2006 and 2017/18 but by a different observer. Phenotypic trait codes are defined in Fig. 2 and Table S1.

Supplementary references

Altschul, S. F., Gish, W., Miller, W., Myers, E. W., & Lipman, D. J. (1990). Basic local alignment search tool. *Journal of Molecular Biology*, *215*(3), 403–410. https://doi.org/10.1016/S0022-2836(05)80360-2

Andrews, S., Krueger, F., Seconds-Pichon, A., Biggins, F., & Wingett, S. (2010, January 1). FastQC. A quality control tool for high throughput sequence data. Retrieved February 24, 2020, from https://www.bioinformatics.babraham.ac.uk/projects/fastqc/

Arnqvist, G., & Mårtensson, T. (1998). Measurement error in geometric morphometrics: Empirical strategies to assess and reduce its impact on measures of shape. *Acta Zoologica Academiae Scientiarum Hungaricae*, *44*(1–2), 73–96.

Catchen, J., Hohenlohe, P. A., Bassham, S., Amores, A., & Cresko, W. A. (2013). Stacks: An analysis tool set for population genomics. *Molecular Ecology*, *22*(11), 3124–3140. https://doi.org/10.1111/mec.12354

Caye, K., Jumentier, B., Lepeule, J., & François, O. (2019). LFMM 2: Fast and accurate inference of gene-environment associations in genome-wide studies. *Molecular Biology and Evolution*, *36*(4), 852–860. https://doi.org/10.1093/molbev/msz008

Chambers, J. M. (2013). *SoDA*: Functions and examples for "Software for Data Analysis". R package version 1.0-6. Retrieved June 12, 2020, from https://cran.r-project.org/package=SoDA

Chhatre, V. E. (2018). Distruct v2.3: A modified cluster membership plotting script. Retrieved from http://distruct2.popgen.org.

Cullen, A. C., & Frey, H. C. (1999). *Probabilistic techniques in exposure assessment* (1st ed.). New York: Plenum Press.

Danecek, P., Auton, A., Abecasis, G., Albers, C. A., Banks, E., DePristo, M. A., … Durbin, R. (2011). The variant call format and VCFtools. *Bioinformatics*, *27*(15), 2156–2158. https://doi.org/10.1093/bioinformatics/btr330

Delignette-Muller, M. L., & Dutang, C. (2015). *fitdistrplus*: An R package for fitting distributions. *Journal of Statistical Software*, *64*(4), 1–34. https://doi.org/10.18637/jss.v064.i04

Do, C., Waples, R. S., Peel, D., Macbeth, G. M., Tillett, B. J., & Ovenden, J. R. (2014). NeEstimator v2: Re-implementation of software for the estimation of contemporary effective population size (Ne) from genetic data. *Molecular Ecology Resources*, *14*(1), 209–214. https://doi.org/10.1111/1755-0998.12157

Dray, S., Bauman, D., Blanchet, G., Borcard, D., Clappe, S., Guenard, G., … Wagner, H. H. (2020). *adespatial*: Multivariate multiscale spatial analysis. R package version 0.3-8. Retrieved April 22, 2020, from https://cran.r-project.org/package=adespatial

Drenovec, F. (2012). Hrvatski jadranski otoci, otočići i hridi. http://www.hrvatskiotoci. com/. Retrieved from internal-pdf://221.138.58.193/hrvatskiotoci_info_islands.pdf

Duplačić Leder, T., Ujević, T., & Čala, M. (2004). Coastline lengths and areas of islands in the Croatian part of the Adriatic sea determined from the topographic maps at the scale of 1:25 000. *Geoadria*, *9*(1), 5–32.

Ewels, P., Magnusson, M., Lundin, S., & Käller, M. (2016). MultiQC: Summarize analysis results for multiple tools and samples in a single report. *Bioinformatics*, *32*(19), 3047–3048. https://doi.org/10.1093/bioinformatics/btw354

Excoffier, L., & Lischer, H. E. L. (2010). Arlequin suite ver 3.5: A new series of programs to perform population genetics analyses under Linux and Windows. *Molecular Ecology Resources*, *10*(3), 564–567. https://doi.org/10.1111/j.1755-0998.2010.02847.x

Fick, S. E. (2017). WorldClim 2: new 1-km spatial resolution climate surfaces for global land areas. *International Journal of Climatology*, *37*(12), 4302–4315.

https://doi.org/10.1002/joc.5086
Foll, M., & Gaggiotti, O. (2008). A genome-scan method to identify selected loci appropriate for both dominant and codominant markers: a Bayesian perspective. *Genetics*, *180*(2), 977–993. https://doi.org/10.1534/genetics.108.092221
Frichot, E., & François, O. (2015). LEA: An R package for landscape and ecological association studies. *Methods in Ecology and Evolution*, *6*(8), 925–929. https://doi.org/10.1111/2041-210X.12382
Garcia-Gonzalez, F., Simmons, L. W., Tomkins, J. L., Kotiaho, J. S., & Evans, J. P. (2012). Comparing evolvabilities: Common errors surrounding the calculation and use of coefficients of additive genetic variation. *Evolution*, *66*(8), 2341–2349. https://doi.org/10.1111/j.1558-5646.2011.01565.x
Gautier, M. (2015). Genome-wide scan for adaptive divergence and association with population-specific covariates. *Genetics*, *201*(4), 1555–1579. https://doi.org/10.1534/genetics.115.181453
Goslee, S. C., & Urban, D. L. (2007). The ecodist package for dissimilarity-based analysis of ecological data. *Journal of Statistical Software*, *22*(7), 1–19. https://doi.org/10.18637/jss.v022.i07
Gruber, B., Unmack, P. J., Berry, O. F., & Georges, A. (2018). *dartR*: An R package to facilitate analysis of SNP data generated from reduced representation genome sequencing. *Molecular Ecology Resources*, *18*(3), 691–699. https://doi.org/10.1111/ijlh.12426
Günther, T., & Coop, G. (2013). Robust identification of local adaptation from allele frequencies. *Genetics*, *195*(1), 205–220. https://doi.org/10.1534/genetics.113.152462
Hadfield, J. D. (2010). MCMC methods for multi-response generalized linear mixed models: The *MCMCglmm* R package. *Journal of Statistical Software*, *33*(2), 1–22. https://doi.org/10.18637/jss.v033.i02
Heidelberger, P., & Welch, P. D. (1983). Simulation run length control in the presence of an initial transient. *Operations Research*, *31*(6), 1109–1144. https://doi.org/10.1287/opre.31.6.1109
Herrel, A., Huyghe, K., Vanhooydonck, B., Backeljau, T., Breugelmans, K., Grbac, I., … Irschick, D. J. (2008). Rapid large-scale evolutionary divergence in morphology and performance associated with exploitation of a different dietary resource. *Proceedings of the National Academy of Sciences of the United States of America*, *105*(12), 4792–4795. https://doi.org/10.1073/pnas.0711998105
Houle, D. (1992). Comparing evolvability and variability. *Genetics*, *130*(1), 195–204.
Jombart, T. (2008). *adegenet*: a R package for the multivariate analysis of genetic markers. *Bioinformatics*, *24*(11), 1403–1405. https://doi.org/10.1093/bioinformatics/btn129
Jombart, Thibaut, & Ahmed, I. (2011). *adegenet* 1.3-1: New tools for the analysis of genome-wide SNP data. *Bioinformatics*, *27*(21), 3070–3071. https://doi.org/10.1093/bioinformatics/btr521
Keenan, K., Mcginnity, P., Cross, T. F., Crozier, W. W., & Prodöhl, P. A. (2013). *diveRsity*: An R package for the estimation and exploration of population genetics parameters and their associated errors. *Methods in Ecology and Evolution*, *4*(8), 782–788. https://doi.org/10.1111/2041-210X.12067
Langmead, B., & Salzberg, S. L. (2012). Fast gapped-read alignment with Bowtie 2. *Nature Methods*, *9*(4), 357–359. https://doi.org/10.1038/nmeth.1923
Li, H., Handsaker, B., Wysoker, A., Fennell, T., Ruan, J., Homer, N., … Durbin, R. (2009). The Sequence Alignment/Map format and SAMtools. *Bioinformatics*, *25*(16), 2078–2079. https://doi.org/10.1093/bioinformatics/btp352
Lischer, H. E. L., & Excoffier, L. (2012). PGDSpider: An automated data conversion tool for

connecting population genetics and genomics programs. *Bioinformatics*, *28*(2), 298–299. https://doi.org/10.1093/bioinformatics/btr642

Luu, K., Bazin, E., & Blum, M. G. B. (2017). *pcadapt*: an R package to perform genome scans for selection based on principal component analysis. *Molecular Ecology Resources*, *17*(1), 67–77. https://doi.org/10.1111/1755-0998.12592

Mueller-Dombois, D., & Ellenberg, D. (1974). *Community Sampling: The Relevé Method*. *Aims and methods of vegetation ecology*.

Muff, S., Niskanen, A. K., Saatoglu, D., Keller, L. F., & Jensen, H. (2019). Animal models with group-specific additive genetic variances: Extending genetic group models. *Genetics Selection Evolution*, *51*(1), 1–16. https://doi.org/10.1186/s12711-019-0449-7

Mussmann, S. M., Douglas, M. R., Chafin, T. K., & Douglas, M. E. (2019). BA3-SNPs: Contemporary migration reconfigured in BayesAss for next-generation sequence data. *Methods in Ecology and Evolution*, *10*(10), 1808–1813. https://doi.org/10.1111/2041-210X.13252

Oksanen, J., Blanchet, F. G., Friendly, M., Kindt, R., Legendre, P., Mcglinn, D., … Wagner, H. (2019). *vegan*: Community ecology package. R package version 2.5-6. Retrieved from https://cran.r-project.org/package=vegan

Paradis, E. (2010). *pegas*: An R package for population genetics with an integrated-modular approach. *Bioinformatics*, *26*(3), 419–420. https://doi.org/10.1093/bioinformatics/btp696

Parchman, T. L., Gompert, Z., Mudge, J., Schilkey, F. D., Benkman, C. W., & Buerkle, C. A. (2012). Genome-wide association genetics of an adaptive trait in lodgepole pine. *Molecular Ecology*, *21*(12), 2991–3005. https://doi.org/10.1111/j.1365-294X.2012.05513.x

Pembleton, L. W., Cogan, N. O. I., & Forster, J. W. (2013). *StAMPP*: An R package for calculation of genetic differentiation and structure of mixed-ploidy level populations. *Molecular Ecology Resources*, *13*(5), 946–952. https://doi.org/10.1111/1755-0998.12129

Peterson, B. K., Weber, J. N., Kay, E. H., Fisher, H. S., & Hoekstra, H. E. (2012). Double digest RADseq: An inexpensive method for de novo SNP discovery and genotyping in model and non-model species. *PLoS ONE*, *7*(5), e37135. https://doi.org/10.1371/journal.pone.0037135

Plummer, M., Best, N., Cowles, K., & Vines, K. (2005). *CODA*: Convergence diagnosis and output analysis for MCMC. *R News*, *6*, 7–11.

Purcell, S., Neale, B., Todd-Brown, K., Thomas, L., Ferreira, M. A. R., Bender, D., … Sham, P. C. (2007). PLINK: A tool set for whole-genome association and population-based linkage analyses. *American Journal of Human Genetics*, *81*(3), 559–575. https://doi.org/10.1086/519795

QGIS Development Team. (2015). QGIS Geographic Information System. http://www.qgis.org/: Open Source Geospatial Foundation Project. Retrieved from http://www.qgis.org/

R Core Team. (2017). A language and environment for statistical computing.

Raj, A., Stephens, M., & Pritchard, J. K. (2014). fastSTRUCTURE: variational inference of population structure in large SNP data sets. *Genetics*, *197*(2), 573–589. https://doi.org/10.1534/genetics.114.164350

Rochette, N. C., Rivera-Colón, A. G., & Catchen, J. M. (2019). Stacks 2: Analytical methods for paired-end sequencing improve RADseq-based population genomics. *Molecular Ecology*, *28*(21), 4737–4754. https://doi.org/10.1111/mec.15253

Rosenberg, N. A. (2004). DISTRUCT: A program for the graphical display of population structure. *Molecular Ecology Notes*, *4*(1), 137–138. https://doi.org/10.1046/j.1471-8286.2003.00566.x

Schneider, C. A., Rasband, W. S., & Eliceiri, K. W. (2012). NIH Image to ImageJ: 25 years

of image analysis. *Nature Methods*, *9*(7), 671–675. https://doi.org/10.1038/nmeth.2089
Sherrill-Mix, S. (2021). *taxonomizr*: Functions to work with NCBI ccessions and Taxonomy. R package version 0.8.0.
Simão, F. A., Waterhouse, R. M., Ioannidis, P., Kriventseva, E. V., & Zdobnov, E. M. (2015). BUSCO: Assessing genome assembly and annotation completeness with single-copy orthologs. *Bioinformatics*, *31*(19), 3210–3212. https://doi.org/10.1093/bioinformatics/btv351
Weisenfeld, N. I., Kumar, V., Shah, P., Church, D. M., & Jaffe, D. B. (2017). Direct determination of diploid genome sequences. *Genome Research*, *27*(5), 757–767. https://doi.org/10.1101/gr.214874.116
Wilson, G. A., & Rannala, B. (2003). Bayesian inference of recent migration rates using multilocus genotypes. *Genetics*, *163*(3), 1177–1191. https://doi.org/10.1093/genetics/163.3.1177
Wolak, M. E., & Reid, J. M. (2017). Accounting for genetic differences among unknown parents in microevolutionary studies: how to include genetic groups in quantitative genetic animal models. *Journal of Animal Ecology*, *86*(1), 7–20. https://doi.org/10.1111/1365-2656.12597